Development of an In-Vitro Model to Study the Effect of Shear and Biomaterial on Neutrophil Extracellular Trap Release by Blood Neutrophils and HL-60 Cells

by

Andreea Maria Palage

A thesis

presented to the University of Waterloo

in fulfillment of the

thesis requirement for the degree of

Master of Applied Science

in

Systems Design Engineering

Waterloo, Ontario, Canada, 2023

Author’s Declaration

I hereby declare that I am the sole author of this thesis. This is a true copy of the thesis, including any required final revisions, as accepted by my examiners.

I understand that my thesis may be made electronically available to the public.

Abstract

Cardiovascular biomaterials are essential for the support of damaged or diseased cardiovascular tissue and structures. Their applications include stents, heart valves, vascular grafts, and pacemakers. The success of these biomaterials is crucial for improving patient outcomes and enhancing quality of life. Shear stress, the frictional force exerted by flowing blood on the surface of cardiovascular biomaterials, can directly influence the performance and stability of these materials. Studying the impact of shear stress can aid in the development of improved biomaterials.

Neutrophils (PMNs) are a type of white blood cell that play a crucial role in the body's immune system and defend against infection. In addition to their conventional role in phagocytosing and killing pathogens, neutrophils employ another intriguing defense mechanism known as neutrophil extracellular traps (NETs). These web-like structures are released by neutrophils to immobilize and eliminate microbes and are composed of DNA as well as antimicrobial proteins. With the introduction of a biomaterial into the body, neutrophils respond by releasing inflammatory mediators and forming NETs. Previous studies have revealed that NETs form on the surface of a variety of biomaterials, however, the effect of shear on NETosis in the presence of a biomaterial has not been examined in blood neutrophils or in the neutrophil-like HL-60 cell line model.

In this study, an in-vitro model was developed to assess the effect of shear on NETosis in the presence of silicone, a common biomaterial. Neutrophils isolated from healthy donor blood and differentiated HL-60s were exposed to either static (37°C incubation in polypropylene tubes with or without neutrophil stimulation) or dynamic conditions (cells circulate in flow chambers pre-loaded with plasma-coated silicone at a shear rate of $500s^{-1}$, with or without neutrophil stimulation). Following exposure, NETs and neutrophil activation were measured using a FACSCalibur flow cytometer and the silicone surface was characterized by immunofluorescence.

Preliminary HL-60 results indicate that two populations of cell are present during analysis: healthy and damaged. Damaged cells include both apoptotic and dead cells. With the inclusion of both populations during analysis, results show that shear, in the presence of a plasma-coated biomaterial, increases the number of cells undergoing NETosis and results in a small, elevated, NET marker release as shown by expression levels of the antimicrobial protein myeloperoxidase (MPO) and citrullinated histone (citH3). In blood-isolated neutrophils, shear also increases the number of

cells undergoing NETosis, however there is a minimal change in NET marker expression. For both cell types, immunofluorescence staining reveals that NETs largely aggregated on the silicone surface, presenting the need to further explore and quantify NETosis on the biomaterial. When the complement system is inactivated under shear conditions by ethylenediaminetetraacetic acid (EDTA), the NET signal is reduced in both HL-60 cells and blood neutrophils.

Using the developed model, results support the idea that shear modulates NETosis in the presence of a biomaterial and may play a role in the distribution of NETs between the material surface and circulation. Given the difference in NETosis response between HL-60 cells and PMNs, the HL-60 cell line may not be an accurate and appropriate model to investigate NET and material interactions under shear. To better characterize the mechanisms involved in NETosis on the biomaterial and under shear, the silicone surface and the aggregates found therein should be further analyzed.

Acknowledgements

I am extremely grateful for all the guidance and support that I received during my two years as a graduate student at Waterloo and there are several people that I would like to thank.

I would like to first express my sincere gratitude and appreciation to my supervisor Maud Gorbet for allowing me to work with the MIBS lab and for her unwavering mentorship throughout this project. Thanks to her, I have learned so much about biocompatibility and how to be an effective and engaged researcher.

I am grateful to Miriam Heynen for her assistance in taking blood for this experiment and for all the donors that were willing to give blood so that I could explore my research question. Without them, this thesis would not have been possible.

I would also like to thank my thesis readers Dr Veronika Magdanz and Dr Valerie Ward for their constructive and valuable feedback. I sincerely appreciate their insights. I would like to further thank my fellow lab members: Yutong Jin, Nikan Momenbeitollahi, Sadaf Mohsenkhani and Matt Robichaud. Thank you for sharing your knowledge and experience with me and for always being willing to lend a helping hand. You have all made this an incredible and positive working environment.

I would like to extend my appreciation to the SYDE Department for their support via the Engineering Excellency Fellowship and more broadly to the Engineering Faculty for their assistance with the NSERC Grant.

Finally, I would like to thank my friends and family! To my mom Felicia Moldovan and my brother Cristian Palage, thank you for listening and letting me talk through my ideas even though this is not within your areas of study (Mulțumesc). Thank you to Emma Johnson, Lareb Zahra, Mahtash Nourafkan, and Malek Terry for everything.

Table of Contents

List of Figures

List of Tables

List of Abbreviations

PMNs	Blood Polymorphonuclear Leukocytes (specifically Neutrophils)
dHL-60	Neutrophil Differentiated Promyeloblast Cells
PMA	Phorbol Myristate Acetate
fMLP	N-formyl-methionyl-leucyl-phenylalanine
CI	Calcium Ionophore
IL-8	Interleukin-8
MPO	Myeloperoxidase
citH3	Citrullinated Histone 3
DMSO	Dimethyl sulfoxide
ATRA	All-Trans Retinoic Acid
DMF	Dimethylmethanamide
NETs	Neutrophil Extracellular Traps
PPP	Platelet Poor Plasma
UA	Unactivated
EDTA	Ethane-1,2-diyldinitrilotetraacetic acid
ANOVA	Analysis of Variance
FSC	Forward Scatter
SSC	Side Scatter
FL	Fluorescence Channel
FITC	Fluorescein isothiocyanate

PE	Phycoerythrin

Chapter 1: Thesis Introduction

1.1 Introduction

Neutrophils, a type of granulocytic white blood cell (leukocyte), are essential components of the innate immune system. Neutrophils represent over 60% of the leukocyte population in blood and play a crucial role in inflammation and fighting infections. Equipped with a distinctive multi-lobed nucleus, and granules containing powerful antimicrobial and pro-inflammatory mediators, neutrophils can eliminate invading microorganisms through phagocytosis, producing reactive oxygen species (ROS), and releasing antimicrobial proteins and peptides, such as lactoferrin (LF), myeloperoxidase (MPO), and elastase (NE). Neutrophils are also capable of releasing extracellular traps to neutralize infections. Additionally, neutrophils contribute to the inflammatory response by releasing proteins known as cytokines, which help recruit other immune cells to sites of infection or inflammation. Moreover, neutrophils interact with other immune cells and regulate immune responses [1], [2].

Biomaterials come into contact with biological systems in a variety of ways such as through implants, drug delivery systems, surgical tools, diagnostic devices, and tissue engineering scaffolds. As key players in the innate immune response, neutrophil response can significantly impact the interactions with biomaterials in tissues as well as cardiovascular biomaterials (ie blood-contacting material). Thus, understanding how biomaterials interact with blood, including neutrophils, is essential in assessing their biocompatibility. The biocompatibility of blood contacting medical devices has been the subject of much research and review. Despite the improvement of current biomaterials and the development of new ones, contact with blood continues to result in the activation of blood components and in adverse reactions, such as thrombus formation, chronic inflammation and impaired healing [3], [4]. Blood-biomaterial interactions are complex and can impact the biomaterial's functionality and longevity (Figure 1.1) [5]. For example, the complement system (part of the body’s innate immune response) is activated in the presence of a biomaterial. As a result of complement protein adsorption to the surface and the chemoattractant particles that they release, leukocytes are recruited to the material leading to further immune system activation via cytokine release [3]. The adsorption of plasma proteins also includes fibrinogen, von willbebrand factor (vWF), and immunoglobulins which further results in platelet activation. This triggers not only coagulation pathways (leading to thrombus formation) but the formation of platelet-leukocyte aggregates that can also contribute to creating an extensive thrombus network [6], [7]. Within this

feedback loop of activation, complement proteins are additionally capable of enhancing platelet adhesion and activation [3].

Subsequently, studying the various elements of blood-material interactions in vitro will allow for more insight into the underlying mechanisms that govern these responses. This knowledge will be valuable in developing strategies to modulate host responses and improve blood compatibility in various biomedical applications. During blood-material interactions, neutrophils can become activated and adhere to the material's surface. This activation triggers the release of inflammatory cytokines, tissue-degrading enzymes, extracellular traps, and reactive oxygen species [8], [9]. As neutrophils adhere to the material, they attempt to phagocytose the surface as part of the immune response. As the material is too large to be engulfed, neutrophils undergo a frustrated form of phagocytosis leading to the release of oxygen metabolites and proteolytic enzymes [10]. The extent of neutrophil activation depends on both the material characteristics and the other proteins adsorbed on the surface. Neutrophils heavily interact with other biological components during the material-induced biological response such as platelets, complement proteins, and endothelium. Given the complexity of these interactions, it is important to isolate the specific effect of the material on neutrophils directly. Hence, blood-isolated polymorphonuclear neutrophils (PMNs) (as opposed to whole blood) can be employed in models investigating leukocyte-material interactions. This thesis will explore neutrophils in the presence of shear and a biomaterial in order to contribute to the growing body of blood biocompatibility research.

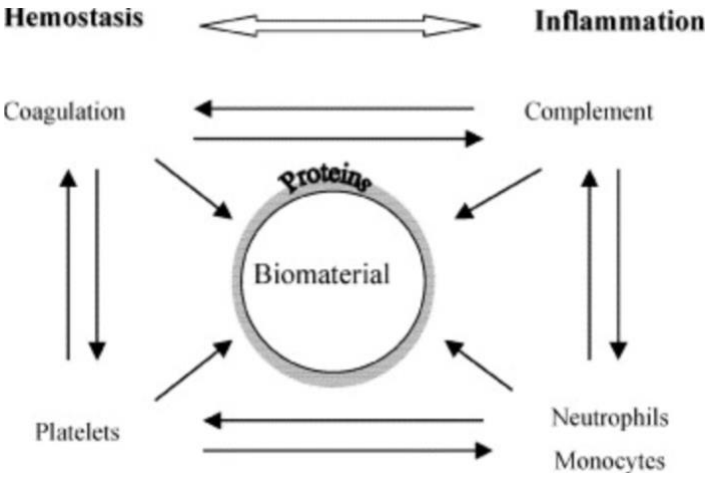

Figure 1.1: The key components of the blood-biomaterial response and their interactions. Reproduced with permission [10].

1.2 Silicone

A widely used biomaterial, particularly in implanted cardiovascular materials, is silicone (also known as polysiloxane). Silicone is made up of a mixture of semi-inorganic polymeric molecules consisting of an array of polydimethylsiloxane monomer chains of varying lengths [11]. It has high elasticity and hydrophobicity and retains flexibility even at extreme temperatures, making it a widely applicable material. Its applications include coating or treatment of medical devices, inserts and implants, catheters, contact lenses, and shunts. Table 1.1 provides a thorough list of silicone's applications in the medical setting. Silicone has good hemocompatibility in the body due to its hydrophobicity and low surface tension [11].

Location	Body parts	Applications
Head and neck	Brain	Hydrocephalus shunts
	Skull	Burr hole covers
	Eye	Scleral bands and buckles Vitreous fluid replacement Intraocular lenses Contact lenses
	Ear	Elastomer tubes for ontological ventilation Cochlear implants (encase in silicone)
	Throat	Voicebox prothesis, post-laryngectomy
Torso	Cardiac	Peacemaker encapsulated and leads insulated with silicone Mechanical heart valves
	Gastric	Gastric band implant (Lap-Band, Realize)
Urinary system	Urinary tract	Silicone urological catheters Urethral stents Artificial urethra
Skeletal joints	Hip	Silicone drainage systems
	Knee	Shock-absorbing silicone bumper for knee replacement
	Foot	Foot and toe joint implants

Table 1.1: Applications of silicone. Adapted from Zare et al (open access article) [11].

1.3 Research Motivation and Objectives

Although NETs and blood-biomaterial interactions have separately been reported to contribute to thrombosis and inflammation, no in-vitro study has yet investigated the mechanisms involved in

material-induced activation and NETs under flow conditions in human neutrophils. The aim of this thesis was to develop an in vitro model and flow cytometry methodology to characterize NETosis under shear conditions in the presence of a biomaterial. It was hypothesized that contact with a biomaterial under physiological shear using a parallel plate model, and in the presence of an inflammatory mediator, would activate NETosis that could be characterized by flow cytometry.

This thesis is also motivated by the lack of characterization around using the HL-60 cell line to study NETosis. HL-60 is a human-derived immortal cell line that is often used as an alternative to isolating human neutrophils. They are promyelocytes that can be differentiated into macrophage-like cells through exposure to various chemicals, such as PMA and dimethyl sulfoxide (DMSO), [6]. They are convenient for in-vitro studies as they proliferate rapidly (doubling time of 20-45 hours) and can remain in suspension with minimal growth supplements and thus can be readily available for experiments. While they can successfully mimic neutrophils, discrepancies exist in their phenotype, including the lack of lactoferrin-specific granules and additional deficiencies observed in some of their oxidative killing mechanisms [12][13]. Despite these discrepancies, HL-60 cells have been used to study NETs [14]. No comprehensive study has yet examined HL-60 NETosis under flow conditions, nor have any utilized flow cytometry as an analysis method to characterize and quantify NETosis in this model cell line. Thus, the other objective of this thesis was to determine if HL-60 cells are an appropriate model for investigating NETosis in leukocyte-biomaterial interactions under shear.

1.4 Thesis Outline

This thesis will begin by presenting a review of the current understanding of biomaterial-related NETosis in-vitro in Chapter 2. This review will cover both neutrophils and the HL-60 cell line. Chapter 3 will focus exclusively on the HL-60 experimental process including materials, methods, results, and discussion. Chapter 4 will examine blood neutrophils and will similarly outline the materials, methods, results, and discussion related to those investigations. Conclusions and future work will be presented in Chapter 5.

Chapter 2: Literature Review

2.1 Introduction to Leukocyte Biology and Cells Lines

2.1.1 Introduction

Neutrophils are a crucial component of the inflammatory response induced by biomaterials. This chapter focuses on presenting what is currently understood about neutrophil-biomaterial interactions. It will begin by briefly outlining the function of neutrophils, the definition of NETs, and the mechanisms of NET release. It will then present how NETs are assessed, followed by what has so far been done to study NETs on biomaterials in-vitro. Further, it will explore how the HL-60 cell line has been used to model neutrophil activation upon contact with materials. In the final section, this review will discuss how the HL-60 cell line has been used to further the understanding of NETosis mechanisms due to the similarities between differentiated HL-60 cells and neutrophils as well as their modifiable phenotype. This will also include a comparison between HL-60 and neutrophil-derived NET structures.

2.1.2 Leukocyte Biology

Neutrophils (also known as polymorphonuclear leukocytes, or PMNs) are leukocytes, a granulitic type of white blood cell that play a critical role in the innate immune system. Neutrophils, with a concentration ranging from 2.5 to 7.5 million per mL, represent between 40 to 70% of the circulating leukocytes and are primarily responsible for combating infections and protecting the host against foreign bodies. While in circulation, they average a lifespan of approximately 24 hours. They possess a distinctive multi-lobed nucleus and contain granules filled with potent antimicrobial and inflammatory molecules that can neutralize and kill invading microorganisms [2]. PMNs can phagocytose bacteria, fungi, and cellular debris, produce reactive oxygen species (ROS) and release antimicrobial proteins and peptides through degranulation to directly kill microorganisms and control infection. PMNs contain four types of granules: primary (azurophilic), secondary (specific), tertiary and secretory [15]. The antimicrobial proteins myeloperoxidase (MPO) and neutrophil elastase (NE) are released from primary granules when PMNs are activated. This degranulation can be measured by quantifying the increase in CD63, a transmembrane protein that becomes highly expressed on the surface of neutrophils during degranulation [16]. Secondary granules also release antimicrobial proteins including lactoferrin and lysozymes. Within the secondary granules (and also found on the

plasma membrane of PMNs) are the integral membrane proteins CD11b/CD18. During activation, CD11b translocates to the membrane surface to aid with PMN migration and adhesion [17]. CD11b upregulation facilitates the interaction between leukocytes and biomaterials enabling leukocytes to play their role in the immune response. Adherent leukocytes can release various inflammatory mediators that contribute to the recruitment of additional immune cells and the initiation of an inflammatory cascade [3], [18]. As is seen in Figure 2.1 (illustrating the degranulation response), tertiary granules contain metalloproteinases (MMPs) and secretory granules release plasma proteins such as albumin [19]. Some additional PMN surface markers and their function are presented in Table 2.1 [19]–[23]. This is not a comprehensive list but these specific markers were selected based on their use in biomaterial studies to characterize the PMN response [9], [24], [25].

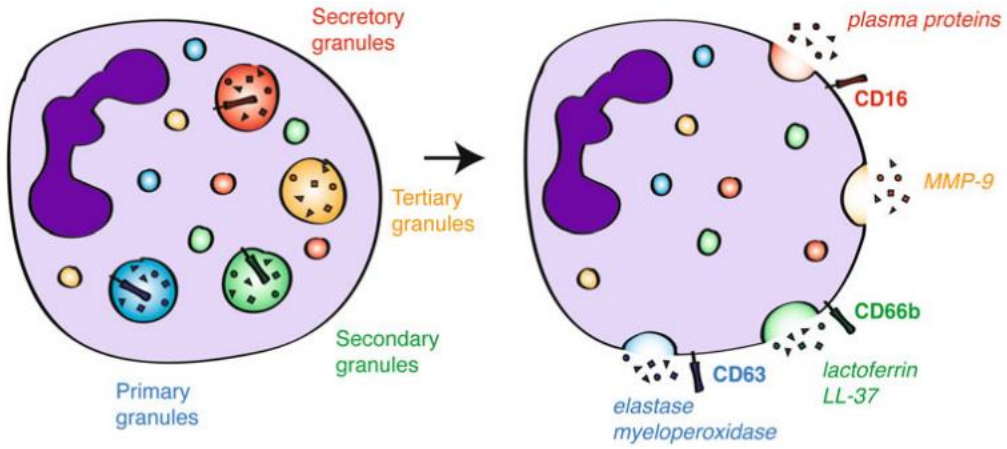

Figure 2.1: Degranulation response of neutrophils upon activation. Image reproduced with permission [15].

Table 2.1: Neutrophil receptors and their function

Receptor	Function
CD11b	Adhesion, migration, phagocytosis
CD15	Mediates neutrophil adhesion to dendritic cells. Common marker for leukocytes
CD16	Phagocytosis. Expressed during maturation
CD35	Complement system regulation
CD63	Degranulation
CD65	Adhesion. Binds E and P-selectin
CD66b	Degranulation, phagocytosis, adhesion, and migration

Besides their role in infection control, neutrophils are the first innate immune cells at an injury site and are essential and critical contributors to the inflammatory response by releasing reactive oxygen species (ROS) and pro and anti-inflammatory proteins known as cytokines [1], [2]. Some of these cytokines, such as interleukin 1 (IL-1), tumor necrosis factor-alpha (TNFα), and macrophage migration inhibitory factor (MIF) aid in recruiting other immune cells to the site of infection or inflammation. A comprehensive list of cytokines released by PMNs, and their functions is presented in Figure 2.2. In the presence of a biomaterial, neutrophils can adhere to, and activate on, the biomaterial surface, thereby impacting the inflammatory response and the overall biocompatibility of the material. Regardless of adhesion, PMNs in circulation will still become activated as part of the inflammatory response [8].

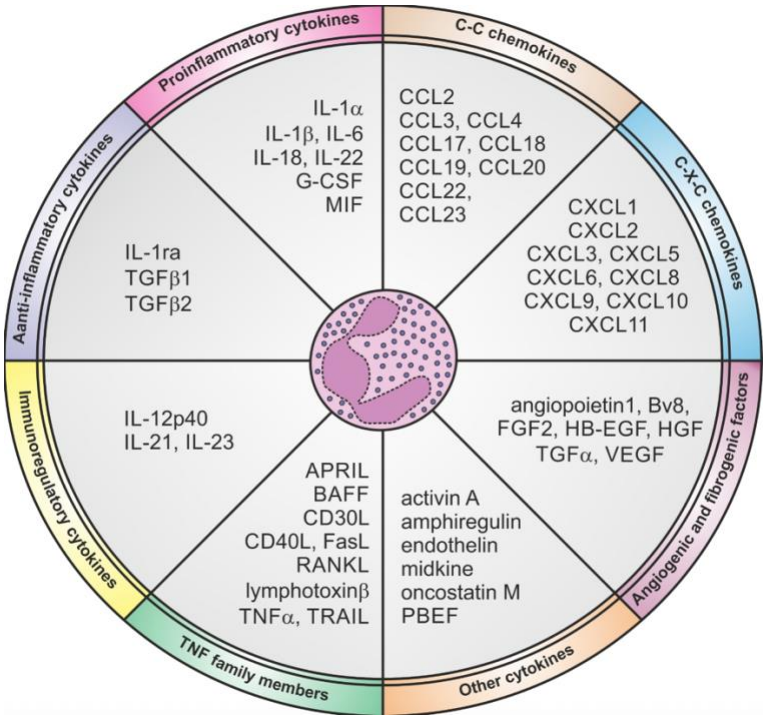

Figure 2.2: Cytokines released by PMNs and their functions. Image reproduced with permission [15].

2.1.3 Neutrophil Extracellular Traps (NETs)

In the study of blood-biomaterial interactions, neutrophils have become increasingly implicated in the inflammatory and thrombotic response to the introduction of foreign material. In recent years, there has been an increased focus on the phenomenon of neutrophil extracellular traps (NETs) that are triggered upon material contact with neutrophils [8], [9]. First reported in 2004, NETosis was initially studied in the context of bacterial infection. Upon activation, neutrophils expel a network of DNA and proteins that bind and eliminate pathogens [26]. Two hallmark steps of NETosis are histone citrullination and protease release. Briefly, citrullination involves the conversion of histone residues (including but not limited to H3) from arginine to citrulline via peptidyl arginine deiminase (PAD4), thereby leading to chromatin decondensation. Concurrently, neutrophils degranulate to release proteins including the antimicrobial enzymes MPO and NE [27]. NETosis is a distinct type of cellular death that differs from apoptosis or necrosis. For example, cells do not display the phosphatidylserine signals typical of apoptotic cells nor do the membranes bleb in the same way.

In fact, plasma integrity is maintained during NETosis to allow granular cargo to mix with chromatin [28]. Despite being a powerful antibacterial tool, NETs have also been implicated in sterile inflammation and can be induced in-vitro by the synthetic stimuli phorbol myristate acetate (PMA) or by physiological stimuli such as calcium ionophore (CI), interleukin- 8 (IL-8) and tumour necrosis factor-alpha (TNF-a)[28]. NETs are pro-inflammatory as well as pro-thrombotic and have been shown to activate complement, platelets, and monocytes [29]. Given the NETosis potential of neutrophils and their importance in the immune reaction towards biomaterials, the interest in studying NETs as a consequence of neutrophil-biomaterial interactions is growing.

2.1.4 Mechanisms of NETosis

While the exact mechanisms and pathways of NETosis continue to be studied, several key features have been elucidated. There are thought to be two types of NETosis: lytic and vital [30]. Lytic NETosis involves extracellular trap expulsion that occurs over several hours following stimulation and ultimately results in the death of the neutrophils involved. In this type of NETosis, reactive oxygen species play a large role. Upon stimulation, neutrophils activate the raf-MEK-ERK signaling pathway that in turn activates the nicotinamide adenine dinucleotide phosphate oxidase enzyme (NADPH) and the subsequent generation of superoxide anions. Crucially, NADPH is not the only source of ROS during NETosis [31], [32]. Exactly how ROS interact with neutrophil proteins to contribute to, as well as further, NETosis, remains unclear. There is evidence, however, that ROS enable the release of granule proteins during NETosis, a hallmark step of the process. Two of the released proteases are MPO and NE. NE has been shown to travel to the nucleus and causes histone degradation, resulting in DNA decondensation [31], [33]. As it moves to the nucleus, NE has also been found to break down actin filaments, hindering the movement of neutrophils. Later, MPO also moves to the nucleus to aid NE in chromatin decondensation, though the exact mechanism is still unknown [31]. DNA decondensation is also triggered by histone citrullination. This process involves the conversion of histone residues (including but not limited to H3) from a positively charged arginine side chain to a polar and uncharged citrulline side chain via peptidyl arginine deiminase (PAD4), thereby leading to chromatin decondensation [32]. The interaction between ROS and histone citrullination continues to be investigated. Eventually, chromatin and granule proteins combine in the cytoplasm, leading to cell membrane lysis and the release of a mixture of nuclear and granule material into the external environment. It is there that MPO produces hypochlorous acid that can kill

pathogens and where NE can degrade bacterial proteins [30], [31], [34]. Figure 2.3 illustrates the release of NETs to the environment.

Vital NETosis involves the expulsion of DNA from the nucleus into the extracellular space while maintaining the viability of the neutrophils. This type of NETosis has been observed in response to specific molecular patterns associated with microorganisms that are recognized by the host's pattern recognition receptors, such as lipopolysaccharides (LPS) and Staphylococcus aureus (S. aureus) [32]. This typically occurs faster than lytic NETosis (beginning in minutes as opposed to hours) and cells maintained their chemotaxis and phagocytic abilities [32], [35]. This investigation will focus on lytic NETosis as opposed to vital.

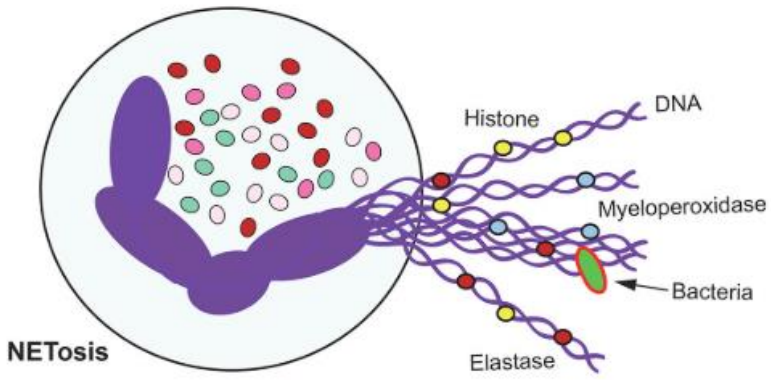

Figure 2.3: NETosis involves the release of DNA, histones and antimicrobial proteins [1]. Open access article.

2.1.5 HL-60 Cells

HL-60 cells are a widely recognized and extensively studied cell line important for studying blood-biomaterial interactions. Derived from a patient suffering from acute promyelocytic leukemia, these immortalized cells exhibit properties of myeloblasts and promyelocytes, making them a valuable model. They can be differentiated into macrophage-like cells using phorbol myristate acetate (PMA) and 12-O-tetra-decanoylphorbol-13-acetate (TPA), or neutrophil-like cells through treatment with dimethyl sulfoxide (DMSO), all-trans retinoic acid (ATRA) or dimethylformamide (DMF) [36]. Their unique characteristics, ease of cultivation, and ability to be induced to differentiate into

different cell types have made them indispensable tools [14], [36]–[39]. These cells provide a simplified and controlled model to explore the responses of blood cells to different biomaterials [14], [39], [40] . By exposing HL-60 cells to biomaterial surfaces, researchers can assess factors such as adhesion, activation, aggregation, and clotting, which are crucial in understanding the biocompatibility and hemocompatibility of these materials. HL-60 cells offer a convenient alternative to working directly with human blood-isolated neutrophils, allowing for repeatable and reproducible experiments [14], [38], [39].

2.1.6 Differentiation Effects on HL-60 Cells

HL-60 differentiation has been more extensively studied to optimize conditions so that differentiated cells (dHL-60) are most susceptible to NETosis. From a method's perspective, this is valuable in establishing effective dHL-60 models to be used in biomaterial-NETosis studies. For example, in an extensive study by Manda-Handzlik and colleagues, HL-60 cells differentiated with ATRA released NETs only when stimulated with PMA and DMSO-differentiated cells only upon CI stimulation. DMF differentiation resulted in HL-60 cells that could respond to both PMA and CI stimulation. In addition, H3 citrullination was observed more so in stimulated cells that had been differentiated with DMSO or DMF as opposed to ATRA [41]. These striking results are at odds with other papers that have reported NETs in CI-stimulated ATRA-differentiated HL-60 cells and PMA-stimulated DMSO-differentiated HL-60 cells [42], [43].

Relating to media used in cell culture, Guo et al found that the serum-free medium X-VIVO was not only effective during HL-60 differentiation with DMSO and ATRA, but that the dHL-60 cells produced were more efficient at generating NETs and ROS upon stimulation. Specifically, they concluded that cells differentiated with DMSO in X-VIVO and stimulated with 100 nM PMA over four hours generated the most NETs (including elevated citH3 levels) [44]. Their findings also contradicted those of Manda-Handzlik as the cells differentiated with ATRA in X-VIVO still generated an elevated level of NETs upon stimulation with CI.

2.2 Characterization of NETs

2.2.1 Immunofluorescent Staining of NETs

There is no gold standard for quantifying NETosis and in fact, there is very little consistency across the literature. For the identification of NETs, most papers employ immunofluorescence staining of both genetic material (either citrullinated histones or chromatin more generally) and NET proteases like MPO and/or NE [45]–[48]. Common dyes for genetic material include 4′,6-diamidino-2-phenylindole (DAPI) or Sytox green which will only stain cells with compromised plasma membranes [49], [50]. Quantification using immunofluorescence often involves expressing the ratio of antibody-positive cells to the total adhered cells on the surface. Groups may also simultaneously employ live/dead cell counts alongside antibody targeting [14]. Within imaging, several software techniques exist to quantify NETs (including image stream systems, NETQuant and Image J) though they can be modified to suit the needs of each group and may still require manual identification of NET-positive events [14],[15].

2.2.2 ELISA for NET Quantification

Another method that is occasionally used is the enzyme-linked immunosorbent assay (ELISA). This assay is used to detect the presence of a certain ligand (typically proteins) in a sample by using antibodies specific to the ligand of interest. In the case of NETs, this is usually MPO, NE or citH3 [51], [52]. In a method development paper, researchers validated ELISA detection of citH3 and MPO in samples from patients with systemic lupus erythematosus [53]. In another work, MPO-DNA complexes were used to study the association between NETs and cardiovascular disease risk factors such as age and sex [54]. Despite their use, there are issues regarding standardization and there remains some debate about the effectiveness of ELISA for identifying NETs as others have reported that it is error prone. Hayden and colleagues found that results obtained using MPO-DNA ELISA did not correlate with other NET parameters such as citH3 and NE release. In addition, Matta et al determined that the quantity and quality of NET structures had an effect on the success of ELISA-based NET detection [55], [56]. Overall, using ELISA as a NET identifying tool was not considered to be particularly effective and therefore was not selected as a primary NETosis analysis tool in this investigation.

2.2.3 Flow Cytometry

Flow cytometry is a measurement technique that can carry out a multi-parametric analysis of cells in solution. Samples are first stained with fluorescent antibodies and then injected into a flow path that is surrounded by a sheath containing faster-flowing fluid (See Figure 2.4). The sheath ensures that cells pass a single file when exposed to the lasers of the machine. Light scattering and fluorescence emission provide information about the cells such as size (Forward Scatter-FSC), granularity (Side Scatter-SSC) and surface receptor presence. Fluorescent probes to label the cells include those in the Fluorescein isothiocyanate (FITC), Phycoerythrin (PE), Peridinin chlorophyll protein complex (PerCP) and Alexa Fluor series. Individual fluorescence (FL) channels then display the final, filtered, optical signal [57]. Flow cytometry can be used to acquire a large number of NETosis events and uses positive identification of NETosis markers including citH3, NE and MPO. The MPO and citH3 combination is the most frequently used in the literature and often involves an additional neutrophil marker such as the CD15 antigen [58]–[60]. This technique has been used on both PMNs and HL-60 cells, however it is not standardized and cannot track the progression of NETosis. As such, it is mainly used at defined experimental endpoints.

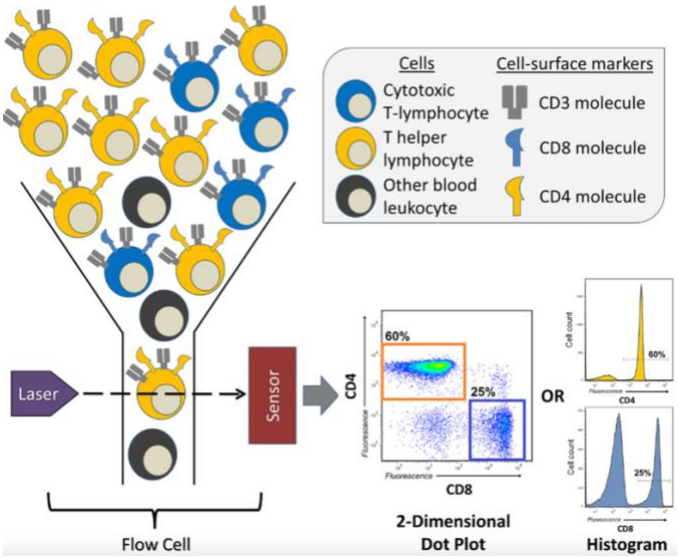

Figure 2.4: Flow cytometry mechanism. Labelled cells pass through the laser and the signal is detected by a sensor. Open access article [56].

In flow cytometry, a gate refers to a range of values that are used to separate a particular group of cytometric events from a vast collection. Gating allows for the identification of a specific cellular population of interest by using a panel of markers that are visualized via their fluorescent signal or side scatter as mentioned above. Figure 2.5 illustrates an example of a gating strategy used in this investigation. Each singular dot in Figure 2.5A-B represents a single cell in the solution, regions were drawn around specific cell population to define gates; the fluorescent histogram and associated statistics of this gated population are shown in Figure 2.5C-D. The mean fluorescence value is commonly reported when flow cytometry is used as an analytical tool [57], [61]. Additional information that is provided includes the total number of cells within that gate (Gated events) and the total percentage of cells in G1 relative to the total number of cells (% Gated). In this particular example, a large number of cells have very low fluorescent intensity, indicating that marker expression (in this case citH3) is low and following activation, a greater fluorescent intensity is observed.

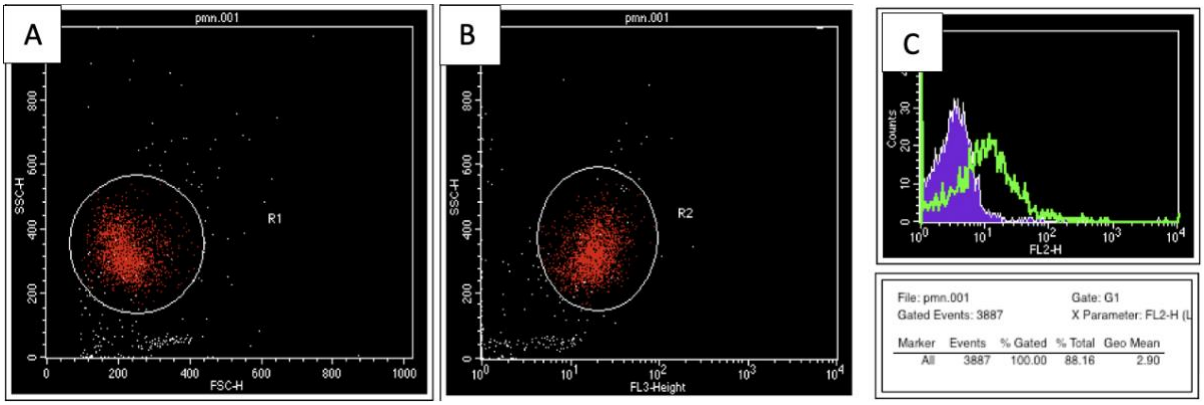

Figure 2.5: Representative images of flow cytometry data. A) Neutrophils of a characteristic FSC and SSC in Region 1 (R1). B) The same neutrophils from (A) were further selected by their expression of a neutrophil-identifying marker in FL3 (CD15-PerCy5) identified in Region 2 (R2). C) Fluorescent histogram for flow cytometry analysis. Y-axis indicates the number of cells, and the x-axis indicates the intensity of the fluorescence. Cells in the gate G1 (cell population in R1 and R2) express the marker of interest and that overall fluorescence is indicated by the "Geo Mean" value in the histogram statistics panel (D). The purple histogram represents cell events for a sample that is not activated while the green line overlay represents data of an activated sample.

2.3 In-Vitro Investigations of Blood Neutrophils, Biomaterials and NETosis

2.3.1 NETosis on Titanium

The literature related to blood-biomaterial interactions is extensive and continuously expanding due to the need to better understand the mechanisms related to the foreign body response. Much of this work directly relates to understanding or preventing thrombosis [3], [62], [63]. To date, there has been much less focus on understanding the impacts of biomaterials on NETosis in-vitro, however various materials and in-vitro models have been explored. Vitkov and colleagues identified that PMNs in whole blood attached to the surface of sandblasted large-grit acid-etched (SLA) titanium implants and generated NETs after 4 hours of incubation [64]. Their presence was confirmed by co-staining of H3, NE, and DAPI. Interestingly, there was no significant difference between control conditions and those pre-treated with albumin, suggesting that Fc-gamma-receptors (Fcγ) do not influence the initiation of NETosis [64]. Abaricia and colleagues similarly characterized the neutrophil response to titanium though the surface topography was modified to better understand how physical cues can modulate NETs [65]. In this work, NETosis was characterized by measuring the area and circularity of DAPI-stained DNA. As the release of NETs includes the expulsion of DNA and genetic material, a greater area would be indicative of a strong NETosis response. Given that the DNA also unravels during NET release, measuring circularity was also important for this work. Neutrophils on smooth titanium showed large NET formation by 4 hours while rough surfaces did not generate NETs until 8 hours post-plating and showed lower levels of pro-inflammatory cytokines including IL-1beta, IL-6 and CCL22. Further, incubation on rough hydrophilic surfaces (generated in a nitrogen environment to retain surface wettability) did not result in NET formation [65](Figure 2.6).

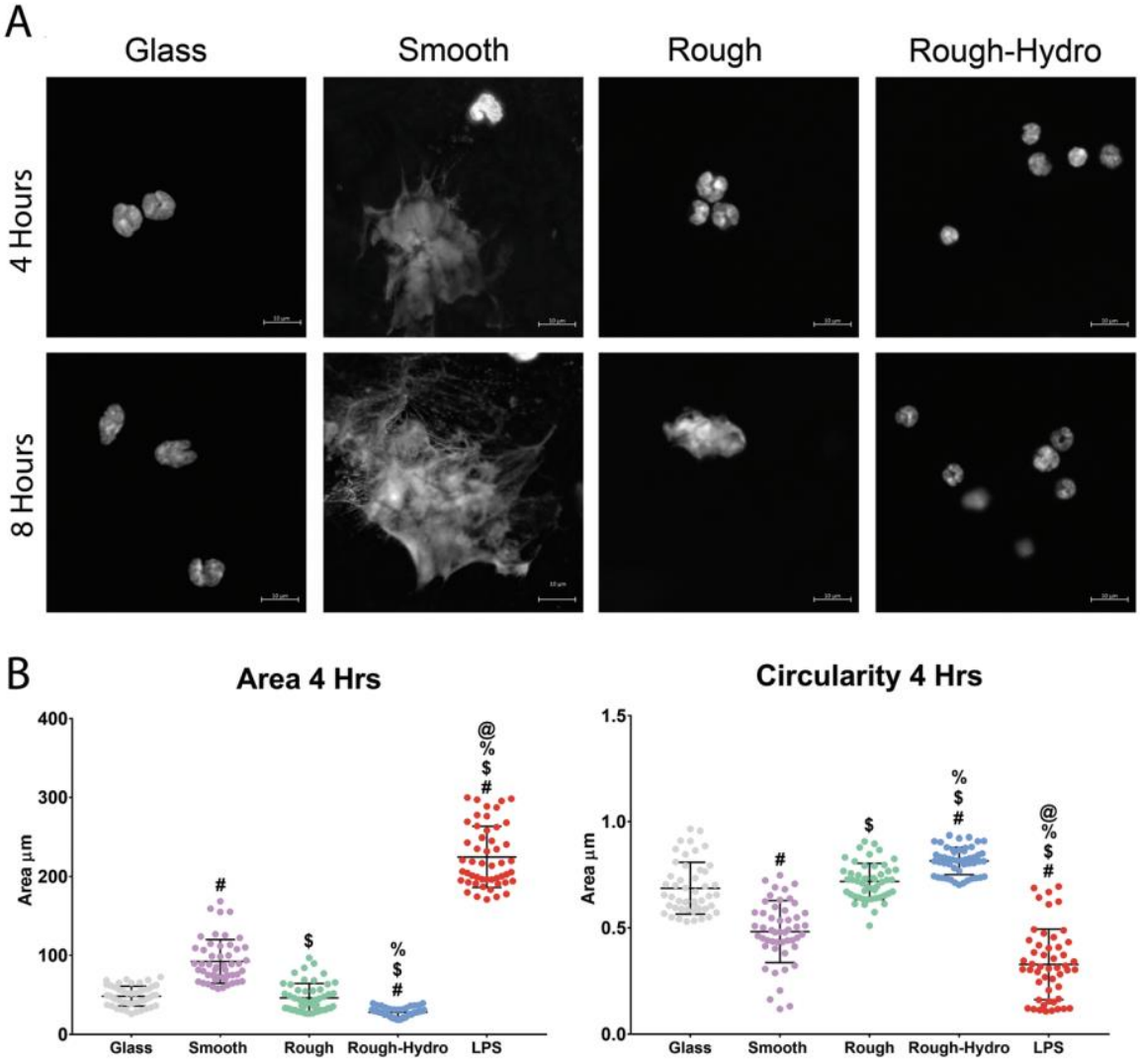

Figure 2.6: NETosis events and quantification on titanium surfaces as presented by Abaracia and colleagues. NETosis events were considered to be those that had a large DNA area and low circularity [65]. Rough-hydro indicates rough hydrophilic surfaces. Open access article.

2.3.2 Surface Cue Modulation of NETosis

In a later study, Abaricia et al further characterized the neutrophil response to varying stiffnesses of polydimethylsiloxane (PDMS)[66]. As surface stiffness increased, so too did NET formation, coupled with an increase in pro-inflammatory cytokines. The group further implicated the integrin-dependent focal adhesion kinase (FAK) pathway in NETosis by observing that FAK

inhibition attenuated the stiffness-dependent increase in NETs [66]. While these two papers contribute greatly to the understanding of sterile material-induced NETosis, the group's use of murine neutrophils, as opposed to human ones, indicates that additional confirmation is required as their respective properties differ. For example, murine neutrophils have different surface receptor expressions (e.g., less CD16 receptor expression compared to human neutrophils), a shorter lifespan, and differences in cytokine production as well as regulation [67]–[69]. Furthermore, other groups have not thoroughly validated their method of quantifying NETs through the spread and shape of nuclear DNA, nor is their use of MPO-DNA complexes an effective indicator of NETosis without the additional identification of histones [56].

Abaricia and colleagues were not the only group to examine how surface cues modulate NETosis in-vitro. Erpenbeck and colleagues examined how adhesion and substrate elasticity of polyacrylamide (PAA) gels affected NETosis [70]. Neutrophils were cultured on integrin-coated PAA surfaces with physiologically relevant elasticities ranging from 1-128 kPA before being stimulated with either 5nM PMA or 75 μg/mL LPS for 3 hours. NETosis was quantified microscopically by examining MPO staining and chromatin decondensation. It was determined that PMA-induced NETs were not impacted by either the substrate elasticity or the collagen and fibrinogen used to coat the surface [70]. This can partly be explained by PMA's mechanism of NETosis which acts intracellularly to directly generate reactive oxygen species [70], [71]. In contrast, LPS-stimulated NETs increased with increasing substrate elasticity – a novel finding. Also of note, LPS-induced NETs increased with an increased cell contact area thus implying the importance of adhesion signalling. PMA-induced NETs did not require adhesion as they did not correlate with spreading. These results further contribute to the notion that both the NETosis trigger, and the material microenvironment can dramatically alter the progression of NETosis [70].

NETosis was also taken into consideration by King and Bowlin during their use of the near-field electrospinning (NFES) technique to generate novel polydioxanone (PDO) scaffolds. Scaffolds generated via NFES had a 50% reduction in NETs relative to traditional electrospinning scaffolds at both the 3 and 6-hour mark [72]. This group was not the only one to explore the interaction between neutrophils and PDO in-vitro. In a series of papers by Fetz and colleagues, the interactions between polydioxanone and human neutrophils have been extensively examined. In 2017, investigations were carried out on the ability of PDO to regulate NETosis in-vitro. PDO and PDO-type I collagen blended templates were fabricated with either small or large diameter fibers before their interactions with

neutrophils were evaluated for 3-24 hours [73]. NETs were co-stained with DAPI and Sytox while template-bound citrullinated histone (citH3) expression was quantified using an infrared-on-cell Western blot. The authors determined that large fiber diameters (1.0-2.00 μm) reduced NETosis on PDO templates while the addition of collagen attenuated NET formation independent of fibre diameter. Small fibers (0.25-0.35 μm) rapidly induced NETosis and led to the expression of 8.06 ± 2.64 ng of CitH3 at 3 hours, a value five times higher than the large fibers [73]. This highlighted the importance of designing scaffolds that can effectively modulate the immune response to limit NETs. The authors incorporated chlorine-amidine to further elucidate whether PDO templates could act as a delivery system to attenuate template-induced NETosis [74]. This was intended to inhibit peptidyl arginase deiminase 4 (PAD4); an enzyme that mediates histone citrullination and is heavily involved in NETosis, however, the results obtained were inconclusive. As the drug concentration increased, NETosis decreased on small diameter templates (0.4 um) while the opposite trend was observed for large diameters (1.8 um). Regardless of drug content, both small and large fibre templates triggered nearly equivalent levels of NETosis by the 6-hour mark [74]. This suggests that other pathways, besides that of PAD4, can regulate NETosis in the presence of PDO. To further elucidate these pathways, a 2021 paper by the same group examined how IgG adsorption on PDO of varying fibre sizes might regulate NET release [75]. On both small and large fibres, amounts of IgG ranging from 100 μg to physiological concentrations increased NET release in a dose-dependent manner. When the IgG receptor Fcγ RIIIb was inhibited, NET release was reduced on small fibres. Interestingly, none of the other receptors tested (Fcγ RI, Fcγ RIIa, and CD11b) altered NET release, nor was NETosis impaired on large fibres in any condition. Further analysis revealed that the TAK1 signalling enzyme was responsible for the Fcγ RIIIb activation pathway. This work demonstrated that the release of NETs on biomaterials is in part regulated by IgG adsorption and subsequent engagement of the Fcγ RIIIb/TAk1 signalling pathway [75]. This is in contrast to the study by Vitkov and colleagues that did not find a role for Fcγ receptors in NETosis [64]. This could, in part, be due to their use of titanium and not PDO however those authors did not further investigate specific Fcγ receptors in their work.

While the above papers focus on modifying a singular material's surface, Sperling et al compared NET release on a range of hydrophilic and hydrophobic material surfaces simultaneously [76]. Glass, poly(ethylene-alt-maleic anhydride) (PEMA), self-assembled monolayers of methyl-terminated alkanethiols (SAM-CH3), and Teflon AF™ were incubated for 4 hours with isolated

human neutrophils after pre-adsorption with plasma proteins. NETs were visualized using citH3 and NE but were quantified by determining the relative Sytox green staining. Their results showed a significantly higher amount of expelled DNA on the hydrophobic surfaces SAM-CH3 and Teflon compared to the hydrophilic surfaces. NET structures were identified on these surfaces through co-staining of individual NET components though the authors did not present that data. Further testing on Teflon with whole blood revealed a similar pattern of NETs that stained positively for citH3, NE, and expelled DNA [76]. The increased retention of plasma proteins on the hydrophobic surfaces likely contributed to the elevated NET formation on these surfaces. The significance of this work lies in the relevance of hydrophobic surfaces in medical devices such as oxygenators and some vascular grafts. [71].

2.3.3 NETosis on Graphene Oxide and Nanomaterials

A handful of additional materials have been tested as the importance of NETs becomes increasingly clear. Lu and colleagues exposed PMNs to graphene oxide biomaterials for an hour before NET formation was evaluated via confocal microscopy and staining of MPO and NE[77]. Visualization revealed DNA smears and enzyme staining that was indicative of NETosis while also confirming that their NETs were generated in a ROS and NADPH-dependent fashion. Interestingly, graphene oxide functionalization with carboxyl (GO-COOH) and polyethylene glycol (GO-PEG) resulted in NET levels that were four times lower than that of unfunctionalized GO thus re-affirming the importance of biomaterial surface modifications on modulating NETosis [77].

In one of only two studies examining nanomaterials, Bilyy et al showed that agglomerations of non-stabilized superparamagnetic iron oxide nanoparticles (SPIONs) induce NET formation in human neutrophils after 3 hours[78]. In the presence of serum, however, NET formation was abrogated. Similarly, Munoz et al reported that nanodiamonds also triggered NETs although this was size-dependent [79]. It is difficult to directly interpret the results of these studies as they both used high concentrations (200 μg/mL) of nanomaterial that would typically not be present [78], [79]. Other groups have reviewed neutrophil-nanomaterial interactions more thoroughly [80]–[82].

The groups have all used human neutrophils to directly explore the effect of biomaterials on NETosis. On the other hand, some have opted to take advantage of the HL-60 cell line to study the effects of biomaterials on neutrophil activation. The next section of this literature review will summarize how HL-60 cells have been used as a way to model neutrophil activation by biomaterials.

2.4 HL-60 Cells as a Model of Neutrophil-Biomaterial Interactions

Literature on using HL-60 cells to study biomaterial-induced NETosis is scarce. As such, for this particular section, criteria were expanded to include other types of neutrophil activation more broadly such as apoptosis and oxidative burst.

2.4.1 Macrophage-Like HL-60 Cells

One of the only papers that used HL-60 cells as a model of NETosis on biomaterials was a recent study conducted by Clarke and colleagues. To study the impact of biomaterial surface chemistry on the release of NETs, undifferentiated HL-60 cells were incubated on poly(methyl methacrylate) (PMMA) functionalized with either carboxylic acid or amine groups[14]. The HL-60 cells were activated with 50 nM PMA over 48 hours which induced a semi-differentiation and allowed the cells to adhere to the PMMA surface. Cells incubated on aminated PMMA had higher cell adhesion and overall NETosis (as visualized using Sytox green and citH3) after 48 hours compared to HL-60 cells incubated on both carboxylated and unfunctionalized PMMA. Crucially, the ratio of NETs to total adhered cells was not statistically significant between cells on all three surfaces thus indicating the importance of adherence to overall NETosis. These results would seem to suggest that amine-functionalized biomaterials are more immune-activating than other types of functionalization[14]. This paper is unique in its approach toward HL-60 cell differentiation. Activation with PMA typically induces more of a macrophage-like phenotype as opposed to neutrophil-like which raises questions about their validity as a NET model [83]–[87]. Macrophage-like differentiated HL-60 cells were also used by Iwasaki et al when investigating the inflammatory reaction of HL-60 cells to blended 2-methacryloyloxyethyl phosphorylcholine (MPC) and poly(lactide-co-glycolide) (PLGA) polymers. The addition of MPC was found to reduce the inflammatory response as indicated by a decreased level of IL-1 beta mRNA [88]. In a separate study by Shin and colleagues, macrophage-like HL60 cells were used to study pressure regimes at the soft-tissue-material implant interface. Here, superoxide production was used as a marker of cell death with all pressures tested (5–40 mmHg) eliciting significantly less superoxide relative to controls [89]. In all of the above studies, HL-60 cells were induced to differentiate to provide a more accurate model of blood leukocytes.

2.4.2 Undifferentiated HL-60 Cells

Not all investigations use differentiated cells in their experiments as shown by Ciapetti et al who used undifferentiated HL-60 cells to investigate the in-vitro apoptosis-inducing potential of PMMA-based bone cement [38]. Undifferentiated HL-60 cells were selected alongside osteoblast-like MG-63 cells due to their sensitivity to apoptotic stimuli. The viability of HL-60 cells was reduced (down to a minimum of 50% on one material) on three of the four types of cement tested, however the MG-63 cells were more sensitive to the cytotoxic effects of the materials than HL-60s, as evidenced by an increase in DNA fragments in the medium [38]. It is difficult to directly apply this result to the in-vivo environment given the stark difference between undifferentiated and differentiated HL-60 cells. Furthermore, when considering undifferentiated HL-60 cell NETosis, a proteomic analysis of NETs by Scieszka and colleagues revealed significant differences in the expression levels of proteins known to be associated with NETs when undifferentiated and differentiated HL-60 cell NETosis was compared [90].

2.4.3 Differentiated HL-60 Cells

One of the only other studies using HL-60 cells to study NETosis in-vitro was conducted by Abri and colleagues. Specifically, a fluorinated methacrylamide chitosan (MACF) hydrogel was used to determine if neutrophil function is influenced by the presence of oxygen and/or the antibacterial agent polyhexamethylene biguanide (PHMB)[39]. The results revealed that the ability of differentiated HL-60 (dHL-60) cells to form NETs on the scaffold and in the presence of oxygen and PHMB depended on the type of stimulation. NETs were maximally produced when chemically induced with PMA as opposed to *Staphylococcus aureus*. A similar trend was observed for ROS production. This study presented an intriguing in-vitro model to study the immune response via HL-60 cells, however their quantification of NETosis was incomplete. The authors opted to use a double-stranded DNA quantification assay to quantify extracellular DNA which was used as an indicator of NET formation. While extracellular DNA is a useful NET marker, relying solely on expelled DNA is not recommended as a method of quantifying NETs as it does not distinguish NETosis from apoptosis or necrosis of the cells [91]–[93]. This is further compounded by the issue that the HL-60 differentiation process results in gradual apoptosis [94]–[97]. Indeed, the authors noticed that there was a 68% reduction in cell number upon differentiation of the HL-60 cells [39]. Cells may have

already been undergoing apoptosis before stimulation thus resulting in an overall inflated ROS and apoptosis result.

2.4.4 HL-60 Cells Compared to Neutrophils on Biomaterials

In a study by Verdon and colleagues, the following responses to nanomaterials were compared between PMNs and HL-60 cells: metabolic activity, cytokine production and cell death [40]. Interestingly, while NETs were examined in blood PMNs, the authors state that NETosis was not examined in dHL-60 cells because of the challenges associated with their suspension. This is likely an obstacle specific to the paper's experimental design and not the inability of HL-60 cells to generate NETs in-vitro. The authors present a handful of key results. NETs were released by PMNs after 4 hours of exposure to 62.5 μg/mL of silver nanomaterial (Ag) and were stained with DAPI and NE to confirm their characteristic spread and composition. Copper oxide (CuO) nanomaterials at a concentration of 62.5 μg/mL were found to reduce the metabolic activity of blood PMNs to 13% and of dHL-60 cells to 59%. Exposure to silver and CuO also increased pro-inflammatory cytokine release, mainly IL-8, in both cell types in a concentration-dependent manner. This was observed alongside a reduction in the secretion of the cytokine interleukin-1 receptor antagonist (IL-1Ra). Strikingly, zinc oxide (ZnO) nanomaterials at a concentration of 15.6 μg/mL reduced dHL-60 metabolic activity to 35% and killed the cells at concentrations over 62.5 μg/mL but had no effect on PMN metabolic activity [40]. This highlights the behavioral difference between dHL-60 cells and PMNs, something that should be considered when selecting HL-60 cells as a model for PMNs and when applying conclusions obtained from HL-60 cells to PMNs in the biomaterial environment. Indeed, several studies have reported differences between the behavior of HL-60 cells and PMNs and are cited here for reference but are, once again, outside of this chapter’s current scope ([98]–[100]). HL-60 cells and neutrophils can also be compared and contrasted based on their use in studying the mechanisms that drive NETosis. Hence, the final part of this section will focus on NETosis mechanisms and whether differences exist between HL-60 and PMN-driven NETs.

2.5 The NETosis Process in HL-60 Cells vs Neutrophils

2.5.1 The Role of Protein Arginine Deiminase (PAD4) in NETosis

PAD4 is an enzyme that converts arginine residues to citrulline on protein substrates in a process referred to as citrullination/deamination [101]. Since NETs were first identified, there has been substantial work to elucidate the role that PAD4 plays in their mechanism, and it is now widely accepted that PAD4 is vital for NETosis (thorough reviews of PAD4 activation in NETosis can be found below [102], [103]). Two of the landmark papers that studied this phenomenon utilized dHL-60 cells. In 2008, Neeli and colleagues investigated the PAD4-mediated H3 citrullination in both PMNs and dHL-60 cells exposed to CI, LPS, TNF, lipoteichoic acid, f-MLP, or hydrogen peroxide [104]. CI treatment of dHL-60 cells resulted in detectable H3 citrullination starting 15 minutes after stimulation and plateaued after 2 hours. Similar responses were observed with TNF and LPS. In PMNs, histone citrullination was also observed as early as 30 minutes after stimulation but plateaued at 3 hours. Crucially, these increases in histone citrullination did not occur during apoptosis thus demonstrating that NETosis and apoptosis are separate, distinct, processes. This paper also successfully demonstrated that PMNs respond more robustly than HL-60 at lower concentrations of neutrophil stimuli [104]. For example, PMNs responded to TNF at concentrations as low as 0.5 ng/ml while dHL-60 cells required a concentration that was four times higher (2 ng/ml). This same trend was observed for LPS (0.1 vs 1 ng/ml). In an extension of this work, Wang et al used dHL-60 cells to demonstrate that hypercitrullination of histones by PAD4 mediates chromatin decondensation [105]. Their work confirmed Neeli's observations of dHL-60 histone citrullination (both H4 and H3) after just 15 minutes of CI stimulation and demonstrated that TNF treatment of PMNs results in approximately 10% of neutrophils showing an increase in histone citrullination by 15 minutes. For their additional analysis of PAD4 activity, the authors relied exclusively on dHL-60 cells and did not confirm their results with PMNs. PAD4 activity was confirmed by inhibition with chlorine amidine which resulted in significantly decreased histone staining during stimulation. To study the effect of citrullination on nuclear structure, chromatin decondensation was analyzed through the addition of wild-type or inactivated PAD4. The addition of wild-type PAD4 generated pronounced chromatin decondensation which was not present when inactivated PAD4 was added. In an interesting sub-set of results presented by the authors, it was demonstrated that H3 citrullination was rarely observed in undifferentiated HL-60 cells despite stimulation with IL-8 and bacteria, however, it was observed

after differentiation [105]. This further supports the use of dHL-60 cells over undifferentiated cells as a model for NETosis. This paper has been cited by others as support for the notion that HL-60 cells generate fewer NETs than PMNs. While this has been observed in the literature and will be discussed in a later section of this review, it is difficult to directly compare the results in this paper given the difference in stimuli used between dHL-60 cells and PMNs [104]–[106].

In a more recent study involving dHL-60 cells and PAD4, Thiam et al performed high-resolution time-lapse microscopy to thoroughly track the NETosis process [34]. In all three cell types tested (mouse neutrophils, PMNs, and dHL-60 cells), the cellular sequence of events was largely conserved upon ionomycin stimulation. NETosis began with the rapid disassembly of the actin cytoskeleton, followed by plasma membrane vesicle shedding, endoplasmic reticulum vesiculation, nuclear rounding, and chromatin decondensation. PAD4 was found to accumulate and remain expressed in the nucleus up to nuclear rupture and was then expelled alongside NE and chromatin once plasma membrane breakdown occurred. Human PMNs did not exhibit the same form of nuclear rounding as the dHL-60 cells during DNA decondensation despite the overall similarities. This may have been due to differences in the cell type's nuclear mechanical properties. Interestingly, the authors report that after the 4-hour 4μM ionomycin stimulation, 45% of the human PMNs went on to complete NETosis as opposed to the 56% of dHL-60 cells [34]. This can be attributed to several factors including the choice of stimulus, the differentiation conditions of the HL-60 cells, and the subjectivity of defining a NETosis endpoint.

2.5.2 Signalling Pathway Receptors Involved in NETOsis

When it comes to investigating the specific role of different receptors and signalling molecules in the NETosis process, there is a significant advantage to using HL-60 cells. PMNs cannot readily be genetically manipulated; thus, HL-60 cells are often used as surrogates [107]. Several studies have leveraged this feature of dHL-60 cells. Kawakami et al studied the contribution of GTPase Rab27a to NETosis using ATRA-differentiated HL-60 cells [108]. In this work, Rab27a was found to be recruited to decondensing chromatin within 3 hours of PMA stimulation and histone release into the medium gradually increased. In dHL-60 cells where expression was knocked down, NET structures were barely visible after 4 hours of PMA treatment and this was accompanied by a decrease in ROS production. This implies that Rab27a promotes NETosis through a ROS-dependent mechanism. The authors also found that for both wild-type dHL-60 cells and PMNs, similar NET

structures and release of citH3 were observed, however, there is very little comparison of the two responses beyond this observation[108].

To confirm the role of nucleotide oligomerization domain (NOD) receptors in NETosis, NOD1 and NOD2 knockout dHL-60 cells were generated by Alyami et al [109] . When stimulated with the bacterium *Fusobacterium nucleatum* for 12 hours, these cells showed significantly fewer NETs than the controls. Further, it was observed that NOD1 but not NOD2 was associated with histone release though both receptors were equally associated with MPO and NE release as shown via ELISA. Similarly, direct inhibition of NOD 1/2 receptors in PMNs stimulated with *F. nucleatum* also resulted in reduced receptor expression and reduced IL-8 levels. However, the authors did not examine a NETosis end point in these cells and so no comparison can be made to the knock-out dHL-60s. Interestingly, in neutrophils, *F. nucelatum* upregulated NOD 1/2 receptors but stimulation with 100 nM PMA did not alter NOD1 expression [109]. This points to stimuli-specific differences in the mechanism.

In a study to understand the relationship between cellular lipid peroxidation and MPO/NE during NETosis, Tokuhiro and colleagues also leveraged HL-60 cell manipulation [110]. MPO knockout cells had suppressed lipid peroxidation and reduced NETosis when stimulated with PMA. However, NE knockout cells did not impact the degree of peroxidation or NETosis induced by PMA. Despite this, NE-deficient cells still had a reduced citH3 signal thus highlighting the differing functions of NE when compared to MPO. These two trends were also confirmed using MPO and NE knockout mice neutrophils and through direct inhibition of PMNs. While this group leveraged knock-out cells, Xu and colleagues overexpressed kindlin-3, an essential integrin activator, in dHL-60 cells to study the effect on NETosis [42]. In this short report, overexpression of kindlin-3 resulted in reduced ROS generation and NETosis, as determined by DNA fiber SYTOX quantification. An additional crucial finding of this paper was that overexpression of kindlin-3 defective in interacting with integrins still resulted in reduced ROS/NETosis thus demonstrating that the effect of kindlin-3 is independent of integrin binding. While this paper presents important findings, their quantification of NETosis via DNA fragments in solution was not very comprehensive. HL-60 cells have also been called upon to answer mechanistic questions without manipulating protein expression.

2.5.3 Adopting HL-60 Cells to Model NETosis

Other groups have also utilized HL-60 cells as a model to explore NETosis interactions. To determine the impact of circulating IgG on NET formation, Lu and colleagues used dHL-60 cells pre-treated with components of IgG. The authors found that the IgG1 and IgG2 subclasses as well as the IgG Fc fragment were capable of augmenting PMA-stimulated NETs in dHL-60 cells. This was found to be via the specific engagement of FcyRIII and the Syk-ERK-NF-κB pathway that activates the transcription factor NF-κB [111]. This aligns with the results previously mentioned in section 2.3.2 where the Fcγ RIIIb activation pathway was found to be involved in NETosis on small fibre PDO templates. Notably, however, the concentrations of IgG used were below levels found in human serum, so this remains to be explored in further detail. Furthermore, whether the Syk-ERK signaling pathway can induce the activation of PAD4 is currently being investigated [111]. Another group has also explored the interaction of immune system components with NETs in dHL-60 cells. Mendes et al found that the monoclonal antibody 2C5 had a strong specificity towards dHL-60 generated NETs both in static and dynamic flow conditions and argue it could be used as a tool to identify and target NETs for therapeutic intervention [112].

2.5.4 Comparing HL-60 and PMN Responses

Section 2.4 of this chapter has already commented on some of the direct differences observed in the NETosis response between HL-60 cells and PMNs [34], [104], [105]. There are, however, some papers that are better suited to their own section as they more directly compare the two. In another study by Manda-Hadzlik and colleagues, dHL-60 cells failed to release NETs upon stimulation with reactive nitrogen species whereas PMNs responded vigorously and generated NETs over 3 hours (Figure 2.7 and Figure 2.8) [113]. In one of the sole papers aimed at characterizing the suitability of dHL-60 cells as a model for PMNs, Yaseen et al analyzed the antibacterial response to *S. aureus* in dHL-60 cells and PMNs [106]. This study revealed that after a 4-hour stimulation with *S. aureus*, only 28% of dHL-60 cells released NETs as opposed to almost 100% in the PMN sample. A similar trend was observed with PMA stimulation where NET formation was evident by 2 hours and complete by 4 in PMNs, but dHL-60 cells released significantly fewer NETs at both time points. Three groups mentioned in this chapter have all observed that the NETs released by dHL-60 cells are shorter and less diffuse than those released by neutrophils. Overall, however, many papers do not

directly draw comparisons between the NETosis response in HL-60 cells and PMNs despite the fact that many utilize both types of cells in their analysis[42], [100], [104]–[106], [112].

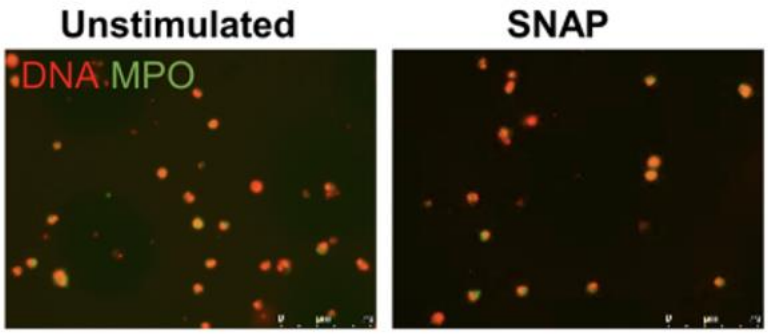

Figure 2.7: dHL-60 cells fail to release NETs when stimulated with reactive oxygen nitrogen species. (SNAP: S-Nitroso-N-acetyl-DL-penicillamine, a nitric oxide donor added to generate reactive nitrogen species) (adapted from Manda-Hadzlik et al, open access article) [113].

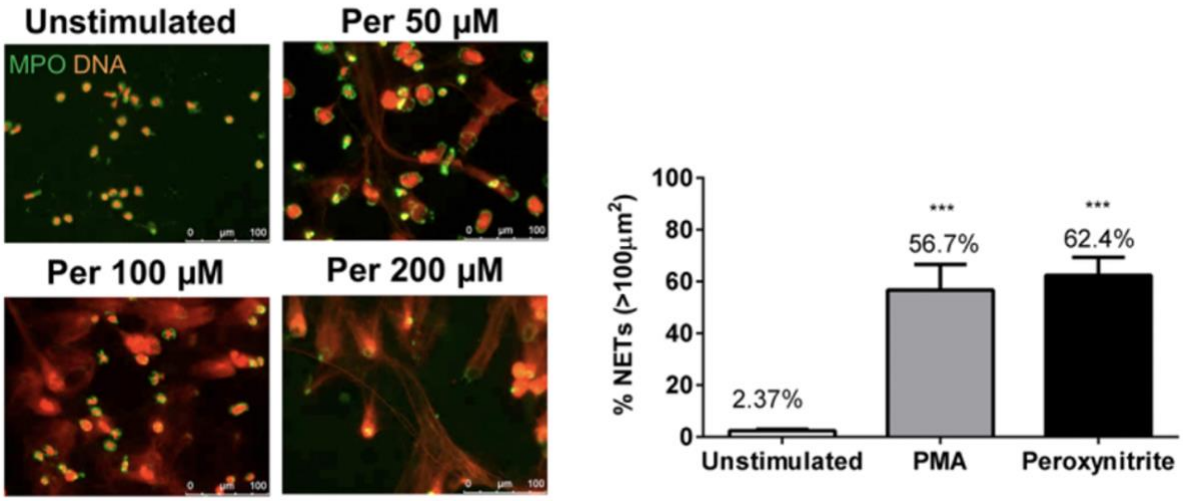

Figure 2.8: PMNs release NETs in the presence of reactive nitrogen species at levels similar to those induced by PMA. (Adapted from Manda-Hadzlik et al, open access article). PER: Peroxynitrate [113].

2.6 In-Vitro Flow Models

Studying the effect of dynamic flow conditions on cells and tissue components requires the use of an in vitro model that is capable of simulating a variety of physiological flow rates and shear stresses. Commonly used systems include the cone and plate, the rotating disk, microfluidic devices, and parallel plate flow chambers.

2.6.1 Cone and Plate Model

Cone and plate systems consist of a stationary plate and a rotating cone, creating a defined shear rate in the sample. The sample fluid is placed in the plate, and the rotation of the cone generates a shear force that causes the fluid to flow. The viscosity can be calculated from the shear stress (from the torque) and the shear rate (from the angular velocity) (Figure 2.9). These devices are often used to measure the viscosity and rheology of fluids but can also be used to study cell behaviour under flow [114]–[117]. While useful for cell studies, this model often requires larger sample volumes in order to obtain accurate measurements [118].

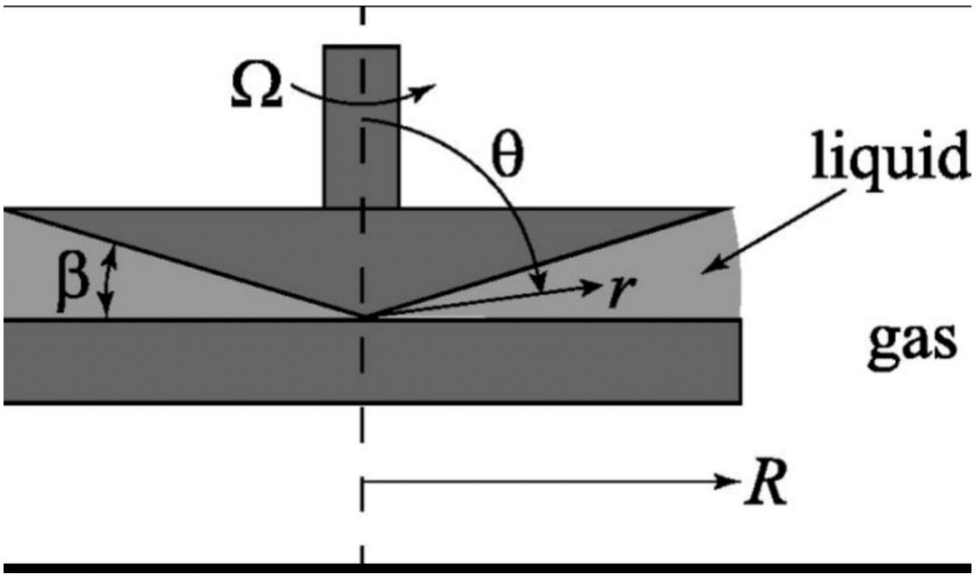

Figure 2.9: Schematic of a cone and plate system. The cone rotates with an angular velocity (Ω). Reproduced with permission [115].

2.6.2 Rotating Disk

Rotating disc systems are used to measure the flow properties of fluids under shear (Figure 2.10). The instrument consists of a circular disk that is rotated at a constant angular velocity while immersed in the fluid being studied. The fluid forms a thin layer on the surface of the disk, and the shear rate is varied by adjusting the speed of rotation of the disk. The shear stress exerted by the fluid on the disk is measured using strain gauges or other sensors attached to the disk, which convert the mechanical deformation of the disk into an electrical signal that can be recorded and analyzed. Coating the surface of the disk with a layer of extracellular matrix proteins or other adhesion molecules allows for cells to be cultured on the disk and subjected to controlled shear stresses that mimic physiological conditions. The cells can be observed, and their behavior analyzed using various techniques. The system has been used to study the effect of shear stress on cell adhesion, migration, proliferation, and differentiation, as well as to investigate the mechanisms underlying these cellular responses [119], [120]. While advantageous for certain types of studies, the system's flow patterns, and shear rates can be challenging to control and the model operates at a relatively low throughput.

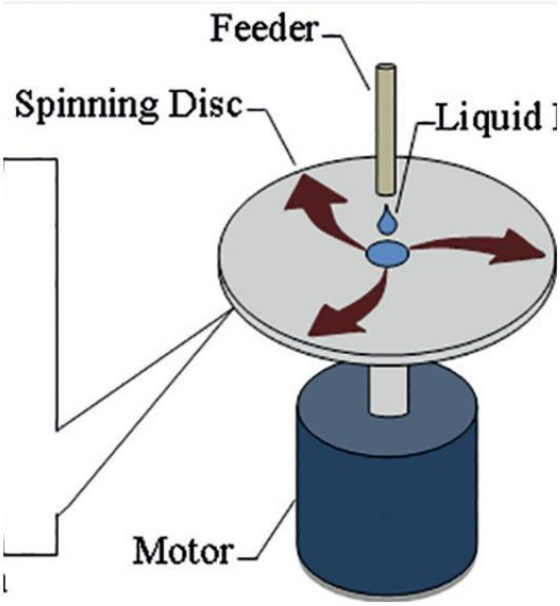

Figure 2.10: Schematic of a rotating disk system [116]. Open access article.

2.6.3 Microfluidic System

Microfluidic devices are miniaturized systems that use microfabrication techniques to control and manipulate small volumes of fluids in channels and chambers on the micrometer to millimeter scale. These devices typically consist of a network of channels, valves, pumps, and sensors etched onto a substrate such as glass or silicone. They can be adapted to study cell adhesion, migration, and cell signaling [121], [122]. A common material used in the fabrication of microfluidic devices is silicone rubber polydimethylsiloxane (PDMS), an inexpensive and relatively biocompatible material [123]. The advantage of such systems is that they are highly adaptable and multiple channels on the same device can be modified to run parallel experiments simultaneously under different shear conditions. Furthermore, microfluidic models allow for small volumes to be used. As a disadvantage, these models can generate shear stress gradients (despite the often-precise control over the fluid) that can affect cell behavior and introduce variability in experimental results [124]. Also, they have limited scalability, accessibility, and standardization when it comes to studying blood-biomaterial interactions.

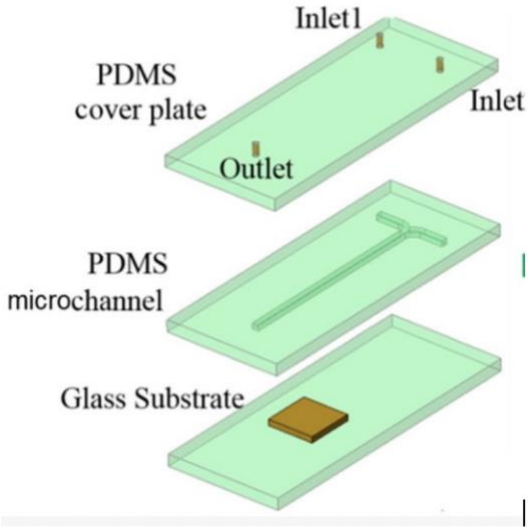

Figure 2.11: Schematic of a PDMS microchannel (adapted from [121], open access article).

2.6.4 Parallel Plate Flow Chamber

Parallel plate flow chambers have been widely used in biomaterial studies [125]–[127]. A circular parallel plate flow chamber typically consists of two parallel plates (typically made of glass

or plastic) that are circular in shape and sandwich a circular flow channel between them. The flow channel has an inlet and an outlet, and the fluid (usually a buffer or cell culture medium) is pumped through the channel at a controlled rate to generate a defined shear stress on the cells (Figure 2.12). The overall chamber environment may also be equipped with other components, such as temperature and gas controllers, to maintain a stable and controlled environment for the cells during the experiment. The flow chamber can produce a constant shear rate from 1 to 10^4 s^{-1} and does not require large volumes thanks to a syringe or roller pump that provides continuous re-circulation [128]. The parallel plate chamber can house a variety of biomaterials and cellular monolayers. For the purposes of this investigation, the chamber was well-suited to house a disc of silicone material. Furthermore, the parallel plate made it possible to effectively study the effect of constant shear stress on the neutrophil's capacity to generate NETs over the longer periods of time required for NETosis and supported by continuous re-circulation with the syringe pump.

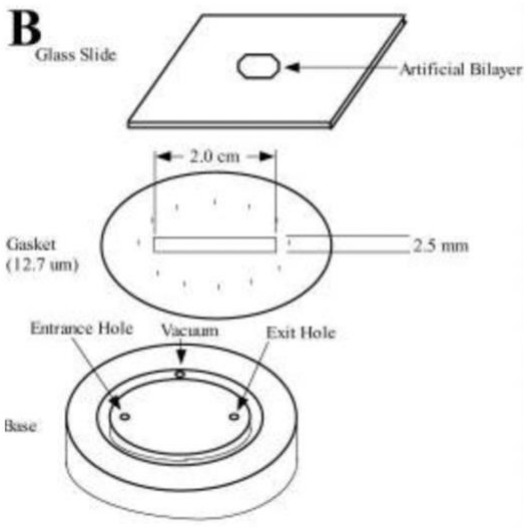

Figure 2.12: Schematic of a circular parallel plate flow chamber [126] Open access article.

2.7 Conclusion

Neutrophil extracellular traps are web-like structures released by activated neutrophils. They are composed of granule proteins (MPO and NE) as well as DNA and they play a crucial role in the immune response against pathogens. Dysregulation of NETs can lead to exacerbation of the inflammatory response. The importance of NETs in driving the immune response towards

biomaterials has become increasingly clear in recent years. NETs can be studied in static conditions on biomaterials and under shear via the use of various shear-generating devices. Identification of NETs may be done visually using microscopy and NET marker expression can be further quantified using flow cytometry. So far, only a handful of groups have explored the direct impact of biomaterials on NETosis in-vitro. Those findings have demonstrated that surface properties, topography and modifications can modulate NETosis in various inflammatory conditions. It has also become evident that the time frame during which NETs are generated on biomaterials depends on both the material properties and the inflammatory stimulus [64]–[66], [70], [74]–[77]. The study of neutrophil activation, and more specifically NETosis, has also employed HL-60 cells in their various forms. Undifferentiated, neutrophil, and macrophage-like HL-60 cells have been used in-vitro to model biomaterial responses. In general, undifferentiated HL-60 cells release NETs less effectively than dHL-60 cells and have different properties upon activation [38], [90]. The similarity between dHL-60 and PMNs has resulted in their use for understanding the mechanisms of NETosis, particularly through genetic manipulation. While the use of HL-60 cells has aided in identifying key players in the NETosis pathway (including PAD4, NOD receptors and Rab27a), their sensitivity to stimuli and the overall response observed differs from PMNs [34], [42], [104]–[106], [108]–[110], [113]. This difference in response appears to be highly stimulus-specific and it cannot be said with certainty that HL-60 cells will generate equivalent NETs to PMNs in every in-vitro experimental design.

Chapter 3: In-vitro model and flow cytometry analysis of HL-60 NETosis under shear conditions in the presence of a biomaterial

3.1 Introduction

Neutrophils release neutrophil extracellular traps (NETs) as a defense mechanism against invading pathogens. While this is meant to be a protective mechanism, recent research has suggested that NETs may also contribute to a range of inflammatory and autoimmune diseases [1], [2]. As a result, there has been increasing interest in studying NETs and their role in disease pathogenesis and potential therapeutic interventions to target these structures. Studying neutrophil extracellular traps (NETs) under flow conditions is essential as it allows for the simulation of the physiological conditions under which NETs are formed in vivo. In the body, NETs are produced by neutrophils and are released into the bloodstream. Blood flow exerts shear forces on cells and the extracellular matrix, which can affect the formation, structure, and function of NETs [3], [4]. By studying NETs under flow conditions, the effect of shear stress and flow dynamics on the properties of NETs (their size, shape, stability, and composition) can be examined. This information may help better understand the mechanisms of NET formation and the role they play in various inflammatory conditions. Furthermore, studying neutrophil extracellular traps (NETs) on biomaterials is also crucial as it allows for a deeper understanding of the interactions between NETs and the surfaces of medical devices and implants. When biomaterials are implanted or inserted into the body, they come into contact with blood and tissues, and this can trigger an immune response that involves the formation of NETs [5]– [12]. These NETs can adhere to the surface of cardiovascular biomaterials and contribute to inflammation and thrombosis on the biomaterial surface. Cardiovascular biomaterials can be composed of metals, polymers, or diamond-like carbon. While some are permanent, others are made to be bioabsorbable over time (specifically those made of polymers). These materials must be stable under exposure to shear and limit inflammation. A truly biocompatible cardiovascular material does not exist and therefore designs focus on minimizing complications [7].

In-vitro, NETs can be generated by synthetic stimuli like phorbol 12-myristate 13-acetate (PMA) or by physiological stimuli such as calcium ionophore (CI), interleukin-8 and N-formylmethionyl-leucyl-phenylalanin (fMLP). PMA is a potent chemical stimulator that stimulates

NETosis by inducing reactive oxygen species (ROS) production, calcium influx, and the activation of downstream signaling pathways. These pathways include protein kinase C (PKC), Raf/MEK/ERK, and p38MAPK. Downstream activation of these pathways results in cytoskeleton changes and alterations in nuclear envelope structure that allows for the expulsion of chromatin from the nucleus [13]–[15]. In a similar manner, fMLP (a bacterial-derived chemotactic) is thought to trigger a ROS cascade via the activation of the protein nicotinamide adenine dinucleotide phosphate oxidase (NADPH oxidase), leading to NET release [16][17][18][19][23].

HL-60 cells are a human promyelocytic leukemia cell line commonly used in biomedical research, and are an attractive research alternative for blood-isolated cells because they can be induced to differentiate into various types of myeloid cells, including neutrophils [19], [20] [24]–[26]. HL-60 cells can be differentiated into neutrophil-like HL-60 cells (dHL-60) using dimethyl sulfoxide over five days [17]–[19]. The exact mechanism by which DMSO induces differentiation is not fully understood however it is thought to involve several signaling pathways and transcription modulation. DMSO has been shown to downregulate the c-myc gene resulting in terminal differentiation [20], [21]. DMSO has also been shown to suppress proliferation by activating the tumor suppressor PTEN, known to arrest proliferation during the G1 cell phase [22], [23]. Yet another implicated signaling pathway is the Wnt/B-catenin pathway whose activation via DMSO contributes to the final neutrophil-like phenotype of dHL-60 cells [24]. Differentiation of HL-60 cells can be confirmed using several markers. Undifferentiated HL-60 cells express high levels of CD71, also known as transferrin receptor 1 (TfR1), on their surface as they are rapidly dividing and require it for proliferation. Following differentiation, CD71 levels decrease [25], [26]. Differentiation also results in the up-regulation of the surface marker CD11b, a crucial protein involved in adhesion and activation [26]. Once differentiated, HL-60 cells can be activated by a variety of stimuli, resulting in an increase in CD11b expression on the surface of cells so that they can carry out their immune response, and an increase in degranulation [27], [28]. Degranulation can be measured by CD63, a protein marker that is translocated from the dHL-60 granule membrane to the cell surface. In addition, dHL-60 cells can generate NETs upon stimulation with PMA [29], [30]. Clarke and colleagues present one of the only papers that use HL-60 cells specifically as a model of NETosis on biomaterials, finding that undifferentiated HL-60 cells incubated on poly (methyl methacrylate) (PMMA) functionalized with amine groups had elevated levels of cell adhesion and overall NETosis

compared to cells on carboxylated PMMA [31]. HL-60 cells were also the main model used by several groups to identify the role of PAD4 in the mechanism of NET release [32], [33].

Flow cytometry has been used as an analytical tool for HL-60 cells. It can confirm the differentiation of cells by quantifying surface proteins [34]. In addition, HL-60 phagocytosis, apoptosis, and ROS production have all been measured using flow cytometry following activation with various stimuli and following differentiation under differing conditions [29], [34]. HL-60 chemotaxis and rolling have been studied by exposing cells to shear-biomaterial models prior to analysis by flow cytometry to quantify and examine the expression of surface migration and adhesion proteins [26], [35]. While NETs can be quantified by flow cytometry using fluorescently labeled antibodies against NET components including myeloperoxidase (MPO) and citrullinated histone (citH3) [8], [34]–[36], for NETosis in dHL-60s, only one study used flow cytometry with citH3 being the sole marker examined [29]. The various properties of HL-60 cells have been leveraged to study both the mechanisms of NETosis and biomaterial-induced NETs in different environments. Despite this work, no study has examined biomaterial-induced HL-60 NETosis in a shear environment, nor have any utilized a full panel of NET markers on flow cytometry to fully characterize and quantify NETosis in this model cell line.

Parallel plate flow chambers are in vitro systems used to study cell populations under flow conditions that mimic physiological shear stresses [34] [35], [36][43]. The effect of shear and biomaterial on neutrophils has been explored by other groups using flow generating devices. Tomczok and colleagues exposed PMNs to different biomaterials under shear and found that adhesion of activated PMNs was significantly greater on hydrophilic surfaces as opposed to hydrophobic. They also observed that PMN migration on the biomaterial surfaces varied depending on the material [36]. On polyether-urethane urea (PEUU), Shive et al noted that shear induced neutrophil apoptosis [37]. Transient exposure to high mechanical shear stress has also been found to increase neutrophil activation, aggregation, and phagocytic ability [38]. Despite investigations like these into PMN activation in the presence of shear and a biomaterial, gaps in knowledge remain. Specifically, PMN NETosis has been primarily investigated on biomaterials only under static conditions and has not been explored under shear [12], [39], [40]. NETs have also been found to have prothrombotic activity due to their interaction with platelets [7]. Given the exposure of biomaterials, particularly cardiovascular ones, to shear in the body, and the contribution of NETs to immunothrombosis, it is important to understand how physiological shear modulates NETosis on biomaterials.

In this investigation, the parallel plate flow chamber made it possible to effectively study the effect of shear stress in the presence of plasma-coated biomaterial on the HL-60 cell's capacity to generate NETs over the longer periods of time required for NETosis. Silicone was chosen as our model biomaterial due to its extensive use in the medical setting, specifically in catheters and other blood-contacting devices [41]. Following exposure to the biomaterial under shear conditions with or without PMA stimulation, flow cytometry was used to quantify NETosis (via the NET markers MPO and citH3) and dHL-60 activation (via CD11b and CD63 expression). The central hypothesis of this study was that the presence of shear as an additional stimulus to the biomaterial would result in an elevated NET release compared to static samples.

3.2 Materials and Methods

3.2.1 Reagents and monoclonal antibodies

The experiments in this chapter utilized the following antibodies: PerCP-Cy™5.5 Mouse Anti-Human CD15 (BD #560828), FITC Anti- Myeloperoxidase (Abcam 11729), Recombinant Anti-Histone H3 (citrulline R2+R8+R17, Abcam 281584), Goat Anti-Rabbit IgG H&L (PE) (abcam 72465), FITC Mouse anti-Human CD11b (BD #562793), PE Mouse Anti-Human CD63 (BD #557305), PE-Cy™5 Mouse Anti-Human CD45 (BD #555484), PE Mouse Anti-Human CD71 (BD #555537). Additional reagents include RPMI Medium 1640 (1X) with 10% Fetal Bovine Serum, 0.5M EDTA, pH 8.0, DEPC-Treated (EMD Millipore #324506-100ML), X-Vivo 15 (Serum-Free, Gentamicin and Phenol Red, Lonza #04-418Q), Dimethyl Sulfoxide (DMSO, Sigma #67-68-5), Fluoroshield with DAPI (GeneTex #GTX30920), PMA (Sigma #P8139) and fMLP (Sigma, F3506-5MG). Phosphate Buffered Saline 1X (PBS) (Corning #21-040-CV).

3.2.2 HL-60 cell culture and differentiation

HL-60 cells (ATCC, Toronto, Canada) were cultured in untreated flasks with X-Vivo-15 media at 37°C and with 5% CO_2 [29]. Media was changed every 24-48 hours and cells were passaged weekly. Cells no older than 12 passages were used for experiments. Prior to experiments, cells were differentiated with 1.3% DMSO for 5 days at a concentration of 5 x 10^5 to generate neutrophil-like HL-60 cells (dHL-60) [19]. To prepare the cells for exposure to shear, cells were spun down at 1200rpm (277g) for 5 minutes to remove X-Vivo-15 and were then resuspended in RPMI with 10% FBS before counting.

3.2.3 HL-60 Shear Experiments Using the Circular Parallel Plate Flow Chamber

Glass coverslips were covered with an FDA grade silicone sheet (0.005" NRV G/G 40D 12" X 12" (SMi). The following conditions were tested: silicone without plasma, silicone coated with platelet-poor plasma and silicone coated with a combination of platelet-poor plasma and 10 mM EDTA. This study was conducted in accordance with the tenets of the Declaration of Helsinki and received ethics clearance from the University of Waterloo Human Research Ethics Committee (#44502, Waterloo, ON, Canada). To obtain plasma, blood was drawn via venipuncture from healthy donors who were medication-free for at least 3 days. Platelet-poor plasma was obtained by spinning down donor blood for 10 minutes at 100g, removing the top layer of plasma, and another 7378 g (10,000 rpm) centrifugation for 10 minutes to remove platelets. Silicone was incubated with 50% plasma (diluted in PBS) or with a 50% plasma/10 mM EDTA solution for 30 minutes at 37°C. EDTA, a calcium and magnesium chelator, was used to chelate the calcium ions necessary for activation of the classical and lectin complement pathways [43].

To assemble the system, coverslips (GlycoTech #31-008, 35mm diameter) were secured to a round parallel plate chamber lined with a gasket (Width 2.5 mm, thickness 0.01 in, GlycoTech #31-003). Inlet and outlet medical silastic tubing (0.062" X 0.125" (SMi)) were securely connected to the chamber ports, ensuring that no air bubbles were present. Syringes were used to draw up HL-60 cells suspended in RPMI with 10% FBS (either with or without 25 nM PMA). The syringes were connected to the inlet tubing and outlet tubing was placed in a microcentrifuge tube to allow for re-circulation of the cell suspension. The chamber system was then connected to a Cole Parmer 75900-50 programmable 6-channel syringe pump which allowed for continuous circulation. The total length of tubing in the system was 140 mm. This length was optimal for running experiments in the 37°C incubator and also prevented an excess of biomaterial surface area. The number of HL-60 cells per shear experiment to be circulated through the system was selected to be 2×10^6 based on recommendations in the literature and the parameters of the chamber [48].

The shear rate in the parallel plate flow chamber was calculated according to the equation:

$$\gamma = \frac{6Q}{wh^2}$$

where γ is the shear rate, Q is the flow rate, w is the flow chamber width and h is the chamber height. Based on the parameters described above, a flow rate of 0.78 ml/min was required to produce a shear of $500s^{-1}$. To ensure full circulation of the HL-60 cells, a volume of 1.3 mL was selected. Flow within the chamber was assumed to be continuous and experiments were run for 2 hours at 37°C. The full experimental setup is illustrated in Figure 3.1. After 2 hours, the bulk solution was then collected for flow cytometry analysis.

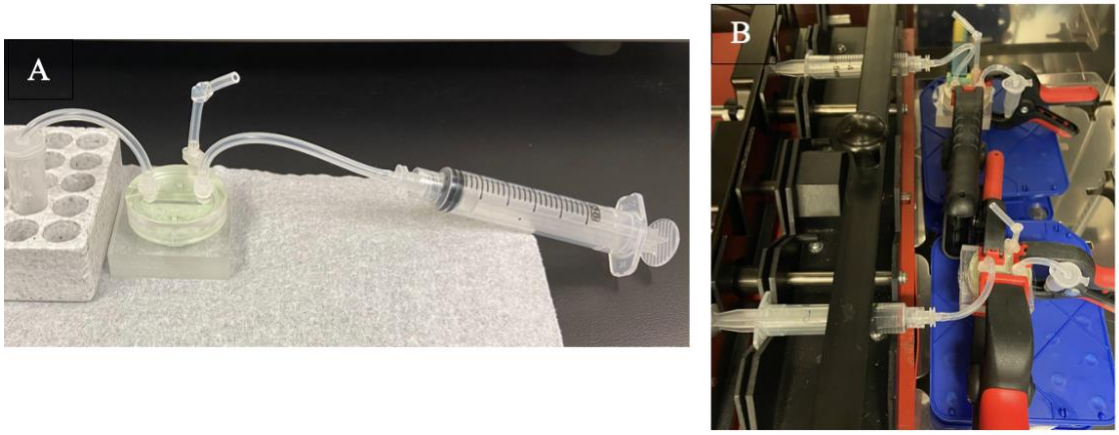

Figure 3.1: Parallel plate set up for shear experiments run with undifferentiated or differentiated HL-60 cells. A) The chamber connected to the syringe that will hold the cell suspension. Cells will flow from the syringe, through the chamber, and into the microcentrifuge tube. B) Chamber attached to the parallel plate with clamping to create a leak-proof seal. Cell suspension is circulated back and forth between the syringe and the tube via the parallel plate.

3.2.4 Controls and Experimental Conditions

Several controls were selected for these experiments. A sample was incubated without exposure to flow and without plasma or PMA for 2 hours at 37°C (negative control). Static samples were incubated in 5mL round bottom polypropylene tubes (Falcon Corning #352063) as opposed to the chamber. The chamber would not have allowed for enough volume and cells. As a positive control, a sample was incubated with 25 nM PMA for 2 hours at 37°C without plasma. To further test a more physiological stimulus, 1μM fMLP was also tested for 2 hours at 37°C. Experimental conditions were tested on both undifferentiated and differentiated HL-60 cells in order to generate a more comprehensive understanding of the HL-60 cell line as a model for NETosis. Plasma coating was included to create more physiologically relevant conditions and EDTA was also included to

explore the potential effect of complement activation on NETosis via the chelation of calcium and magnesium ions [42]. The experimental conditions tested are presented below.

Table 3.1: Experimental conditions for HL-60 cells for shear and static samples

Stimulus	**Surface Treatment**	**Abbreviation**
-	Platelet Poor Plasma	PPP
-	Platelet Poor Plasma + 10 mM EDTA	PPP/EDTA
PMA	-	PMA
PMA	Platelet Poor Plasma	PMA + PPP
PMA	Platelet Poor Plasma + 10 mM EDTA	PMA + PPP/EDTA
fMLP	-	fMLP

Cells were circulated in the presence of a stimulus: PMA (25nM) or fMLP (1 μM). PPP: platelet-poor plasma with or without 10 mM EDTA.

3.2.5 Flow Cytometry

All samples were adjusted to a cell number of 75,000 per tube by carrying out a cell count of the bulk solution following shear and prior incubation with antibodies. To assess NETosis, samples were first incubated with a primary anti-citrullinated histone (citH3) antibody for 30 minutes at room temperature. This first incubation was immediately followed by a secondary IgG PE antibody for citH3, a FITC anti-MPO antibody, and a PE-Cy™5 anti-CD15 myeloid cell identifying antibody. Samples were then incubated for an additional 30 minutes at room temperature in the dark. Following incubation, samples were washed with 1mL RPMI with 10% FBS and centrifuged at 1200 rpm for 5 minutes. The supernatant was removed, and the cells were resuspended before being analyzed immediately.

For leukocyte activation, samples were incubated with FITC anti-CD11b (Mac-1 upregulation), PE anti-CD63 (a neutrophil degranulation marker), and PE-Cy™5 anti-CD45 (a

leukocyte identification marker) for 30 minutes at room temperature in the dark, then diluted before being read immediately.

Samples were read on a four-color FACS Calibur flow cytometer (Becton Dickinson, Franklin, New Jersey, USA). Data acquisition and analysis were performed using CELL-Quest software (Becton Dickinson). Results are expressed as total fluorescence (geometric mean fluorescence of the detected antibodies) and the fluorescence of a sub-group of HL-60s that have undergone NETosis (known as marker 1 or M1 cells).

3.2.6 Apoptosis Protocol

To determine if HL-60 cells had undergone or were undergoing apoptosis, the FAM-FLICA Poly Caspase Assay (FAM fluorescent-labeled inhibitors of caspases) (ImmunoChemistry Technologies Catalog #92) was used. The protocol was followed according to the manufacturer's instructions. Briefly, FLICA was diluted 1:5 and added to each sample at 1:30 followed by a one-hour incubation. Cells were washed three times with 1X apoptosis buffer. Samples were labelled with Propidium Iodide and immediately analyzed using flow cytometry.

3.2.7 Immunofluorescent Microscopy

To assess adherent cells on the silicone biomaterial, the nuclear DNA stain 4′,6-diamidino-2-phenylindole (DAPI) was used. At the end of the experiment, the silicone sheet was removed from each flow chamber slide with tweezers and placed in a well plate. 200 μL of PBS was added over top of the samples before immediately staining with DAPI for 2 minutes. The slides were gently tilted to allow the PBS and DAPI to slide off before the silicone was removed using tweezers and inverted onto a glass slide. Slides were imaged using a TE2000-S microscope and photos were acquired using the NIS-Elements AR Nikon program (Nikon, Melville, New York, USA).

3.2.8 Statistical Analysis

All results are reported as the mean ± standard deviation (SD). For cell apoptosis assays, a parametric paired t-test was used to determine significance. To analyze the percentage of cells in the NETosis region, independent t-tests were used. To determine the effect of shear and dHL-60 activation via PMA on both NETosis and additional dHL-60 activation markers, a two-way ANOVA was conducted followed by simple main effects posthoc test with a Bonferroni correction. A p-value

of less than 0.05 was required for statistical significance. The number of experiments was always equal to three.

3.3 Results and Discussion

3.3.1 HL-60 cell populations

In this study, differentiation of the cells was confirmed via a decrease in CD71 expression (CD71 expression level on undifferentiated and 5 day differentiated cells were 84 AFU and 27 AFU respectively) [25]. However, when dHL-60 cells were analyzed by flow cytometry, all samples demonstrated a double population as illustrated in Figure 3.2. Following stimulation with PMA, the number of cells shifting size and granularity and found in the region R2 (see Figure 3.2) increased, suggesting that healthy cells in the R1 population that underwent NETosis changed size scatter and contributed to the cell population found in the R2 region. The R2 population of cells displayed FSC and SSC characteristics of apoptotic cells (a reduction in cell size as indicated by low FSC and enhanced granularity as indicated by higher SSC). To further characterize the nature of this second population, apoptosis levels in dHL-60 cells were assessed by flow cytometry.

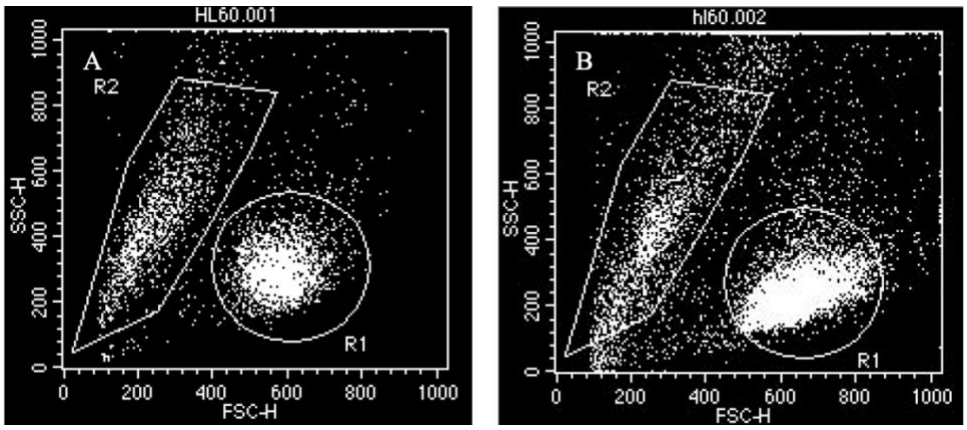

Figure 3.2: Representative images of the two distinct dHL-60 cell populations present during analysis with cytometry. **Size scatter dot plots of a control/unstimulated cell sample (A) and of cells stimulated with 25nM PMA (B). The R1 region represents a healthy population of dHL-60 cells as determined by the characteristic FSC (forward scatter – related to cell size) and SSC (side scatter – related to cell granularity). The R2 region outlines the second, unidentified, population of cells.**

3.3.2 HL-60 cells undergo apoptosis during differentiation

Apoptosis levels were determined using caspase (apoptosis marker) and propidium iodide (secondary necrosis and necrosis marker). Cells that stained positive for caspase but negative for propidium iodide were identified as apoptotic cells while those that stained positive for both markers were identified as having undergone secondary necrosis. Details of analysis are provided in Figure 3.3 and illustrates the increase in apoptosis and secondary necrosis induced by PMA stimulation as well as the presence of cells undergoing apoptosis in day 5 of differentiation even in the absence of stimulation.

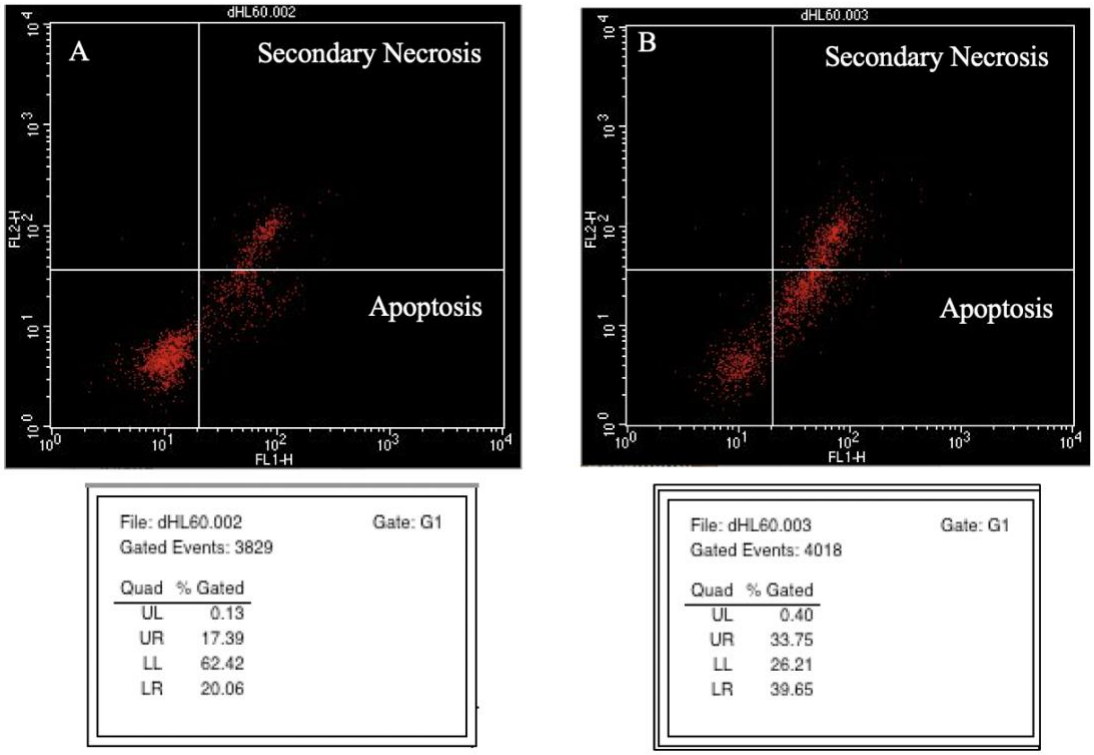

Figure 3.3: Representative image of dHL-60 cells analyzed by flow cytometry to characterize apoptosis. A) unstimulated dHL60 cells, differentiated for 5 days. B) Day 5 dHL-60 cells following PMA (25nM) stimulation for 2 hours. FL1 channel: Caspase (casp) and FL2 channel: Propidium iodide (PI). Three distinct cell populations can be identified: healthy ($casp^-/PI^-$) in lower left quadrant (LF), apoptotic ($casp^+/PI^-$) in lower right quadrant (LR) and secondary necrotic ($casp^+/PI^+$) in upper right quadrant (UR). No cell displayed the necrosis phenotype ($casp^-/PI^+$) in upper quadrant (UL). The percentage of the total number of gated cells that is present in each quadrant is obtained from the quadrant statistics.

Undifferentiated HL-60 cells were found to have a very low level of apoptotic cells. Over the course of differentiation with DMSO, the percentage of cells that were positive for apoptosis markers increased but not significantly (Figure 3.4A). The flow cytometry analysis also confirmed that cells present in the R1 region were non apoptotic cells while cells in the R2 region were undergoing apoptosis or were necrotic. By day 5 of differentiation, approximately 10 to 15% of HL-60 cells were apoptotic. Over the course of differentiation, secondary necrosis increased significantly by day 5 ($p=0.0138$) to more than 20% (Figure 3.4B). In the literature, Guo et al report a percentage survival rate of around 90% on day 5 following differentiation with DMSO. They noted a steep drop in survival only following day 5, however, while they mentioned using an apoptosis Annexin V staining kit, it is unclear from their results whether this value considered both apoptosis and cell death [29]. In another study by Waters, necrosis was identified through a trypan blue exclusion cell count and 30-35% of cells were identified as dead cells by day 5 of differentiation with DMSO [43]. This is in line with our results as just over 20% of differentiated cells were found to be dead by day 5, as identified by a PI+ signal. Waters' study did not use flow cytometry to quantify cell death which may account for some of the difference in the findings. Our results thus indicate that both apoptotic and dead cells are present at day 5 of differentiation in the experimental cell population. Following 25 nM PMA stimulation, apoptosis and secondary necrosis increased to approximately 30% and 50% respectively (Figure 3.4), doubling these populations compared to unstimulated dH-L60 cells. This indicates, that while PMA is a known NET inducer, some dHL-60 cells were likely undergoing apoptosis, as opposed to NETosis, during PMA stimulation. How these cell populations responded to shear and a NET inducer in the presence of a biomaterial was then examined in both undifferentiated and differentiated HL-60 cells.

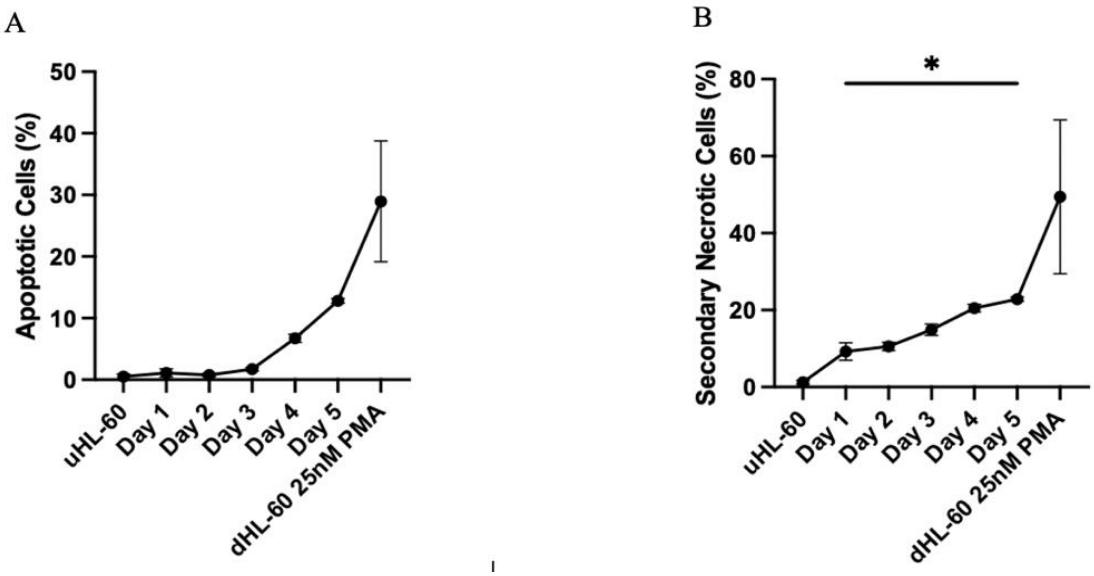

Figure 3.4: Apoptosis (A) and secondary necrosis (B) of HL-60 during differentiation and following stimulation with 25nM PMA for 2 hours. * $p < 0.05$ (parametric paired t-test). mean standard ± deviation, n = 3.

3.3.3 Undifferentiated HL-60 cells fail to generate NETs

No NETosis and no changes in HL-60 activation phenotype (as measured by CD11b and CD63) were observed when undifferentiated cells were exposed to shear. Additionally, when undifferentiated HL-60 cells were stimulated with 25nM PMA for 2 hours, both static and parallel plate chamber samples failed to generate NETs: MPO and citH3 expression on HL-60 cells did not increase significantly between samples (Table 3.2). Furthermore, PMA failed to activate HL-60 cells as indicated by a lack of CD11b upregulation and no change in the CD63 degranulation marker (Table 3.3). Clarke and colleagues generated NETs by stimulating undifferentiated HL-60 cells with PMA between 6 and 48 hours, much longer than what was used in this investigation [31]. With respect to CD11b, undifferentiated HL-60 cells increase their expression of CD11b only over stimulation with PMA for several days as reported by two separate groups [44], [45]. Stimulation with PMA (primarily to differentiate HL-60 cells into macrophages) has also been shown to not alter CD63 expression over time [25]. Our results presented in Tables 3.2 and 3.3 thus concur with prior work, as 25nM PMA stimulation for two hours is insufficient to generate significant changes in CD11b, CD63 and NET signals. The presence of shear did not contribute to further activation of the

undifferentiated HL-60 cells. It is interesting to note that CD63 expression was somewhat downregulated under shear conditions, even in the presence of PMA (though this was not significant). No studies have yet examined HL-60 response (both in terms of activation and degranulation) under this level of shear stress therefore further investigation into the HL-60 response to shear is required to draw conclusions.

Table 3.2: Expression of NET markers MPO, citH3, and myeloid cell identifying marker CD15 on HL-60 cells following 2 hour incubation under static condition and with silicone in flow chamber at 500s-1 with or without PMA (25nM).

Sample	**MPO (AFU)**	**citH3 (AFU)**	**CD15 (AFU)**
Static	12.7 ± 0.5	1.7 ± 0.2	234 ± 163
PMA Static	12.0 ± 0.6	1.4 ± 0.2	221 ± 182
Shear	11.9 ± 1.3	1.4 ± 0.1	233 ± 158
PMA Shear	13.1 ± 1.6	1.4 ± 0.1	310 ± 184

Results are reported as mean of total arbitrary fluorescence units (AFU) and standard deviations. n=3.

Table 3.3: Expression of leukocyte activation markers CD11b, CD63, and CD45 on HL-60 cells following 2-hour incubation under static condition and with silicone in flow chamber at 500s-1 with or without PMA (25nM).

Sample	**CD11b (AFU)**	**CD63 (AFU)**	**CD45 (AFU)**
Static	12.0 ± 1.3	23.0 ± 7.6	23.7 ± 8.4
PMA Static	11.8 ± 1.6	21.0 ± 6.7	28.0 ± 11.0
Shear	11.7 ± 1.9	15.6 ± 4.2	14.3 ± 5.7
PMA Shear	12.3 ± 2.7	16.3 ± 5.2	11.6 ± 3.0

Results are reported as mean of total arbitrary fluorescence units (AFU) and standard deviations. n=3.

3.3.4 Identification of dHL-60 cells undergoing NETosis using a histogram marker

Experiments with dHL-60 resulted in significant NETosis; a comprehensive flow cytometry analysis was developed to characterize NETosis, which was identified by expression of MPO and citH3 on dHL-60 cells. To determine which population displayed signs of NETosis, the two separate populations were first examined independently as shown in Figure 3.5. Both cell populations identified in the R1 and R2 regions (Figure 3.5A) were confirmed to stain positive for the leukocyte identifying marker CD15 (Figure 3.5B). Very few PMA-stimulated dHL-60 cells in the R1 region ("healthy" cells as identified in section 3.3.3) exhibited signs of NETosis, as shown by the few events seen in the upper quadrant of Figure 3.5C. On the other hand, PMA-stimulated dHL-60 cells in the R2 region (which was identified as containing apoptotic and secondary necrotic cells earlier) displayed significant signs of NETosis as shown by the high expression of MPO and CitH3 on the cells (upper quadrant in Figure 3.5D). This highlights how eliminating the R2 population would remove a prominent NET population and thus, in this study, R1 and R2 populations were examined in combination (Figure 3.5E).

Note that while apoptosis has been identified before during differentiation of HL-60 cell as discussed in section 3.3.2, the presence of this second population has not been reported in flow cytometry and as far as we know has not been considered while assessing NETosis in dHL-60 cells. Only one study has previously examined dHL-60 cell NETosis using flow cytometry and in that case, only citH3 expression was examined under static conditions [29]. Day 5 DMSO-differentiated and X-vivo cultured HL-60 cells were stimulated with 100nM PMA over 4 hours and the authors reported a singular population of dHL-60 cells as shown in Figure 3.6, with box region indicating the cells that the authors believe to be NET-positive (slightly above the HL-60 population) [29]. The "damaged" dHL-60 cell population identified in our study has a lower size scatter and size threshold settings may have excluded this population when examining dHL-60 NETs by flow cytometry. While Guo et al authors identified a potentially NETosis-positive region via their gating strategy, a significant number of NETosis events may not have been included. While this had not been previously noted for dHL-60, others have previously commented on how neutrophils undergoing NETosis displayed size scatter characteristics that are very different than healthy neutrophils and one has to be very careful when gating cell population as NETosis can easily be underestimated [46].

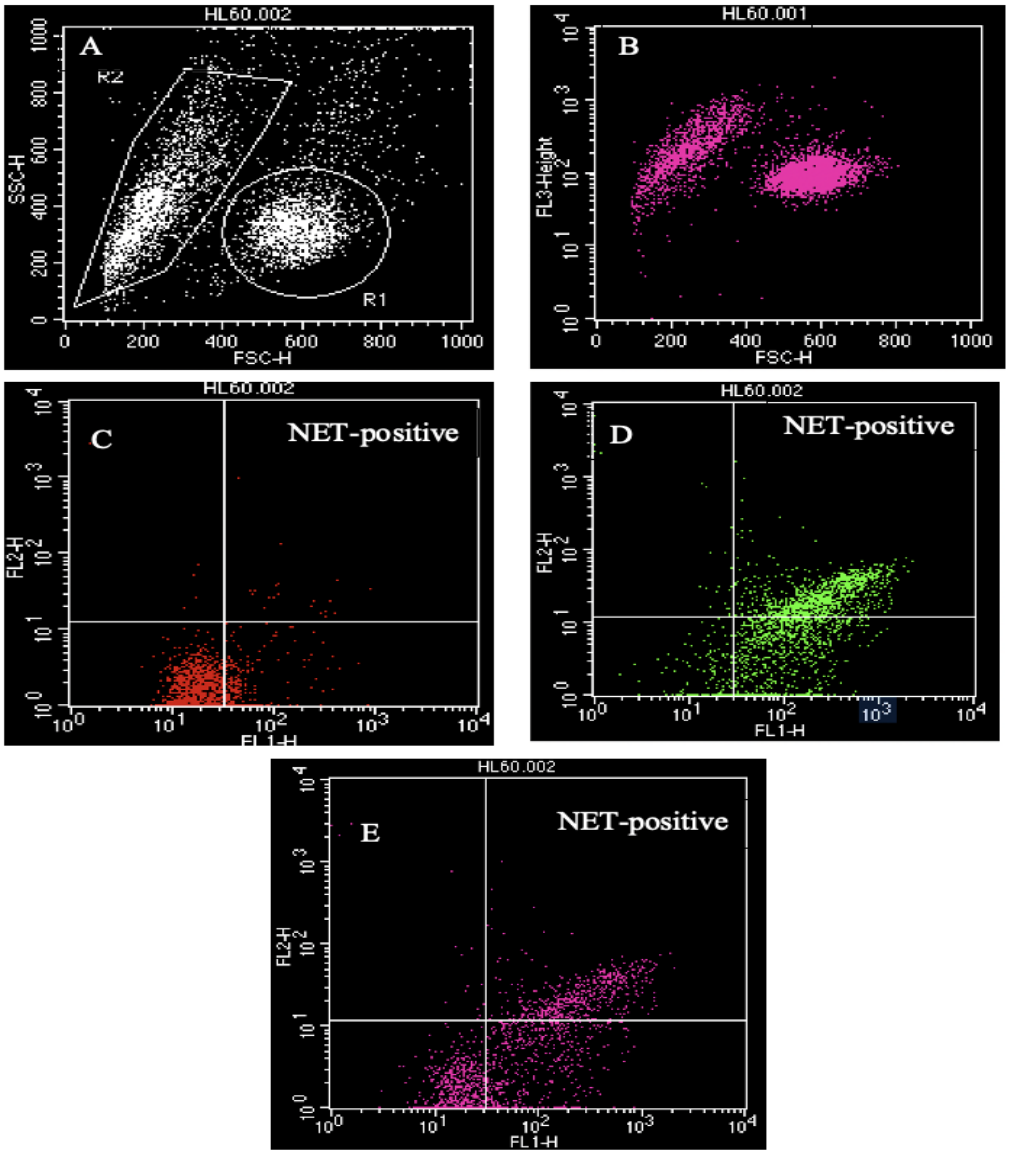

Figure 3.5: Representative flow cytometry plots of dHL-60 staining positive for the presence of NETs, as identified by expression of MPO (FL1) and citH3 (FL2). A) Size scatter of dHL-60 with the double cell population. B) Cells in R1 and R2 stain positive for CD15, a leukocyte marker. In dot plots C to E, cells found in the upper right express both MPO and citH3, markers of NETs. C) R1 cells are rarely NET-positive even following PMA stimulation. D) R2 cells have a high number of NET-positive events. E) Combining R1 and R2 incorporates both the healthy and damaged population to obtain a full representation of distribution of cells staining positive for NETs.

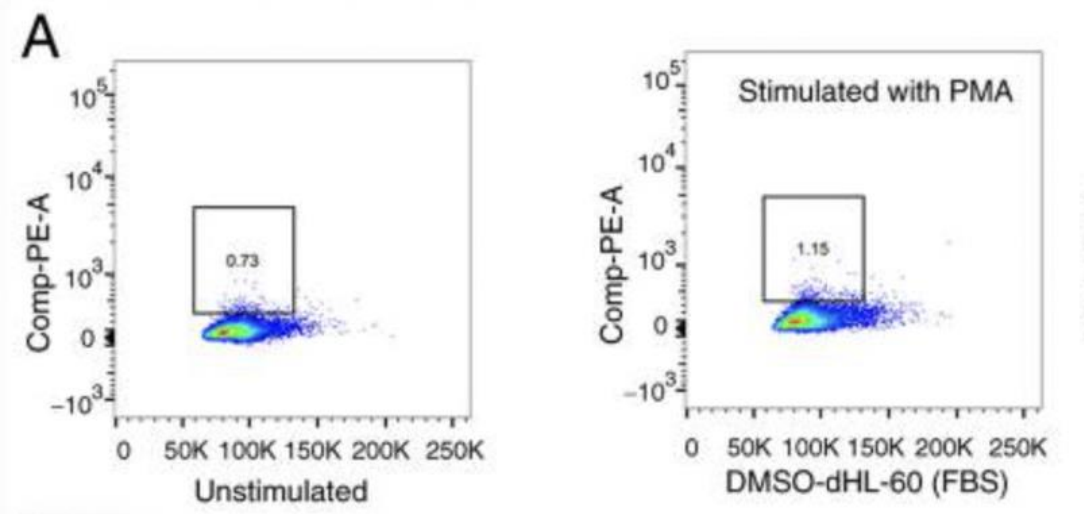

Figure 3.6: HL-60 cell population in an unstimulated and PMA-stimulated sample by Guo and colleagues (open access article) [27]. Comp-PE-A indicates the fluorescence level of citH3.

For all flow cytometry analysis, to ensure a comprehensive analysis of the dHL-60 cell response to PMA stimulation and shear, cells present in R1 and R2 were included, and all results presented are based on this selected total cell population. To improve identifying NETs on dHL-60 cells on the flow cytometry data, a histogram marker (M1) was used when analyzing fluorescent levels of the NET marker (MPO in FL1 and citH3 in FL2), as shown in Figure 3.7. M1 was used to report the "NET signal" more accurately and focus on cells that were positive for the markers of NETosis, ie cells strongly expressing MPO and citH3. The histogram statistics (data table displayed in Figure 3.7) provided the mean fluorescence ("Geo Mean") for cells in M1 as well as the percentage of population within this marker; these values were used as a mean to characterize NETosis in our dHL-60 samples.

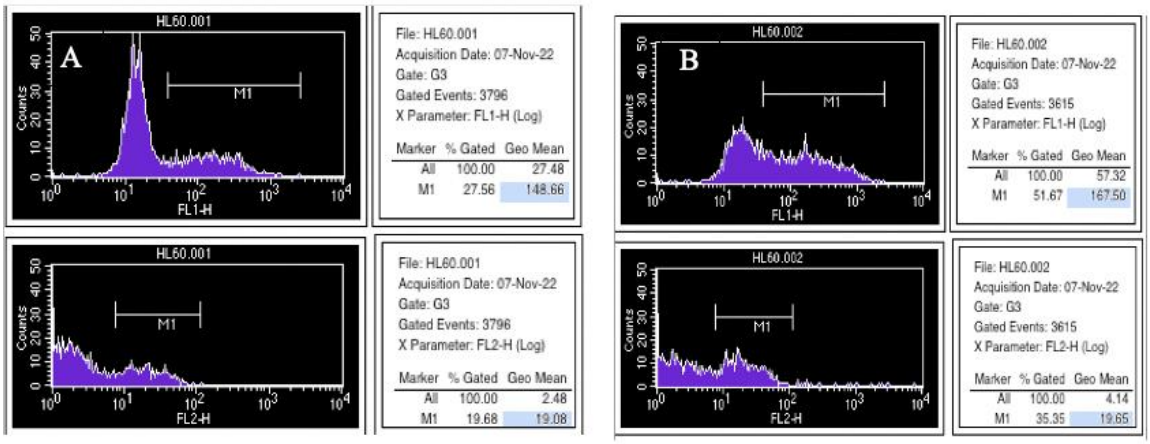

Figure 3.7: M1 marker established for cell analysis. The top two histograms represent the FL1 channel for MPO, and the bottom two panels represent the FL2 channel for citH3. A) Representative panel for an unstimulated, static sample of dHL-60 cells. B) Representative image of the M1 marker following activation with 25nM PMA for 2 hours. Stimulation with PMA results in a greater number of cells with high fluorescence for MPO and citH3. The corresponding histogram statistics tables report the fluorescence value and event number for M1 under the marker column.

3.3.5 Exposing dHL-60 to shear increase NETosis

As shown in Figure 3.8A, the percentage of dHL-60 cells staining positive (ie high FL intensity, as identified by M1) for NET markers MPO and citH3 was not significantly different among any of the control static samples, indicating that less than 20% of cells underwent NETosis in the static control sample even when stimulated with PMA. When examining fluorescence intensity levels of static samples, PMA stimulation did not significantly increase MPO expression (Figure 3.8B), nor did it increase the citH3 signal (Figure 3.8C). The lack of NETosis in PMA-stimulated samples may be explained by the lower concentration of PMA and shorter stimulation times compared to other studies. Studies have previously utilized higher PMA concentrations with dHL-60 cells to trigger significant increases in MPO expression in NETosis [22], [27], [47]. In the case of Lee and colleagues, this included ranges of 100-400nM of PMA [22]. If such high concentrations were used in this investigation, increased NETosis would have been observed in the static control samples, however, it would have been more difficult to detect the effect of shear on samples given that such high concentrations of PMA have been reported to kill dHL-60 cells [48], [49]. Higher concentrations of PMA have also been used to stimulate NET-associated citH3 release. Guo and

colleagues reported that 50nM PMA stimulation for 2 hours resulted in significantly greater citH3 expression in static samples of DMSO-differentiated dHL-60 cells. Similarly, Yoshii and colleagues stimulated dHL-60 cells for 4 hours with 100nM PMA to trigger higher NETs release (as quantified via citH3 expression) in ATRA-differentiated dHL-60 cells. One may note that while few dHL60 cells exhibited signs of the NETosis in the control sample in the absence of plasma, MPO expression was the highest of all conditions. At this time, it is not clear what would explain such phenomena. The reduced MPO expression in the presence of plasma in the static control may be explained by the presence of heparin in the plasma (as blood was anticoagulated with heparin). Heparin has been shown to result in the degradation of NET structures in previous work [50], [51]. It is also possible that some of the plasma proteins present have a protective effect and reduce NETosis.

Exposing dHL-60 cells to shear regardless of biomaterial conditions and the presence of PMA (plasma-coated or uncoated silicone, with or without PMA) resulted in a significant increase in the number of cells exhibiting markers of NETosis (staining positive for CitH3 and MPO; figure 3.8A) when compared to all control static samples ($p<0.05$). As opposed to static control samples, the presence of PMA led to increased NETosis when combined with shear and exposure to biomaterial. Plasma coating appeared to increase the number of cells exhibiting signs of NETosis, and while this may suggest that interactions with adsorbed proteins on the surface may increase NETosis, results did not reach statistical significance. Under shear conditions, minimal changes were observed in expression of MPO and citH3 on dHL-60s showing signs of NETosis (Figure 3.8B and C), indicating that the NET structures were similar across all shear samples. While the results did not reach yet statistical significance and will require additional experiments, there appeared to be a trend whereby higher number of dHL60 cells exhibited signs of NETosis when interacting with plasma-coated silicone under shear (both with and without PMA), suggesting that dHL-60 cells interactions with adsorbed proteins on the biomaterial plays a role in inducing NETosis.

Altogether, our results suggest that exposing dHL-60 to shear in the presence of a biomaterial such as silicone increased NETosis and the presence of plasma proteins on the surface can further trigger mechanisms of NETosis in dHL-60 cells. As the effect of shear had not yet been explored with NETosis in dHL-60, these findings provide a valuable contribution to the existing literature on DMSO differentiated HL-60 cells.

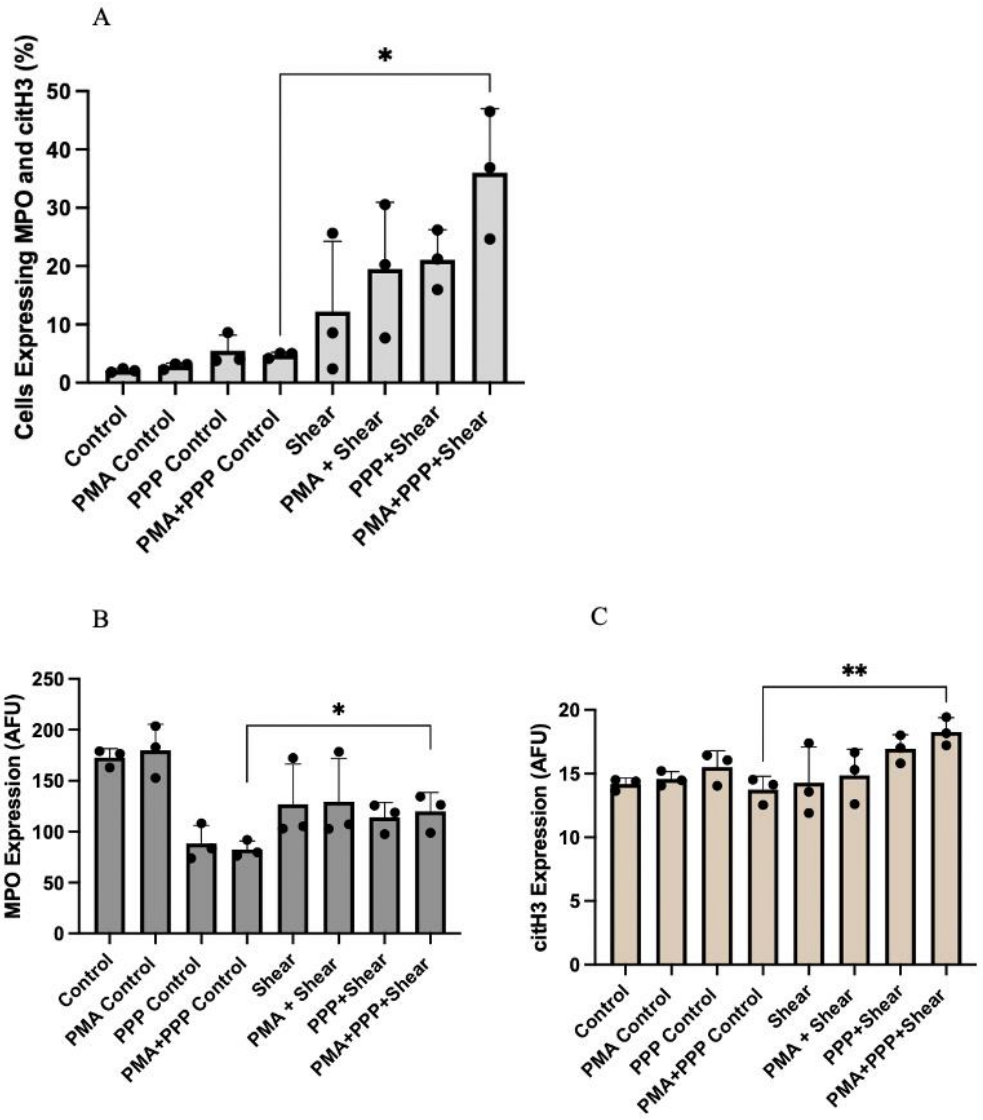

Figure 3.8: A) Percentage of cells showing high level of expression of both MPO (FITC) and citH3 (PE). C) Mean fluorescence of MPO and D) Mean fluorescence of citH3 for static control and samples incubated in the presence of shear with plasma-coated or uncoated silicone. * statistically significant, $p < 0.05$ and ** $p < 0.01$. n = 3, mean ± standard deviation. All experiments were run for 2 hours. PMA: 25nM PMA, PPP: platelet poor plasma, shear: 500s^{-1}.

3.3.6 NET Structures aggregate on the biomaterial

NET structures were identified using DAPI, a stain for genetic material, on both the plasma-coated (Figure 3.9C and D) and non-coated silicone (Figure 3.9A and B) after exposure to shear. The

non-plasma coated silicone had fewer NETs than plasma-coated silicone. Interestingly, non-PMA stimulated samples still demonstrated some signs of NETosis at the biomaterial surface both with and without plasma (10A and 10C), suggesting that material-interaction under shear conditions induced NETosis. Immunostaining with antibodies against MPO and citH3 will be required to confirm the presence of NETs in the biomaterial surface.

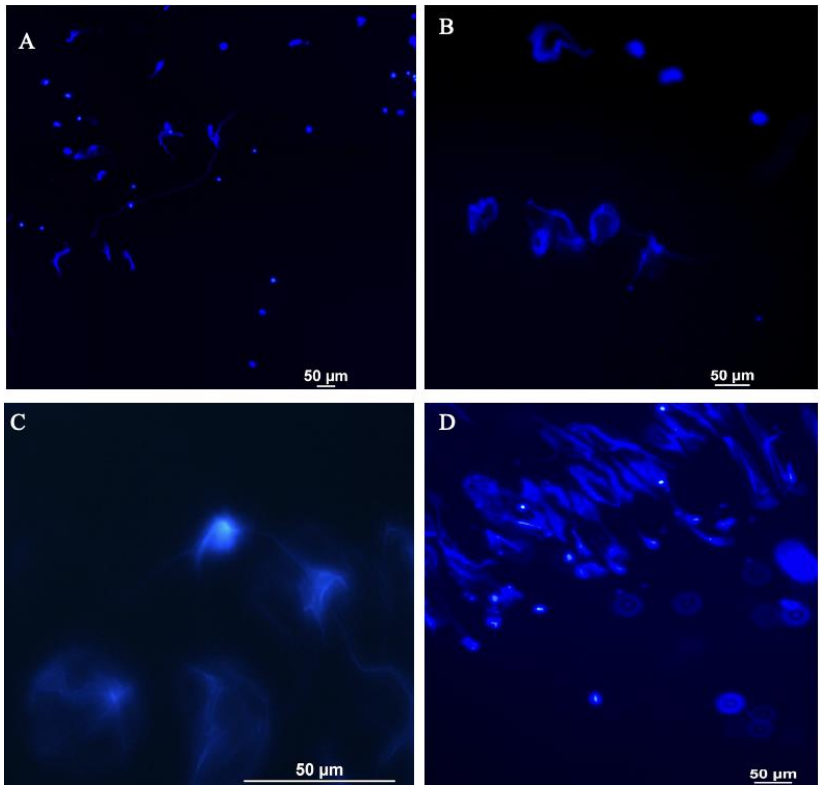

Figure 3.9: DAPI staining of the silicone surface after exposure to shear. A) without plasma coating (Shear), B) PMA-stimulation and without plasma coating (PMA+Shear), C) with plasma coating (PPP+Shear) and D) PMA-stimulation and with plasma coating (PMA + PPP+Shear). PMA-stimulation: dHL-60 cells were resuspended in medium containing PMA (25nM) and were circulated on silicone surfaces for 2hr at 37°C in parallel plate flow chamber at 500s^{-1}.

3.3.7 Shear increases dHL-60 activation (as indicated by CD11b)

In the static control samples, 25nM PMA stimulation was insufficient to significantly increase CD11b expression. As with NETosis, this is likely due to the combination of a low PMA concentration and only two hours of stimulation. CD11b upregulation in dHL-60 cells has only been

observed upon PMA stimulation with concentrations that are eight times greater than what was used in this investigation [52].

Compared to the static control samples, significant CD11b upregulation was observed on dHL-60 cells exposed to plasma-coated silicone under shear conditions regardless of plasma coating or PMA stimulation (Figure 3.10), indicating that shear substantially affected material-induced CD11b upregulation on dHL-60 cells. Interestingly, shear had not been found to result in significant CD11b upregulation in a previous study [53]. However, dHL-60 cells in this previous study were only exposed to shear for 10 minutes in a cone and plate model at a greater shear than in this investigation [53]. The extended period of shear used in this study may play explain the difference in results.

Interestingly, CD11b expression decreases albeit not significantly between PPP+Shear and PMA+PPP+Shear conditions. Stimulation with PMA would be expected to increase CD11b expression however dHL-60 cells may be internalizing CD11b in the presence of shear and increase stimulation. In a previous study where leukocytes were exposed to a similar shear stress and incubation time but were activated with fMLP, it was observed that shear reduced fMLP-induced CD11b integrin activation [54]. While this study used PMNs as opposed to HL-60 cells, dHL-60s have equivalent receptors. The response observed to PMA under shear may be operating by a similar mechanism.

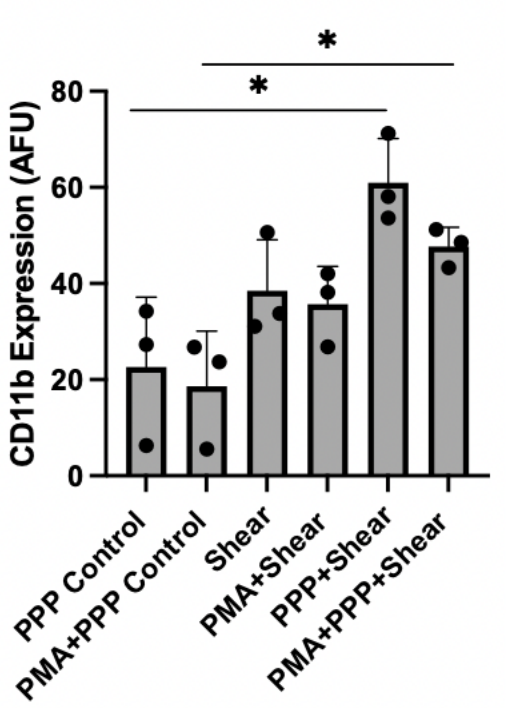

Figure 3.10: CD11b expression on dHL-60 cells in static control and samples incubated in the presence of shear with plasma-coated or uncoated silicone with or without 25nM PMA after 2hr incubation.* statistically significant, $p < 0.05$. mean ± standard deviation, n = 3. PMA: 25nM PMA stimulation, PPP: platelet poor plasma.

3.3.8 Shear increases HL-60 degranulation (as indicated by CD63)

To further examine material-induced dHL-60 degranulation under shear and static conditions, CD63 was selected. CD63 is translocated from the granule membrane to the cell surface, interacting with other proteins, making it a suitable marker for degranulation [55].

As is seen in Figure 3.11, dHL-60 cells exposed to plasma-coated silicone under shear exhibited significantly greater CD63 expression compared to the control static conditions ($p<0.05$). In both the static control sample and in the samples exposed to shear, stimulation with PMA failed to increase CD63 expression even in the presence of plasma. This result is somewhat unanticipated as PMA stimulation has been shown to increase dHL-60 degranulation. However, previous work utilized much greater concentrations of PMA (upwards of 100nM) to stimulate this response [56]. The lack of increased degranulation in the presence of PMA under both static and shear conditions may suggest

that a greater concentration of PMA in combination with shear or the presence of additional blood components like platelets (to interact with neutrophils and increase activation) on the surface may be required to trigger additional degranulation when exposed to the biomaterial.

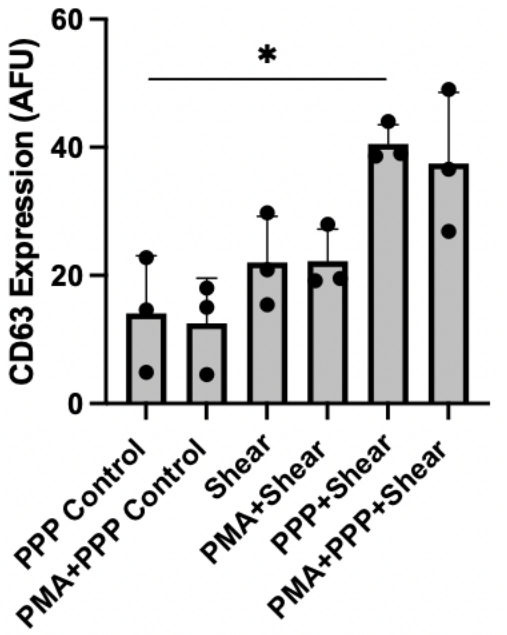

Figure 3.11: CD63 expression on dHL-60 cells in static control and samples incubated in the presence of shear with plasma-coated or uncoated silicone with or without 25nM PMA after 2hr incubation.* statistically significant, $p < 0.05$, $n = 3$, mean ± standard deviation. PMA: 25nM PMA stimulation, PPP: platelet-poor plasma.

3.3.9 Inhibition of complement activation on the plasma reduces NETs formation

To begin investigating the mechanisms involved in triggering NETosis in dHL-60 cells on the biomaterial under shear conditions, the effect of EDTA was studied. Among others, EDTA blocks complement activation by chelating calcium and magnesium ions, which are necessary for the activation of the complement system [42]. To determine if complement activation was contributing to NETosis at the biomaterial surface, silicone was coated with platelet-poor plasma under shear conditions in the presence of 10mM EDTA and incubated for 30 minutes before the addition of circulating dHL-60 cells.

When cells interacted with plasma-coated silicone in the presence of EDTA (PPP/EDTA+Shear and PMA+PPP/EDTA+Shear), a significant lower number of cells exhibiting signs of NETosis ($p < 0.01$)

was observed (Figure 3.12A) when compared to PPP+Shear and PMA+PPP+Shear. The expression of MPO and citH3 on dHL-60 cells also decreased, in some cases reaching statistical significance (Figure 3.12C), when cells interacted with silicone that had been incubated with plasma in the presence of EDTA. In these experiments, activation of the complement system was blocked by EDTA, and thus activated complement proteins were not adsorbed on the plasma-coated silicone. Our results would thus suggest that dHL60 cell interactions with adsorbed complement activation products on the surface play a significant role in triggering NETosis and extensive NET release. Inactivation of complement on the surface may have led to reduced neutrophil interactions with complement plasma proteins, thus limiting the NETosis response and creating smaller NET structures with reduced marker expression. During complement activation, C3 is cleaved into C3b and C3a. The C3b and iC3b can bind or adsorb to biomaterial [55]. There are several pieces of evidence that point to C3 playing a key role in NETosis. In a study by Yipp and colleagues, C3 knockout mice failed to generate NETosis, and their ability was restored upon the addition of C3-containing serum [56]. Furthermore, Palmer and colleagues found that the addition of an antagonist that prevented C3b detection reduced bacteria-induced NETosis [57]. In another study, in PMA-activated human neutrophils, beads coated with C3b not only resulted in significantly greater levels of NETs but also accelerated the NETosis process [58]. PMA-activation of neutrophils also results in the release of C3 from neutrophil granules (that dHL-60 cells also contain). The decoration of NET structures with C3 has also been shown to protect them from degradation [59], [60]. Given these established interactions between C3 and NETs, the reduced levels of NETosis observed on dHL-60 cells following interactions with surfaces that had incubated with plasma in the presence of EDTA suggest that surface interactions with complement activation products play a significant role in material-induced NETosis in dHL60 cells.

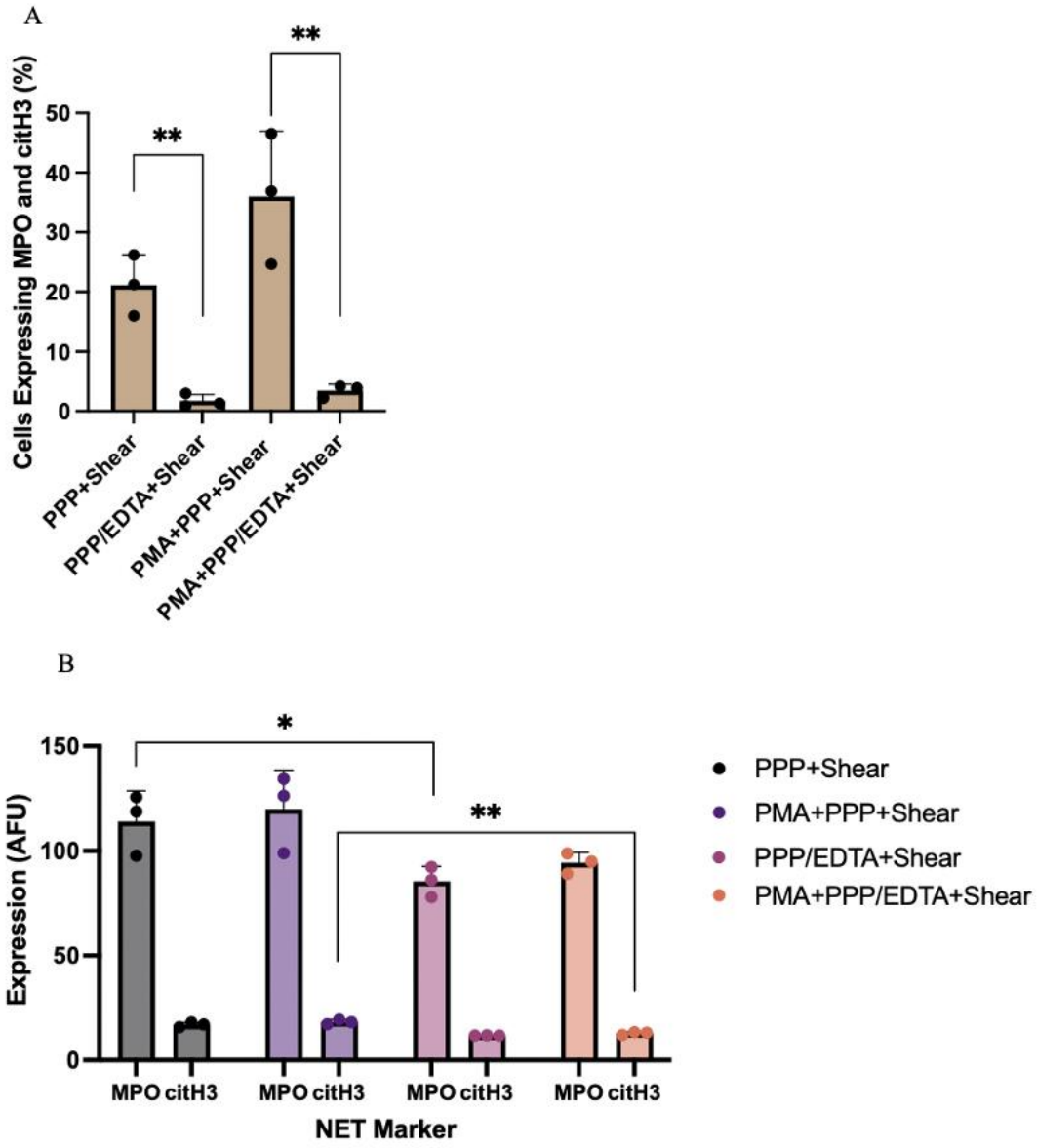

Figure 3.12: Percentage of cells showing high level of expression of A) MPO (FITC) and B) citH3 (PE). C) MPO (FITC) and citH3 (PE) expression on dHL-60 cells following 2-hour exposure to silicone with plasma with or without 10mM EDTA. * Statistically significant, $p < 0.05$ and ** $p < 0.01$. n=3. PMA: 25nM PMA stimulation, PPP: platelet poor plasma, PPP/EDTA: platelet poor plasma with 10mM EDTA.

3.3.10 Inhibition of complement activation on the surface by EDTA decreases dHL-60 activation and degranulation

When platelet-poor plasma-coated silicone was incubated with 10 mM EDTA, and dHL60 cells were then circulated over this surface, as observed with NETosis, dHL-60 activation (CD11b – Figure 3.13A) and degranulation (CD63 – Figure 3.13B) decreased significantly. The presence of PMA to stimulate did not affect outcomes, which is not surprising as PMA stimulation had no effect on CD11b upregulation and degranulation on dHL60 cells as discussed in sections 3.3.7 and 3.3.8. The significant reduction in CD11b and CD63 on dHL-60 suggest that interactions with adsorbed complement proteins on the biomaterial surface play a significant role in degranulation and activation of dHL-60 under shear conditions.

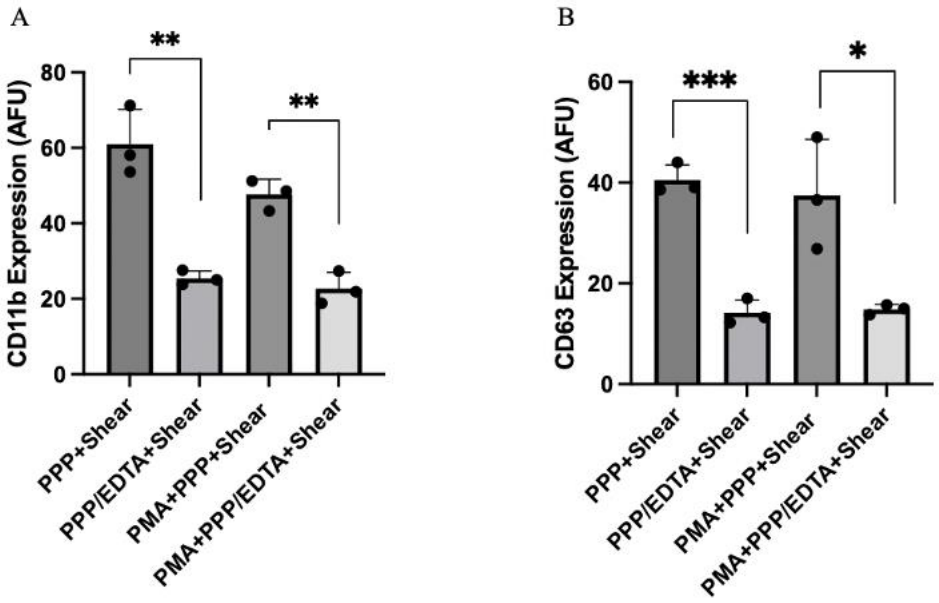

Figure 3.13: CD11b (A) and CD63 (B) expression on dHL-60 cells following 2-hour exposure to silicone with plasma with or without 10mM EDTA.* indicates p < 0.05, ** indicates p < 0.01, and * indicates p<0.001. The mean values illustrated are for samples that were run n = 3. PMA: 25nM PMA stimulation, PPP: platelet-poor plasma, PPP/EDTA: platelet-poor plasma with 10mM EDTA.**

3.3.11 Additional gating does not alter major trends

As is seen in Figure 3.5A, there are clusters of cells outside of the gate that includes R1 and R2. To determine if these cells were also contributing to the NETosis level observed, an additional region

(R3) was added to the gate (Figure 3.14). Figure 3.15 illustrates that some of the cells in R3 are indeed NET-positive.

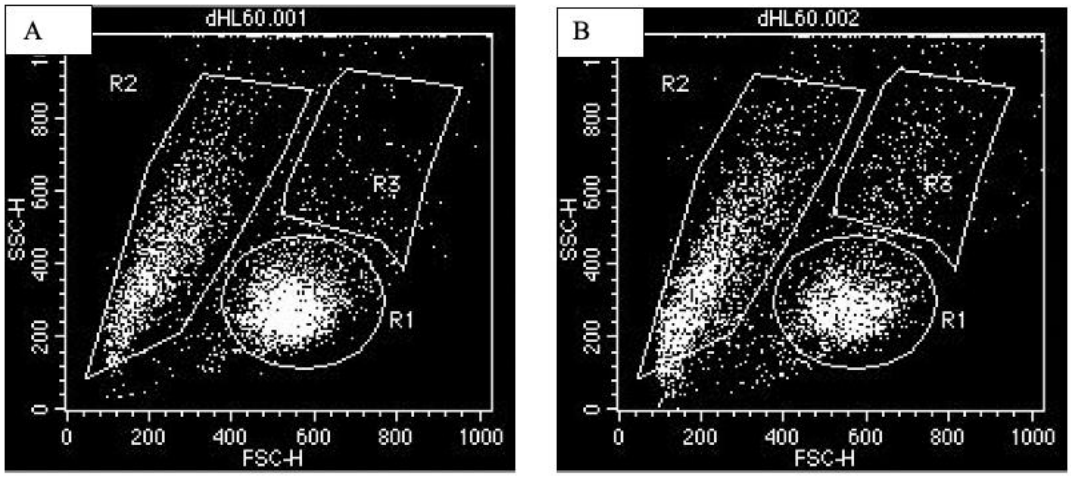

Figure 3.14: Representative images of the three distinct dHL-60 cell populations present during analysis with cytometry. Size scatter dot plots of a control/unstimulated cell sample (A) and of cells stimulated with 25nM PMA (B).

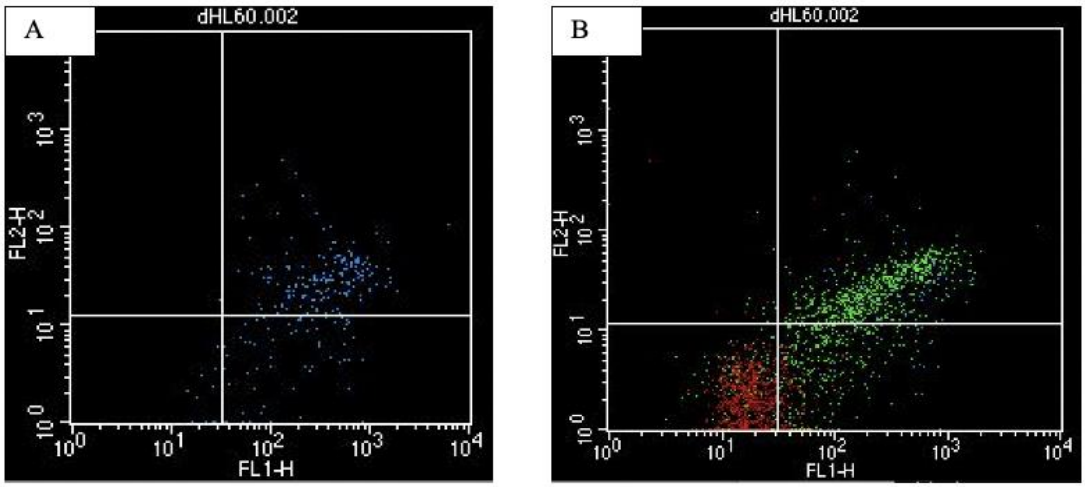

Figure 3.15: A) Cells in R3 that are NET-positive following stimulation with 25nM PMA for 2 hours. B) Overlap of all three regions (R1 in red, R2 in green, and R3 in blue) and the total distribution of NET-positive events from those regions following stimulation with PMA

When R3 is included in the gate, a similar trend of increasing NETosis under shear is observed (Figure 3.16). There is no significant change in NETosis between PMA- stimulated and

unstimulated static control samples (regardless of the presence of platelet-poor plasma). When examining fluorescence intensity levels of static control samples, PMA stimulation did not significantly increase MPO expression (Figure 3.16B), nor did it increase the citH3 signal (Figure 3.16C). This is again likely due to the low concentration of PMA.

For samples exposed to shear, those in the presence of platelet-poor plasma had elevated levels of NETosis relative to no plasma conditions, however this did not reach statistical significance. As has also been previously described, the fluorescence intensity levels of shear samples did not differ significantly (Figure 3.15B and 3.15C). With the inclusion of Region 3, NETosis increased significantly when PMA was added to plasma samples under shear (PPP+Shear vs PMA+PPP+Shear, $p = 0.016$). Despite this, both MPO and citH3 fluorescence did not differ, indicating that the NET structures remained the same between conditions. As in Figure 3.8A, there remains a statistically significant ($p = 0.0179$) increase in NETosis when plasma shear samples are compared to plasma control samples (PMA+PPP Control vs PMA+PPP+Shear). Overall, with the inclusion of R3, there continued to be a trend whereby a higher number of dHL60 cells exhibited signs of NETosis when interacting with plasma-coated silicone under shear (both with and without PMA), suggesting that dHL-60 cells interactions with adsorbed proteins on the biomaterial plays a role in inducing NETosis. Similar to section 3.3.9, the addition of EDTA significantly reduced NETosis in both PMA-stimulated and non-stimulated samples exposed to shear (Figure 3.16D). The fluorescent expression of both MPO and citH3 decreased in the presence of EDTA (Appendix Figure A.1), thereby illustrating that plasma incubation with EDTA reduced NET structure size. Graphs illustrating CD11b and CD63 expression following the inclusion of R3 can be found in the appendix.

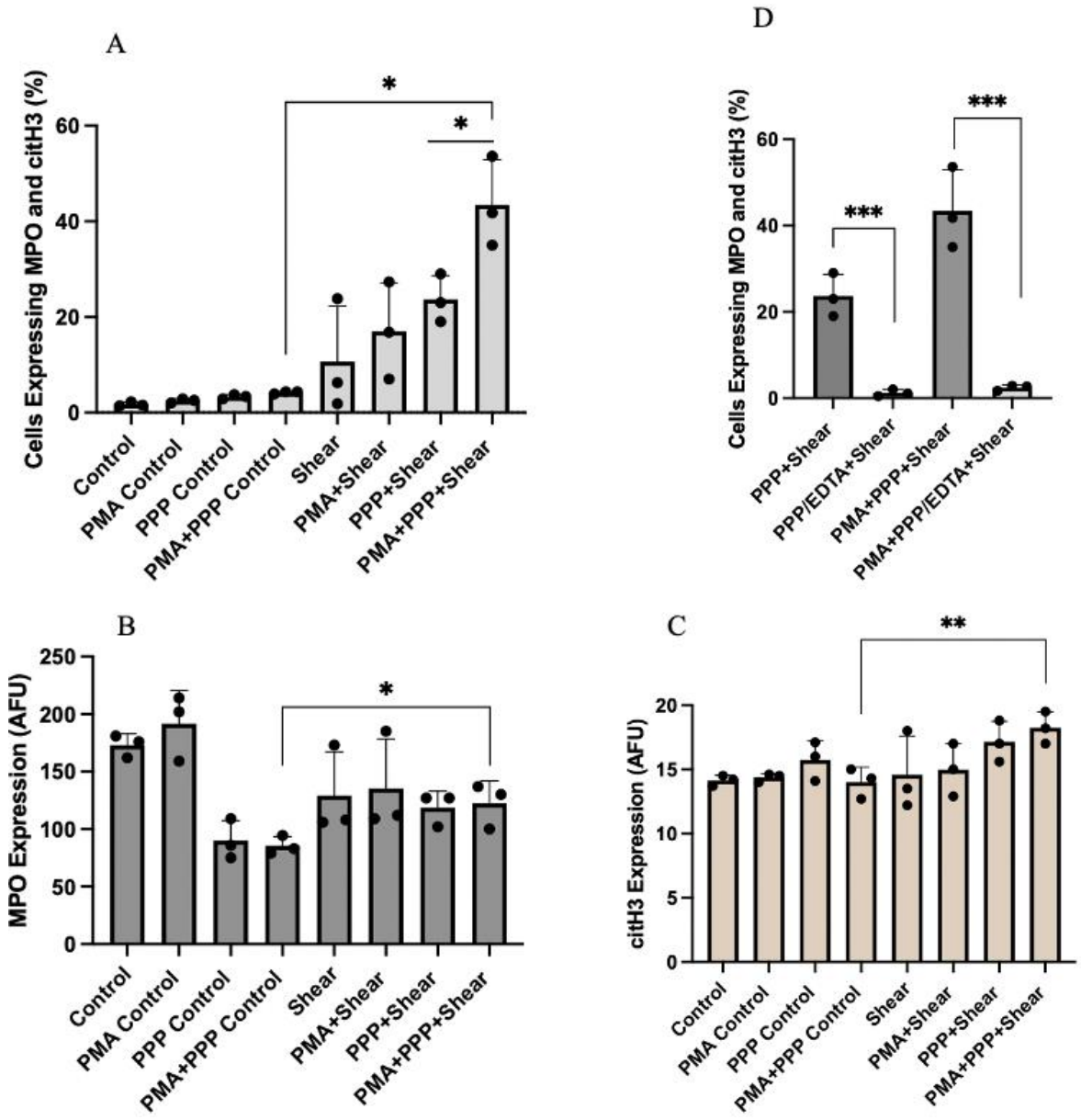

Figure 3.16: Percentage of cells showing high level of expression of both MPO (FITC) and citH3 (PE) (A). B) Mean fluorescence of MPO and C) Mean fluorescence of citH3 for static control and samples incubated in the presence of shear with plasma-coated or uncoated silicone. D) Percentage of cells showing a high level of both MPO and citH3 expression following 2-hour exposure to silicone with plasma with or without 10mM EDTA. * statistically significant, $p < 0.05$ and ** $p < 0.01$. n = 3, mean ± standard deviation. All experiments were run for 2 hours. PMA: 25nM PMA, PPP: platelet poor plasma, shear: 500s^{-1}.

3.3.12 fMLP does not trigger NETosis in dHL-60 cells

PMA is a synthetic stimulus that does not accurately reflect physiological conditions. As such, dHL-60 cells were also activated with 1μM fMLP. Results indicated that fMLP did not trigger NETosis in dHL-60 cells under any conditions (See Appendix Table A.1) This aligns with what has been observed in the literature. HL-60 cells have previously been activated with fMLP and have demonstrated an increase in cytosolic-free calcium ions necessary for activation, leading to cell migration and chemotaxis [63], [64]. The effect of fMLP on dHL-60s has related mostly to chemotaxis and despite their production of ROS (both via NADPH and through other mechanisms), no NETosis has been reported [63], [65], [66]. The results of this investigation confirm that fMLP does not induce NETs in DMSO-differentiated HL-60 cells.

3.4 Conclusion and Future Work

This study examined dHL-60 NETosis under shear and in the presence of a biomaterial. To characterize the NET response, flow cytometry was used to quantify NETosis in this model cell line. In the presence of PMA and following interactions with plasma-coated silicone under shear conditions, an increased number of dHL60 cells expressed both NETosis markers when compared to static control sample. While PMA did not have an effect, shear significantly increased CD11b and CD63 upregulation in dHL-60 cells, suggesting that mechanisms of NETosis, degranulation and CD11b upregulation differ. Inhibiting complement activation on the surface with EDTA resulted in a significant decrease in NETosis in dHL-60 cells suggesting that interactions of dHL-60 cells with adsorbed complement proteins plays a significant role in material-induced NETosis under shear conditions. Large standard deviations in flow cytometry data were often observed, and additional experiments may be required to confirm statistical trends.

To characterize dHL-60 NETosis more accurately under shear in the presence of a biomaterial, the surface of the biomaterial should also be further examined, staining NET structures with not only DAPI but also with specific NET markers such as MPO and citH3. This will help confirm the spread and aggregation of NETs by dHL-60 cells on the biomaterial surface.

When considering blood-biomaterial interactions, our current results with dHL60 cells as model neutrophils suggest that shear has the potential to significantly increase material-induced NETosis when combined with an inflammatory neutrophil stimulus (such as PMA). As such, NETs may play a

role in exacerbating biomaterial-related complications in part due to the effect of physiological shear. Further experiments with blood-isolated neutrophils will be needed to confirm these observations.

Chapter 4: Assessing the effect of shear on neutrophil NETosis in the presence of a biomaterial in the parallel plate flow model

4.1 Introduction

Neutrophils (PMNs) are the most abundant type of granulocyte in blood and are characterized by their multi-lobed nucleus and their specialized intracellular structures called granules, which are categorized into primary (azurophilic), secondary (specific), and tertiary (gelatinase). These granules house a wide array of antimicrobial substances, enzymes, and proteins that contribute to neutrophil's defense mechanisms. Primary granules, also known as azurophilic granules, contain potent antimicrobial enzymes, including myeloperoxidase (MPO) and elastase (NE), which are involved in the destruction of microorganisms. Secondary granules contain proteins such as lactoferrin and lysozyme that contribute to the neutralization of pathogens [1]. Tertiary granules, on the other hand, contain gelatinase enzymes that participate in tissue remodeling. The content and release of these granules are tightly regulated and play a critical role in the neutrophil's ability to combat infections and modulate inflammatory responses and granular proteins such as MPO, NE and lactoferrin have been found on neutrophil extracellular traps (NETs) [1].

Neutrophils release NETs as a defense mechanism against invading pathogens and while they were initially thought to be beneficial, recent research has suggested that NETs may also contribute to a range of inflammatory and autoimmune diseases [2] . As a result, there has been increasing interest in studying NETs and their role in disease pathogenesis, as well as potential therapeutic interventions to target these structures. In vitro, NETs can be generated by synthetic stimuli like PMA or by physiological stimuli such as fMLP. PMA is a potent chemical stimulator that stimulates NETosis by inducing reactive oxygen species (ROS) production [3]–[5]. In a similar manner, fMLP is thought to trigger a ROS cascade via the activation of the protein nicotinamide adenine dinucleotide phosphate oxidase (NADPH oxidase), leading to NET release [6]. Neutrophil stimulation (using PMA and other stimuli) also results in activation and degranulation which can be detected by the expression of receptors CD11b and CD63 respectively [7]–[9] [10], [11]. Current research efforts are focused on understanding the mechanisms of NET formation, identifying the role of NETs in disease, as well as understanding the interactions between biomaterials and NETs [12], [13].

Blood-material interactions refer to the complex interactions that occur between biomaterials and components of the blood when they come into contact. One key player in these interactions is neutrophils. When biomaterials are implanted or introduced into the bloodstream, PMNs are among the first cells to be recruited to the site of interaction. PMNs play a vital role in the response to biomaterials by recognizing them as foreign and initiating an immune response. They adhere to the biomaterial surface, undergo activation, and release various substances such as cytokines, chemokines, and reactive oxygen species. PMNs can also undergo NETosis at the material surface [14]. All biomaterials, both those that are bioabsorbable and those that are temporary, will trigger the immune response, however, excessive activation and prolonged PMN presence can lead to chronic inflammation, tissue damage, and impaired biocompatibility of the biomaterial [15]. Therefore, understanding the interactions between biomaterials and PMNs is essential for improving the design of biomaterials and developing strategies to modulate PMN responses for better clinical outcomes.

In recent years, there has been an increased focus on NETosis triggered upon material contact with neutrophils. On titanium, NETs were found predominantly on smooth surfaces as opposed to rough over the course of eight hours [12]. Furthermore, material stiffness has also been found to have an impact where increased NET formation and release of pro-inflammatory cytokines was observed on stiffer polydimethylsiloxane (PDMS) substrates [16]. A significantly higher amount of expelled DNA on the hydrophobic surfaces SAM-CH3 and Teflon were observed compared to the hydrophilic surfaces [17]. Other biomaterials have also demonstrated an ability to modulate NETosis including polyacrylamide (PAA) gels, graphene oxide, metal and lipid nanoparticles, and polydioxanone [18]–[21]. While several studies have highlighted the role of material topography and other surface cues on NETosis, no in-vitro study has yet investigated the mechanisms involved in material-induced activation and NETs under flow conditions.

In chapter 3, the parallel plate flow chamber was used to explore the effect of shear on NETosis in dHL-60 in the presence of a biomaterial. The results indicated that there was an effect of shear on overall NET release. Ultimately, HL-60s are a model cell line that only mimics neutrophils. To determine if blood-isolated PMNs would react to the presence of shear and a biomaterial in the same way as dHL-60 cells, PMNs were used in the same in vitro model than in chapter 3. In the context of blood-material interactions, the focus of the study was on PMNs in the absence of other cells in the blood system to gain a better understanding on the potential interactions and mechanisms of material-induced NETosis [22]. Following stimulation with PMA or fMLP in the presence of shear

and in the presence of silicone as our model biomaterial, flow cytometry was used to quantify the NET markers, MPO and citH3, as well as PMN activation (via CD11b and CD63 expression). It was hypothesized that contact with a biomaterial under physiological shear, and in the presence of an inflammatory mediator, would trigger NETosis as well as PMN activation to a greater extent than in the static control samples. It was also hypothesized the PMNs would react more readily to stimulation as they are known to be more reactive than dHL-60 cells [22].

4.2 Materials and Methods

4.2.1 Reagents and Monoclonal Antibodies

Neutrophil activation and NETosis were characterized using the following antibodies: PerCP-Cy™5.5 Mouse Anti-Human CD15 (BD #560828), FITC Anti- Myeloperoxidase (Abcam 11729), Recombinant Anti-Histone H3 (citrulline R2+R8+R17, Abcam 281584), Goat Anti-Rabbit IgG H&L (PE) (abcam 72465), FITC Mouse anti-Human CD11b (BD #562793), PE Mouse Anti-Human CD63 (BD #557305), PE-Cy™5 Mouse Anti-Human CD45 (BD #555484), Myeloperoxidase Monoclonal Antibody (2C7) (Invitrogen #MA1-80878), Goat anti-Mouse IgG (H+L), Superclonal Recombinant Secondary Antibody, Alexa Fluor 488 (Invitrogen #A28175) and Alexa Fluor 594 goat anti-rabbit IgG (H+L) (Invitrogen # A-11012). Additional reagents include RPMI Medium 1640 (1X) with 10% Fetal Bovine Serum, 0.5M EDTA, pH 8.0, DEPC-Treated (Millipore #324506-100ML), Fluoroshield with DAPI (GeneTex #GTX30920), PMA (Sigma #P8139) and fMLP (Sigma, F3506-5MG). Phosphate Buffered Saline 1X (PBS) (Corning #21-040-CV).

4.2.2 Neutrophil Isolation and Plasma Preparation

This study was conducted in accordance with the tenets of the Declaration of Helsinki and received ethics clearance from the University of Waterloo Human Research Ethics Committee (#44502, Waterloo, ON, Canada). To obtain neutrophils, blood was drawn via venipuncture from healthy donors who were medication-free for at least 3 days. Neutrophils were isolated using Stem Cell Technologies EasySep Direct Human Neutrophil Isolation Kit (Catalogue #19666). Blood was incubated for 10 minutes at room temperature with EDTA (1/500 diluted), EasySep Direct Human Neutrophil Isolation Cocktail (#19666C) (1/20 dilution), and EasySep Direct Rapid Spheres (#50300) (1/20 dilution). PBS with 1 mM EDTA was then added to a final volume of 10 mL and the blood was

incubated in the magnet for 10 minutes. The solution was transferred to a new test tube and incubated with an additional set of EasySep Direct Rapid Spheres at a 1/20 dilution for 10 minutes in the magnet. This was followed by an additional transfer to a new test tube and a final magnetic incubation for 10 minutes. The isolated cells were then spun down at 1200 rpm for 5 minutes and resuspended in PBS before carrying out a cell count.

Platelet-poor plasma was obtained by spinning down donor blood for 10 minutes at 100g, removing the top layer of plasma, and another 7378 g (10,000 rpm) centrifugation for 10 minutes.

4.2.3 Neutrophil Shear Experiments and Controls

Glass coverslips were covered with a silicone sheet (FDA grade, 0.005" NRV G/G 40D 12" X 12" (Speciality Manufacting inc, Saginaw, MI, USA)). [25], [26] Silicone was coated with 50% plasma or with a 50% plasma/ 10 mM EDTA solution and incubated for 30 minutes at 37°C. EDTA is a calcium and magnesium chelator and can inhibit of calcium- and magnesium-dependent mechanisms, including complement activation [150], [151]. In some cases, 10mM EDTA was added in the circulating solution. The experimental conditions tested are summarized in Table 4.1.

As described in chapter 3, section 3.2.3, the chamber was assembled and connected to a Cole Parmer 75900-50 programmable 6-channel syringe pump which allowed for continuous circulation. The number of neutrophils per shear experiment to be circulated through the system was selected to be 2×10^6 based on recommendations in the literature and the parameters of the chamber [48]. Neutrophils were circulated in RPMI media with 10% FBS at a flow rate of 0.78 ml/min, corresponding to a shear of of $500s^{-1}$. To ensure full circulation of neutrophils, a volume of 1.3 mL was selected. Flow within the chamber was assumed to be continuous and experiments were run for 2 hours at 37°C. The bulk solution was then collected for flow cytometry analysis.

Several controls were included in these experiments. A sample was incubated without exposure to flow and without plasma or PMA for 1 hour at 37°C (negative control, referred to as a static sample). Static samples were incubated in 5mL polypropylene round bottom tubes (Falcon Corning #352063) as opposed to the chamber due to the limited volume and cells that could be added to the flow chamber as a static model. As a positive control, a sample was incubated with 6nM PMA for 1 hour at 37°C without plasma. A more physiological stimulus, 1μM fMLP was also tested for 1 hour at 37 37°C.

Table 4.1: Experimental conditions tested on isolated PMNs

Stimulus/Treatment	Surface Treatment	Abbreviation
-	Platelet Poor Plasma	PPP
-	Platelet Poor Plasma + 10 mM EDTA	PPP/EDTA
PMA	-	PMA
PMA	Platelet Poor Plasma	PMA + PPP
PMA	Platelet Poor Plasma + 10 mM EDTA	PMA + PPP/EDTA
10mM EDTA	Platelet Poor Plasma + 10 mM EDTA	PPP/Circ EDTA
PMA & 10mM EDTA	Platelet Poor Plasma + 10 mM EDTA	PMA+PPP/Circ EDTA
fMLP	Platelet Poor Plasma	fMLP+PPP

PMA: 6nM; fMLP: 1μM. Surface treatment: incubation at 37ºC for 30 min

4.2.4 Flow Cytometry

All samples were adjusted to a cell number of 75,000 per tube. To assess NETosis, samples were first incubated with a primary anti-citrullinated histone (citH3) antibody for 30 minutes at room temperature. This first incubation was immediately followed by a secondary IgG PE antibody for citH3, a FITC anti-MPO antibody, and a PE-Cy™5 anti-CD15 myeloid cell identifying antibody. Samples were then incubated for an additional 30 minutes at room temperature in the dark. Following incubation, samples were washed with 1mL RPMI with 10% FBS and centrifuged at 1200 rpm for 5 minutes. The supernatant was removed, and the cells were resuspended before being analyzed immediately.

For leukocyte activation, samples were incubated with FITC anti-CD11b (Mac-1 upregulation), PE anti-CD63 (a neutrophil degranulation marker), and PE-Cy™5 anti-CD45 (a

leukocyte identification marker). Samples were incubated for 30 minutes at room temperature in the dark, diluted following incubation and analyzed immediately.

Samples were analyzed on a four-color FACS Calibur flow cytometer (Becton Dickinson). Flow cytometry settings of NETosis were optimized to ensure no overlap of fluorescence between the three fluorescent channels used (FL1, FL2, FL3). Data acquisition and analysis were performed using CELL-Quest software (Becton Dickinson). Results are expressed as total fluorescence (geometric mean fluorescence of the detected antibodies)

4.2.5 DNASE Treatment

Generated NETs can be broken down by Deoxyribonuclease (DNAse), an endonuclease that digests the DNA backbone of NET structures [7] [25], [26]. To confirm that the structures present on the silicone surface following shear and activation were NETs, samples were incubated with 1 mg/mL of DNAse for 10 minutes at 37°C [27]. Following treatment, slides were stained with DAPI and visualized using immunofluorescent microscopy.

4.2.6 Immunofluorescent Microscopy

To obtain a thorough confirmation of NET structures, citH3 and MPO NET markers were visualized using immunofluorescence. The protocol was adapted from previous works [28], [29]. Following activation and exposure to shear, silicone samples were removed from the chamber and the attached cells were fixed with 4% paraformaldehyde for 10 minutes at room temperature. Samples were subsequently washed three times with PBS. To prevent non-specific antibody binding, samples were blocked with 5% goat serum for 20 minutes at 37°C and then washed three times with PBS. Samples were incubated with 1/200 diluted primary citH3 (Abcam 281584) and 1/100 diluted primary MPO antibodies (Invitrogen #MA1-80878) for 1 hour at room temperature in the dark. Alexa Fluor™ 594 (2 ug/mL) (Invitrogen # A-11012) and Alexa Fluor™ 488 (1/1000 diluted) (Invitrogen #A28175) secondary antibodies were added for citH3 and MPO respectively and incubated for 45 minutes at room temperature in the dark. Blue nuclear DNA stain 4′,6-diamidino-2-phenylindole (DAPI) for genetic material was added and the silicone was inverted onto a glass slide for imaging purposes. Samples were imaged using an Eclipse TE2000-S microscope and photos were acquired using the NIS-Elements AR Nikon program.

4.2.7 Statistical Analysis

All results are reported as the mean ± standard deviation (SD). To analyze the effect of shear and PMN activation via PMA on NETosis, independent t-tests were conducted. If normality conditions were not met, non-parametric t-tests were conducted using the Kolmogorov-Smirnov test. A p-value of less than 0.05 was required for statistical significance. The number of experiments was always equal to or greater than three.

4.3 Results and Discussion

4.3.1 Flow cytometry analysis of NETosis in neutrophil population

Flow cytometry gates are useful for identifying specific populations of interest cells in samples, using a double-gating strategy. Figure 4.1A illustrates the gating method used for the PMNs in this investigation. As blood-isolated PMNs, most cells presented the characteristic FSC (size) and SSC (granularity) of PMNs (region R1); a few leukocytes, likely lymphocytes, can be observed in the lower part of the size scatter dot plot. Cells were further identified based on their SSC and their expression of the myeloid cell identifying marker CD15 (Region R2); and a gate (G1) was created to focus analysis on cells present in both R1 and R2. Similar to Chapter 3, NET formation in the bulk was identified by changes in the numbers of cells staining positive for NETs as well as fluorescence expression level, through staining with MPO (FL1 channel) and citH3 (FL2 channel) as illustrated in Figure 4.1B (specifically the MPO signal in channel FL1) for those gated cells. The complexity around characterizing NETs in blood-isolated neutrophils in these experiments laid in the fact that the fluorescence signal shifted rather than having a clearer separation between what one may consider positive versus negative (as could be observed with the HL-60 where it was simple to create this M1 mark in the fluorescent histogram). To report NETosis, the percentage of cells that stained positive for both MPO and citH3 was determined as illustrated in Figure 4.1C. Cells in the upper right-hand corner are identified as NET-positive events.

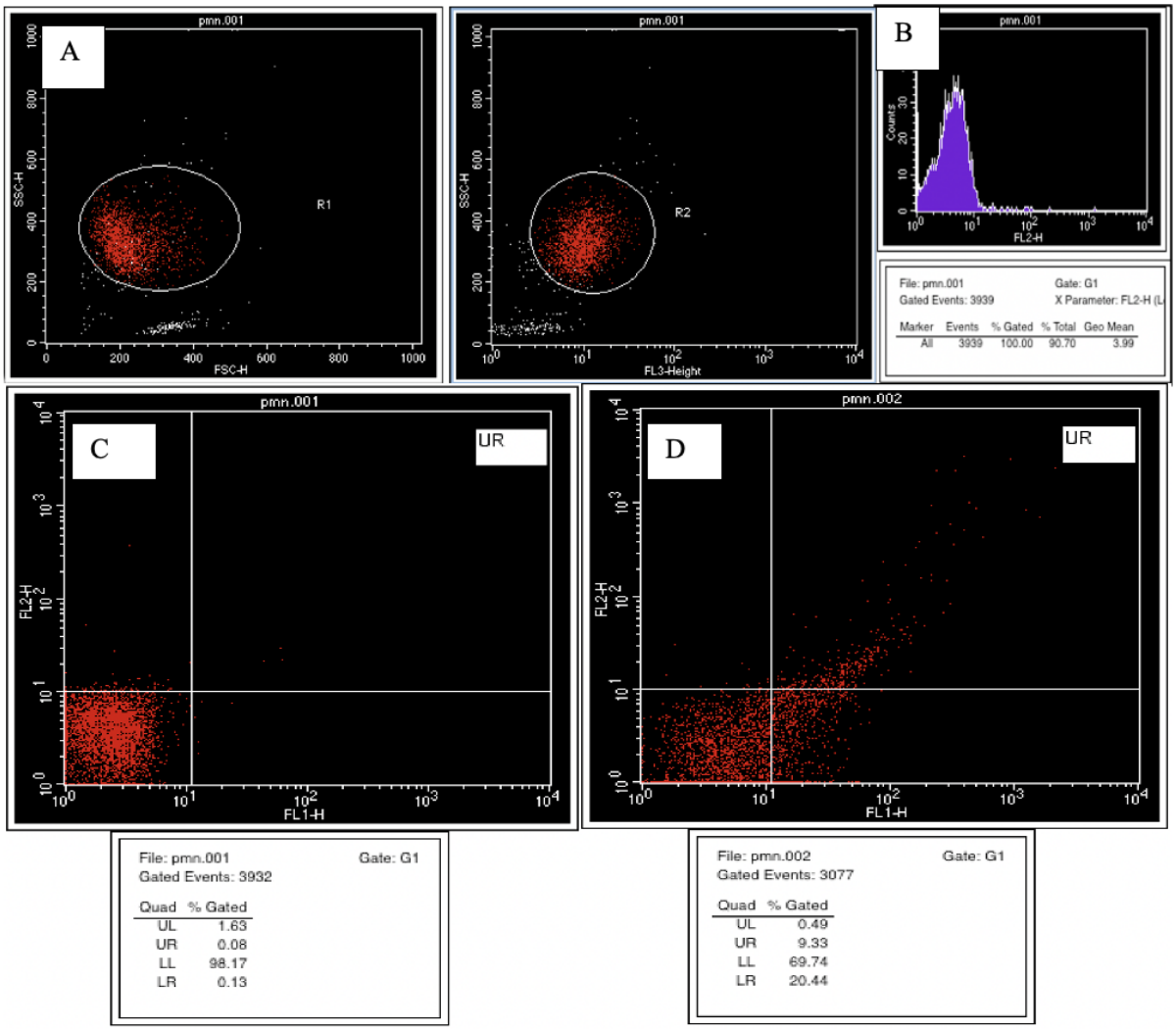

Figure 4.1: Gating strategy and identification of NET-positive events in PMNs. A) Gating strategy including the two regions (R1 and R2) based on FSC, SSC, and CD15 expression in FL3. B) CitH3 fluorescence in FL2 channel and the corresponding mean fluorescence. The fluorescent level in the cell sample, identified as "Geo Mean" in the histogram statistics, is reported throughout the chapter. C) Fluorescent dot plot to identify NET positive PMNs, as identified by the expression of MPO and CitH3 on their surface. Cells in the upper right-hand quadrant of the figure would be those undergoing NETosis D) Fluorescent dot plot for cells activated with PMA.

4.3.2 Shear alone in the presence of a biomaterial does not increase NETosis in the bulk

In the absence of stimulation, less than 5% of PMNs exhibited signs of NETosis and results suggest that shear alone did not increase NET formation in PMNs as shown by the lack of difference between PPP static and PPP+shear (Figure 4.2). The presence of PMA during the 1hr-incubation resulted in NETosis, as shown by the increase in cells expressing NETs markers (MPO and CitH3) and the increase in the fluorescent signal in both the control sample (PMA+PPP static) and PMNs exposed to shear (PMA+PPP+shear) ($p<0.001$) (Figure 4.2). While more PMNs showed signs of NETosis when exposed to shear with PMA when compared to the PMA-stimulated static samples, this did not reach statistical significance (Figure 4.2A). However, a significant increase in MPO expression was observed, highlighting the presence of NETs on PMNs when exposed to 6nM PMA for 1 hour (Figure 4.2B) ($p = 0.0156$, PPP static vs PMA+PPP static). These results are in agreement with prior findings as PMA is known to trigger neutrophil degranulation and NETosis even at low concentrations [10], [30]. Indeed, Erpenbeck and colleagues used 5nM PMA to stimulate NETosis on polyacrylamide (PAA) gels [21]. Additionally, shear conditions (PMA+PPP+ Shear) did not result in a significantly higher MPO expression compared to the control resting sample (PMA +PPP) but was greater overall, indicating elevated MPO levels on the NETs in the presence of physiological flow and PMA (Figure 4.2B).

Furthermore, contrary to MPO, a small but not statistically significant increase in citH3 levels was observed with PMA in the presence of shear (Figure 4.2B). It is possible that 6nM PMA was too low, and 1 hour too short, to sufficiently release enough citH3 into the NETs to have a strong expression. Indeed, lower concentrations and shorter times have not been shown to trigger large amounts of NETosis. Pai and colleagues found that half-maximal NET formation for 3nM PMA occurred only after 120 minutes and concentrations of 10nM only after around 100 minutes [31]. Furthermore, Holsapple and colleagues looked specifically at histone staining within the neutrophils during stimulation with 100 nM PMA. After 60 minutes, histone had accumulated in pockets within the neutrophil membrane but had not yet been released to the environment (even by 150 minutes) [32]. Another potential explanation for the inconsistency between the changes in MPO and citH3 expression is that not all NET structures are equivalent. A study by Obermayer and colleagues found that some NET structures invivo released genetic material but did not citrullinate their H3, resulting in NET structures that would not stain positive for citH3 [33]. Variability in NET structures suggests

that different mechanisms are involved in their release, which may be influenced by interactions with the surface under flow conditions. Overall, our results suggest that in the presence of a plasma-coated biomaterial, shear acts as a priming stimulus for NETosis.

One may suggest that increase PMA stimulation may have allowed to obtain a stronger citH3 expression on NETs, as stimulating PMNs with higher PMA concentrations and longer time period tend to result in equally strong MPO and citH3 expression on NETs [34]–[36]. Indeed, early on in this investigation, higher concentrations of PMA were found to result in a greater citH3 expression but resulted in overall excessive cell loss to the biomaterial (data not shown) [35]–[37]. In this study, 6nM was selected due to its ability to minimize cell loss and cell death in our in vitro model environment. Over the course of protocol development, concentrations of 10-50nM PMA were tested using the parallel plate flow chamber over various time frames. Initially, cells were circulated in the presence of 50nM PMA for an hour. It was found that this led to a high degree of apoptosis and a final cell suspension that could not be analyzed via flow cytometry. Reducing the concentration to 25nM for 1 hour also resulted in a similar issue. The PMNs became excessively activated under shear and the presence of 25nM PMA, resulting in the loss of cells to the biomaterial via adhesion. Further, cells were initially circulated in media supplemented with 30-35% plasma but this was found to exacerbate the cell loss in the presence of 25-50nM PMA and so was not pursued. When PMA was reduced to 12 and 6nM but circulated for 2 hours, a NET signal was observed but low cell counts remained an issue for samples exposed to shear. As such, the final concentration and time were selected to be 6nM PMA stimulation for 1 hour and as mentioned earlier, exposing PMNs to shear appears to have a priming effect as higher level of NETs are observed with PMA stimulation compared to the PMA-stimulated control static sample. In the future, raising the PMA concentration will strengthen the NETosis signal observed but this would need to be balanced by a decrease in incubation time. The lack of the strong presence of NETosis in the bulk/circulating PMNs may also be due to adhesion and where NETosis is taking place, which is discussed in the next section.

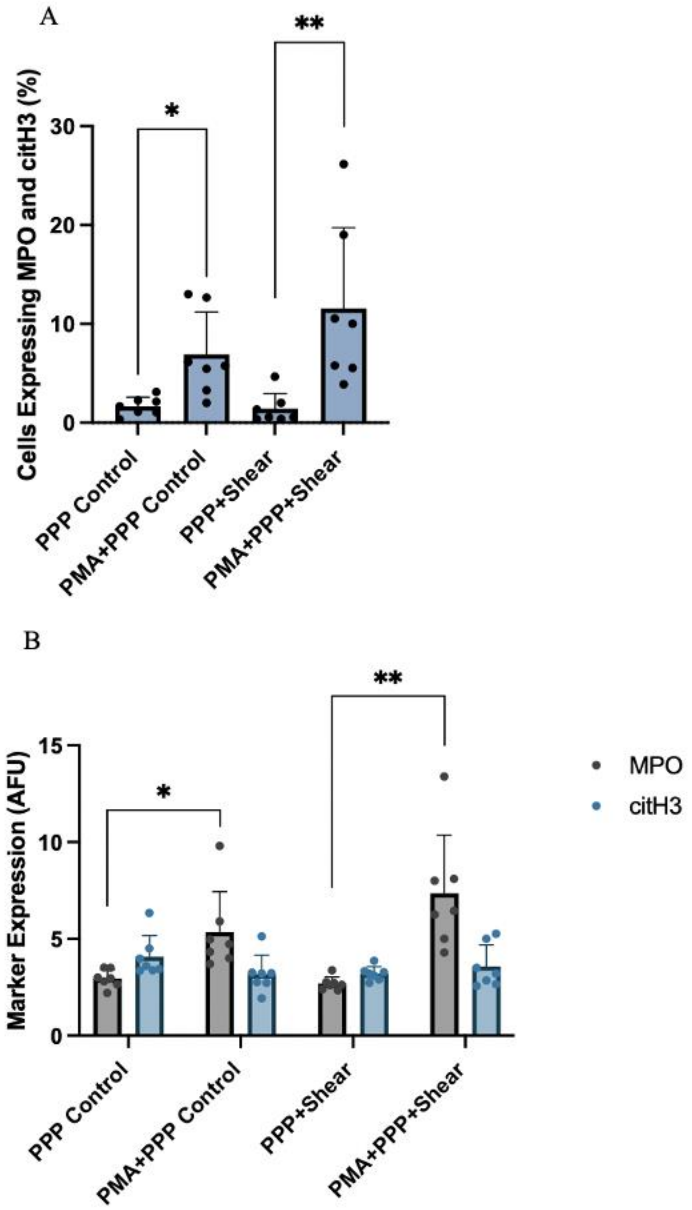

Figure 4.2: NETosis in PMNs in static control and samples incubated in the presence of shear with plasma-coated or uncoated silicone with or without 6nM PMA after 1hr incubation. A) percentage of cells staining for both MPO (FITC) and citH3 (PE). B) MPO and citH3 expression on PMNs cells. * Statistically significant, $p < 0.05$, ** $p < 0.001$. n = 7, mean ± standard deviation. All experiments were run for 1 hour at 37ºC. PMA: 6nM PMA, PPP: platelet poor plasma, shear: $500s^{-1}$. AFU: Arbitrary fluorescent units.

4.3.3 NETs accumulate at the biomaterial surface

A large subset of cells in the solution adhered to the silicone surface and were lost from the circulation. For samples exposed to shear without PMA (PPP+Shear), 68% of cells were lost to the biomaterial environment while samples with PMA (PMA+PPP+Shear) lost a greater number of cells, this was not significantly different (Figure 4.3). This suggested that many of cells adhered to the plasma-coated silicone and adherent PMNs on the surface may exhibit signs of NETosis or be aggregated in NET structures as opposed to circulating in the bulk solution (Figure 4.3) as suggested by Manda-Handzlik and colleagues who found a significant loss of cells from suspension following activation with PMA over several hours [37].

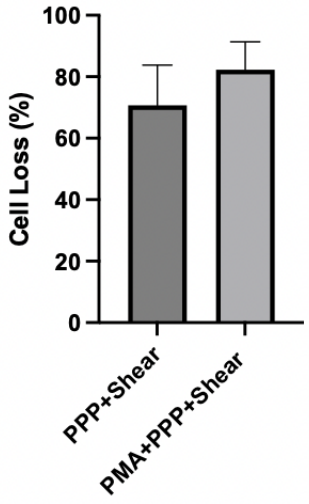

Figure 4.3: Percentage of cells lost the surface of the in vitro model (biomaterial surface and tubing) following exposure to shear for 1 hour with or without 6nM PMA stimulation in the presence of platelet poor plasma. n=7. mean ± standard deviation.

4.3.4 May–Grünwald-Giesma (MGG) staining did not effectively stain NETs

MGG staining is a commonly employed method to image neutrophils [38], [39]. In this stain, nuclei are coloured by an intense blue/purple while the cytoplasm is pink/red. In our lab, the MGG stain was successfully used to visualize tear film neutrophils and thus attempts were also made to identify PMN NETs. Staining with MGG did not reveal easily identifiable NET structures, despite revealing neutrophil aggregates and some strands of genetic material. This likely indicates that the

various steps involved in the staining protocol (which includes different washing steps and fixation) damaged NET structures before imagining could be completed (Figure 4.4).

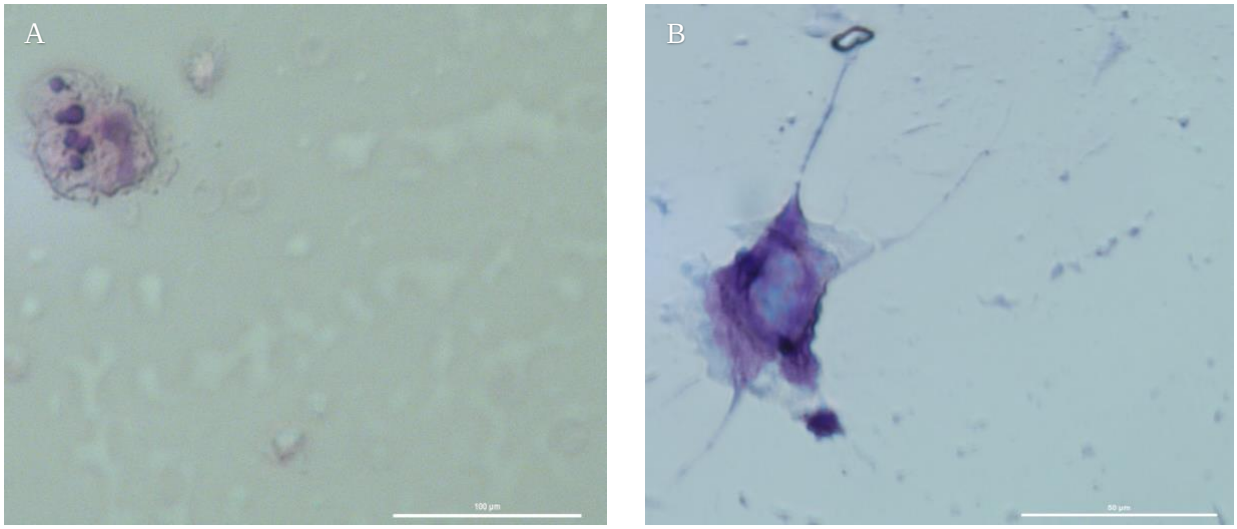

Figure 4.4: MGG staining of neutrophils stimulated with PMA. One NET was identified in B) but overall staining typically revealed activated cells as shown in A) that did not have easily identifiable NET structures.

4.3.5 NETs on the biomaterial surface stain positive for all NET markers

To accurately characterize NETs on the biomaterial surface, samples exposed to shear and activated with 6nM PMA were stained for three NET markers, DAPI, MPO and CitH3 as shown in Figure 4.5. The green fluorescence staining for MPO was observed along the membranes of neutrophils. On strands, citH3 expression often overlapped with DAPI (which stains genetic materials including nuclei of PMNs), particularly in PMN aggregates.

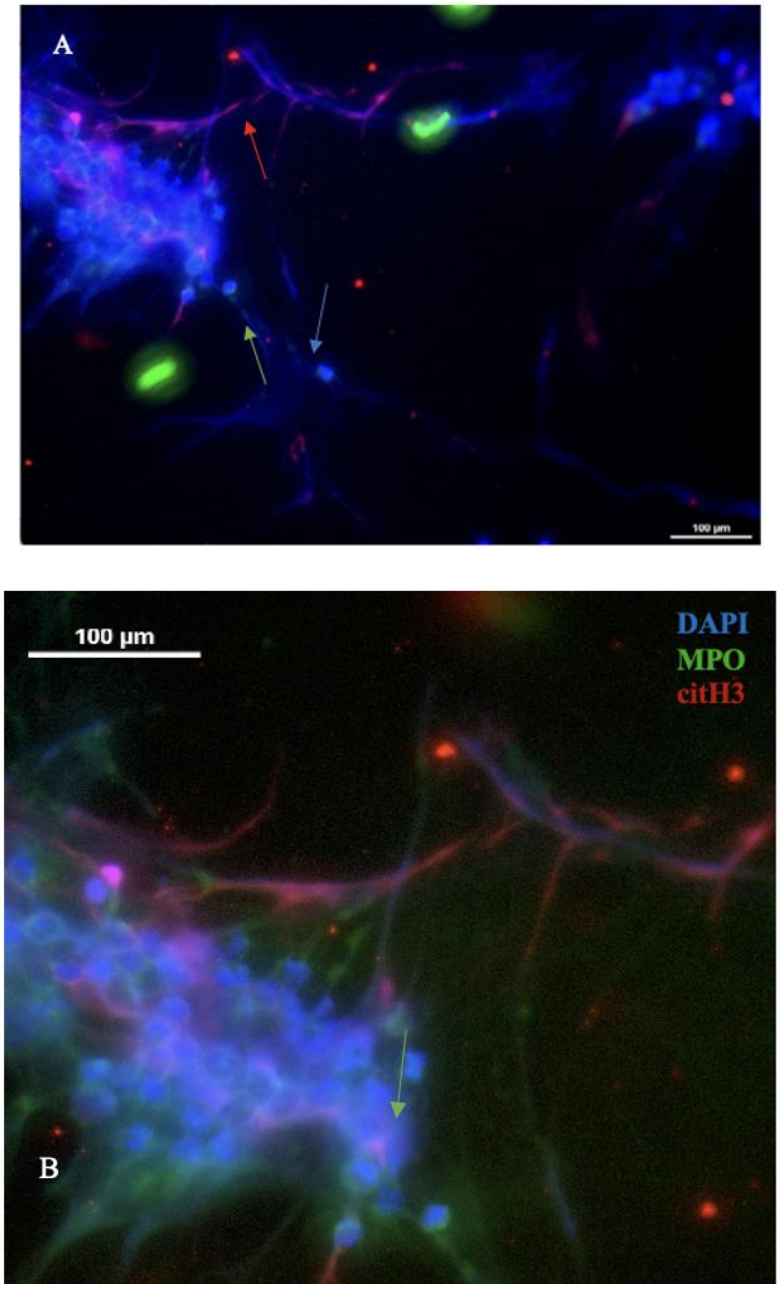

Figure 4.5: Immunofluorescent staining at the plasma-coated silicone surface of samples exposed to shear and activated with 6nM PMA. The blue arrow indicates genetic material stained with DAPI, a green arrow indicates MPO staining, and the red arrow indicates citH3 staining. A) and B) are the same NET structure but B) is magnified to highlight how MPO decorates the surface of the PMNs as NETs are released (as indicated by the green arrow).

These images provide support for the notion that NET structures adhered to the plasma-coated silicone. Highly expressing citH3 cells undergoing NETosis may be remaining adherent to the plasma-coated silicone instead of circulating in the bulk solution. To further confirm that the structures on the plasma-coated silicone were NETs, the biomaterial surfaces were treated with DNAse, a known digestor of NETs for 10 minutes. Prior to DNAse treatment, structures stained positive for citH3, and DNA structures were visible. Following treatment, samples failed to stain for citH3, and DNA strands were eliminated. PMN aggregates remained adhered to the silicone but did not have extracellular structures to connect them (Figure 4.6B).

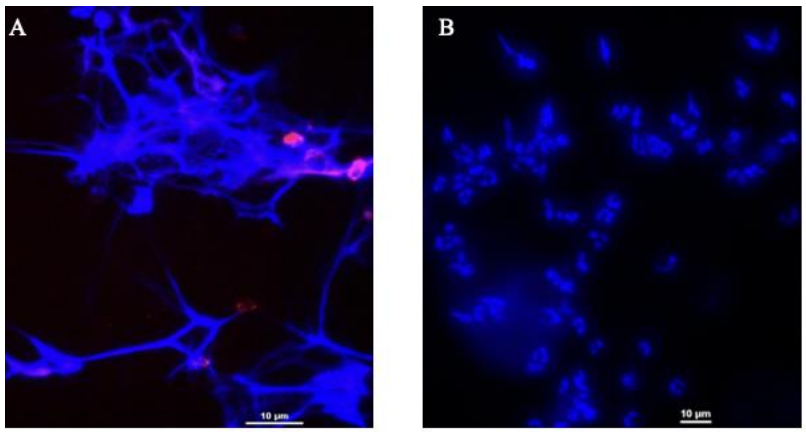

Figure 4.6: Immunofluorescent staining of neutrophils adherent to plasma-coated silicone following shear with 6nM PMA. A) Without DNAse. B) Following DNAse treatment. Blue: DAPI. Red: citH3

These imaging results, taken in combination with Figures 4.5A and 4.5B, indicates that NETosis is occurring at the biomaterial surface or that PMNs that are undergoing NETosis are more adherent, and the NETosis signal in the bulk solution (as measured by flow cytometry), may not accurately reflect the true effect of the material-induced activation in the presence of shear.

4.3.6 Neutrophil markers CD11b and CD63 increase with PMA activation

CD11b is a protein and a member of the integrin family of cell adhesion molecules. It is expressed on the surface of neutrophils and plays a role in adhesion, migration, and signaling. Following activation, CD11b expression increases on the surface of neutrophils so that they can carry out their immune response [40]. As expected, CD11b expression increased upon stimulation with

6nM PMA in static samples ($p \leq 0.01$). In samples exposed to shear, the addition of PMA still resulted in an increase in CD11b expression which is expected due to the PMA-induced activation [172], [190], [191]. However, there was no significant difference between PMA-activated samples that were static and those exposed to shear (PMA+PPP static vs PMA+PPP+Shear). Similarly, samples without PMA (PPP Static and PPP+Shear) did not significantly differ in terms of CD11b expression, indicating that shear was not playing a significant role. This is in agreement with previous work where, at $500s^{-1}$, CD11b expression in blood PMNs did change [43]. CD11b upregulation due to exposure to shear stress only occurs at far greater shear stresses than what the cells were exposed to in our study [43]–[45] .

A similar trend is observed for the degranulation marker CD63. During neutrophil activation, CD63 is translocated from the granule membrane to the cell surface, where it interacts with other proteins. Subsequently, it is used to identify neutrophil degranulation [46]. Stimulation with 6 nM PMA results in significant degranulation in both static and samples exposed to shear as expected ($p < 0.05$) [10], [42], [46]. As with CD11b, no significant difference between PPP+Shear and PMA+PPP+Shear samples was found, indicating that shear was not significantly triggering additional degranulation. This is also in agreement with prior studies as degranulation has not been observed at this level of shear. Transient exposure of neutrophils to extremely high shear has been shown to result in the movement of granules towards the surface but also did not trigger degranulation [44]. As such, it is not expected that the dynamic conditions of this study would trigger excessive degranulation and therefore elevated CD63 levels. Furthermore, the increase in CD11b and CD63 upon PMA stimulation but not shear indicates that the selected 500 s^{-1} shear did not prime the circulating PMNs in this in vitro model.

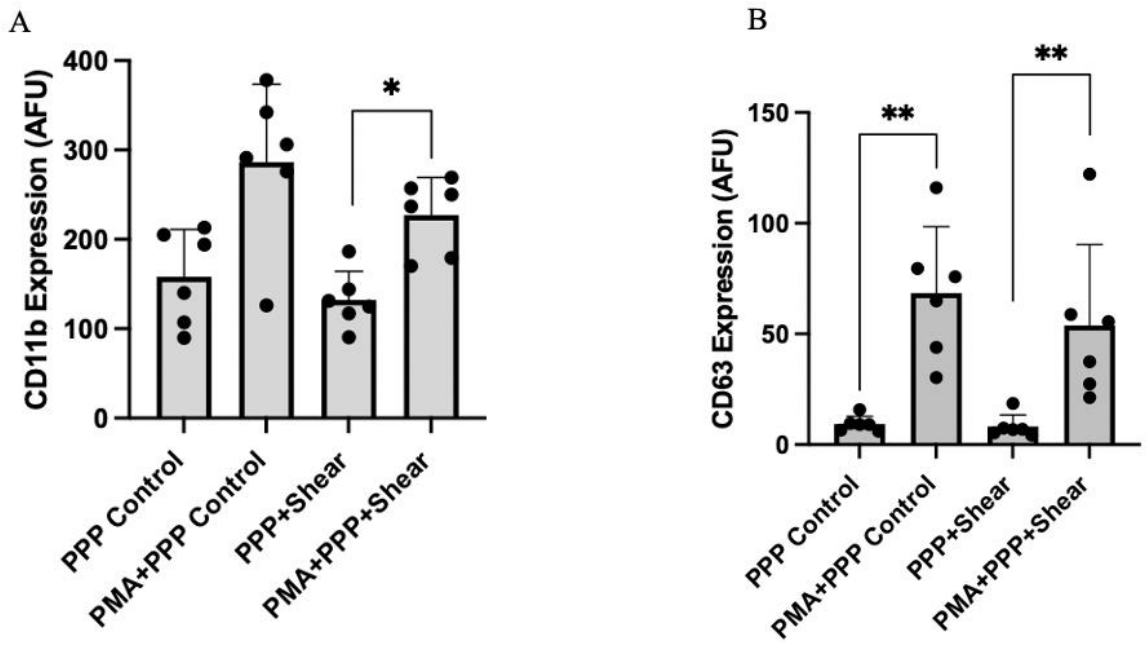

Figure 4.7: CD11b (A) and CD63 (B) expression of PMNs cells in static control and samples incubated in the presence of shear with plasma-coated or uncoated silicone with or without 6nM PMA after 1hr incubation. * Statistically significant, $p < 0.05$. n = 6. PMA: 6nM and PPP: platelet poor plasma.

4.3.7 fMLP did not trigger elevated levels of NETosis

PMA is a synthetic stimulus that does not accurately reflect physiological conditions. As such, this study also attempted to trigger NETosis in PMNs via fMLP. The results using fMLP as a stimulus were inconclusive. Activation of PMNs resulted in a very low percentage of cells that stained positive for both NET markers (anywhere between 0-3% as indicated in Appendix Figure A.4). Staining of the silicone surfaces also did not show conclusive NET aggregates. This aligns with what as previously been reported as the direct effect of fMLP on NETosis is less clear than that of PMA. Some literature suggests that fMLP alone is insufficient to generate NETs without an additional stimulus while others suggest that fMLP first initiates autophagy to trigger NETosis [6], [47], [48]. Regardless, this investigation shows fMLP was not an effective NET inducer in the in-vitro shear and biomaterial model.

4.3.8 EDTA decreased NETosis

To begin investigating the mechanisms involved in triggering NETosis on the biomaterial under shear conditions, the effect of EDTA was studied. EDTA chelates calcium and magnesium and inhibit complement pathways, including the classical, alternate, terminal and lectin pathways, by preventing the activation of complement proteins that require calcium ions for their activity. When activated, the complement system generates a cascade of reactions and has been shown to increase the release of NETs [49]. To determine if complement activation played a role in NETosis at the biomaterial surface, silicone was coated with platelet-poor plasma and 10 mM EDTA for 30 minutes prior to exposure to the PMNs and shear. As shown in Figure 4.8A, the percentage of NET-positive cells decreased when cells were exposed to the EDTA/plasma coated sample. While this did not yet reach statistical significance, the reduction in the number of cells undergoing NETosis points towards a contribution of adsorbed complement proteins on NETosis.

Despite the addition of EDTA, during the plasma coating incubation or during the circulation/flow experiment, both MPO and citH3 expression remained similar to those observed in the absence of EDTA (Figure 4.8B). While no statistical significance was found, the expression of MPO did decrease slightly in the presence of EDTA. As was noted above in section 4.3.2, the overall expression of MPO and citH3 changed very little upon stimulation with 6nM PMA. As such, inhibition of complement via EDTA may have reduced an already low NETosis level that failed to reach statistical significance. As was previously mentioned in Chapter 3, complement proteins such as C3 are known to interact with, and stimulate the generation of, NETs [50]–[53]. Furthermore, adsorption of the plasma protein IgG to material surfaces has also been shown to increase NETosis in a dose-dependent manner [20], [54]. Inhibiting potential calcium-dependent ligand-receptor interactions between adsorbed plasma proteins and circulating PMNs via EDTA may have reduced overall NETosis in the sample. Calcium has also been implicated in intracellular mechanism with the calcium-ion-dependent Raf-MEK-ERK signalling pathway as being required for NET formation. Thus, chelating calcium in the bulk during the experiment would also lead to disruption of calcium signaling that would decrease pathway activation and thus reduce NETosis [55].

Despite incubation with EDTA on the silicone, some NETs were still present on the biomaterial surface (as seen in Figure 4.9), indicating that additional mechanisms may also be at play at the material surface.

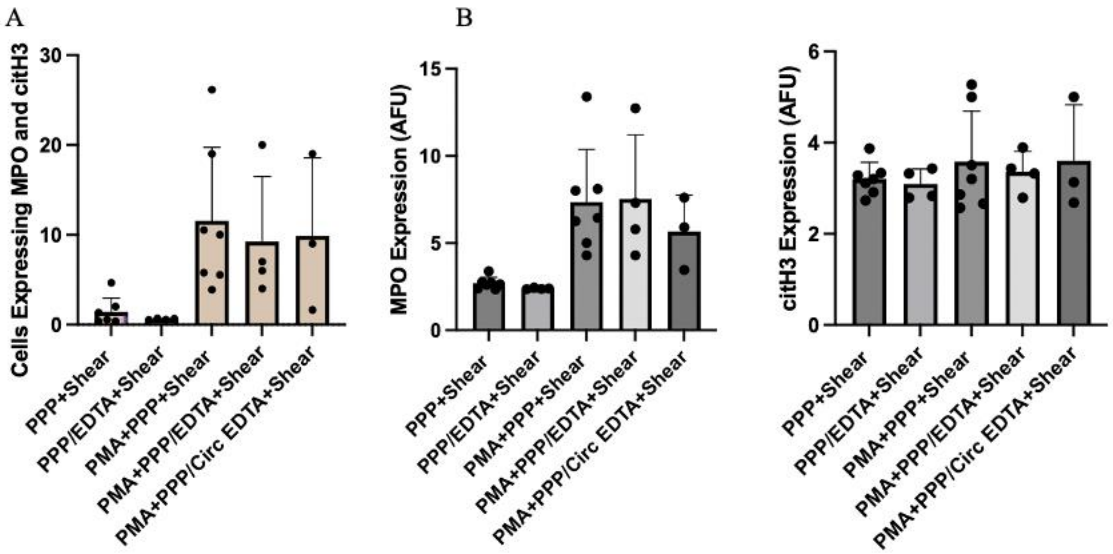

Figure 4.8: NETosis in PMNs in samples incubated in the presence of shear with plasma-coated or uncoated silicone with or without 6nM PMA and 10mM EDTA after 1hr incubation. PPP: platelet poor plasma. PPP/EDTA: platelet poor plasma with 10mM EDTA. PPP/Circ EDTA: platelet poor plasma with 10mM EDTA and an additional 10mM EDTA circulating in the bulk solution. n = 7 for PPP+Shear and PMA+PPP+Shear. n=5 for PMA+PPP/EDTA+Shear. n = 3 for PMA+PPP/Circ EDTA+Shear A) percentage of cells staining for both MPO (FITC) and citH3 (PE). B) MPO and citH3 expression on PMNs cells. mean ± standard deviation. All experiments were run for 1 hour at 37ºC.

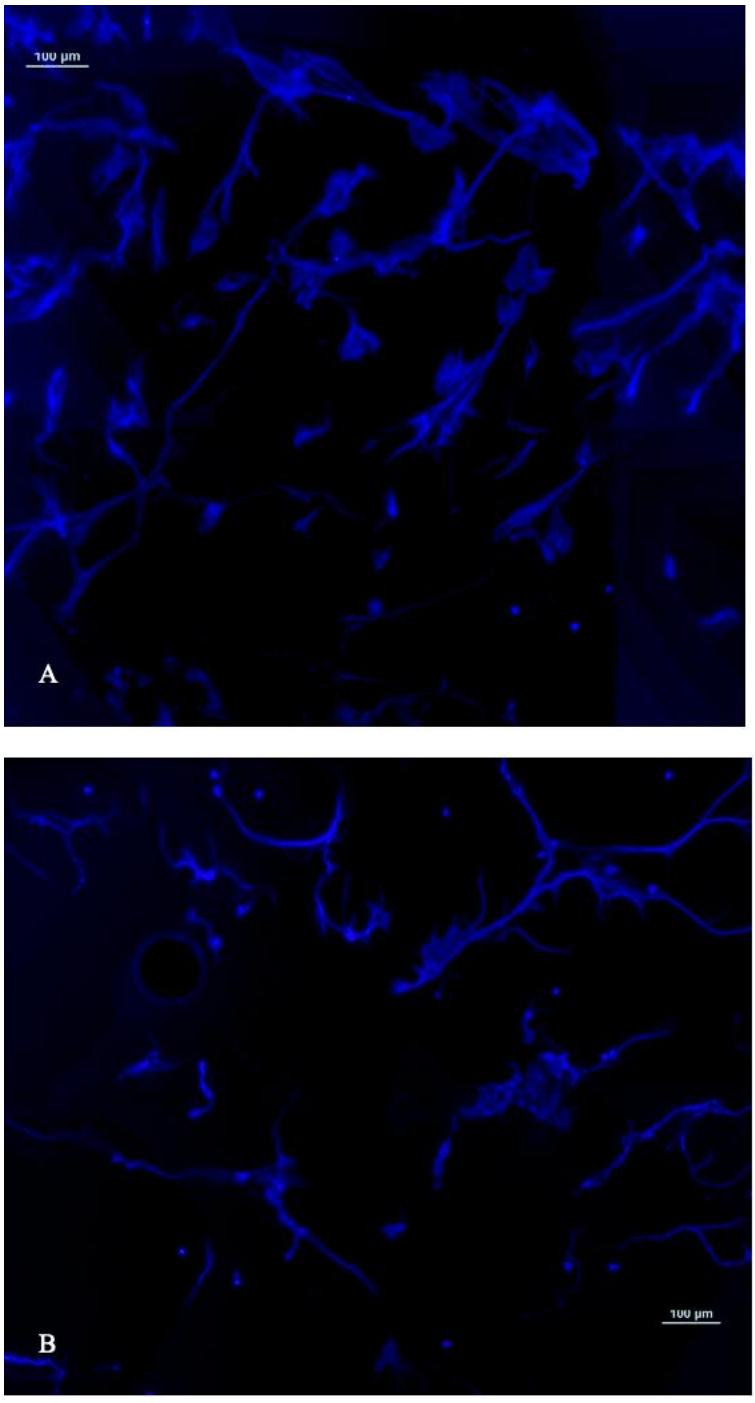

Figure 4.9: Immunofluorescent staining of plasma-coated silicone following shear and activation with 6nM PMA. A) No EDTA on the surface and B) Presence of 10mM EDTA

4.3.9 EDTA did not meaningfully decrease PMN CD11b and CD63 expression

To fully characterize the response of PMNs to EDTA treatment in the presence of plasma-coated silicone under shear conditions, both CD11b and CD63 levels were quantified. Exposure to coating with plasma incubated with 10mM EDTA did not significantly alter the expression of CD11b or CD63 in samples that were activated with 6nM PMA. Additional circulation of 10mM EDTA in the bulk solution was also ineffective at significantly altering CD11b and CD63 expression in samples activated with 6nM PMA (Appendix Figure A.3). This observation aligns with previous works showing that EDTA does not affect overall expression levels [56]–[58]. Treatment with EDTA did not significantly impact PMA-induced PMN degranulation in the presence of shear or a biomaterial as shown by the lack of CD63 expression change. This indicates the mechanisms of material-induced CD11b and CD63 upregulation under shear conditions is independent of adsorbed complement proteins.

Table 4.2: Expression of markers CD11b and CD63 on PMNs following 1 hour incubation with platelet-poor plasma coated silicone under dynamic ($500s^{-1}$) conditions with or without 10mM EDTA and with or without 6nM PMA stimulation.

Sample	**CD11b Expression (AFU)**	**CD63 Expression (AFU)**
PPP+Shear	132 ± 32	8.2 ± 5.2
PMA+PPP+Shear	227 ±42	54 ±37
PMA+PPP/EDTA+Shear	235 ± 42	50±30
PMA+PPP/Circ EDTA+Shear	259 ± 51	22 ± 2

Results are reported as mean of total arbitrary fluorescence units and standard deviations. n= 7 for non-EDTA conditions, n=5 for PPP/EDTA conditions and n=3 for PPP/Circ EDTA conditions.

4.4 Conclusion and Future Direction

This investigation examined the effect of shear on PMN NETosis in the presence of plasma-coated biomaterial. 6nM PMA was used to induce NETs under physiological flow. Our results suggest that while shear was not able to induce NETosis, shear primed PMNs for NETosis. While

limited number of PMNs exhibiting NETosis were identified in the bulk via flow cytometry, imaging of the biomaterial surface indicated a strong presence of NET structures and aggregates. This demonstrated that the NET signal analyzed from the bulk solution did not accurately reflect PMN NETosis as in the presence of a biomaterial under shear, NETs and PMNs were primarily binding to the surface. Complement inhibition by EDTA in both the bulk and on the surface reduced the percentage of cells undergoing NETosis suggesting that interactions between circulating PMNs and adsorbed complement proteins on the biomaterial material surface increased NETosis. Taken together, these results indicate that in the presence of a biomaterial, such as a cardiovascular stent for example, NETs could be induced to aggregate in large structures as a consequence of the immune response at the surface and in combination with exposure to physiological shear. This may play a role in biomaterial-related immune complications.

The results of this study suggest that further investigation of mechanisms at the biomaterial surface, rather than in the bulk, will be crucial in future work. The vast majority of cells adhered to the biomaterial and so it will be important in future work to determine how to quantify NETosis at the surface. Furthermore, as EDTA is a non-specific complement inhibitor, future work will involve complement-inhibition at the biomaterial surface to elucidate mechanisms. Additionally, instead of platelet-poor plasma, the silicone surface can be coated with serum to identify the role of fibrinogen's presence and potential effect on NETosis. Fibrinogen plays a role in creating thrombi and has been shown to scaffold with NETs [59], [60]. To target complement more specifically, complement receptor 3 can be inhibited given its involvement in NETosis [61]–[63]. Testing its inhibition in the presence of shear and a biomaterial environment would provide valuable information regarding NETosis mechanisms at the material surface.

The use of PMA moving forward is also discouraged due to the synthetic nature of the stimulus. fMLP generated inconclusive results about its ability to generate NETs and as a result, additional physiological stimuli, such as lipopolysaccharides (LPS), interleukin-8 (IL-8), and calcium ionophore (CI), should be tested.

Chapter 5: Conclusion

5.1 Final Experimental Conclusions

The purpose of this investigation was to develop an in-vitro model that would allow for the characterization of shear on dHL-60 and blood PMN NETosis in the presence of a biomaterial. To achieve this, a parallel plate model and corresponding flow cytometry analysis tools were developed to study NETosis under these conditions. The hypothesis around both the dHL-60 cells and the blood-isolated PMNs was that in the presence of shear and a biomaterial, PMA-stimulated NETosis would be greater. The results of this study indicate that while an increase in NETosis under these conditions was observed, it was not reflected in the bulk. Rather, NETosis occurred largely at the material surface.

In Chapter 3, dHL-60 cells were first used as a model cell line to study NETosis in the presence of shear and a biomaterial. The impact of various inflammatory mediators including shear, PMA, biomaterial, and plasma components on dHL-60 NETosis was examined. dHL-60 cells analyzed by flow cytometry demonstrated a double population of cells before and after stimulation with PMA. Upon further examination, it was found that this secondary population of HL-60 cells contained a mixture of both apoptotic and necrotic cells. This secondary population increased over the 5-day differentiation period and reached a maximum following PMA stimulation. This illustrates that some of the HL-60 cells undergo apoptosis, as opposed to NETosis, during stimulation with PMA. Furthermore, there remains a percentage of cells that are necrotic and the NET gating strategy included both populations. Despite the elevated presence of apoptotic and dead cells, flow cytometry was still used to analyze NETosis markers.

The number of cells expressing MPO and citH3 increased significantly in PMA-stimulated dHL-60 cells that were exposed to shear relative to static. This was the case for both plasma-coated and non-plasma-coated silicone conditions. As for NET marker expression, both had variable expressions depending on the presence or absence of plasma and PMA. For both MPO and citH3, PMA-activated samples that were exposed to shear in the presence of plasma had significantly greater marker expression than their PMA-activated static counterparts, suggesting that the resulting NET structures were larger, likely due to interactions between the cells under shear. The plasma on the slide may have facilitated these interactions as non-plasma conditions did not have significantly different MPO or citH3 expression between static and shear conditions (indicating no change to NET

morphology in the presence of shear). Taken together, this indicates that shear, in the presence of a plasma-coated biomaterial, modulates NETosis.

During the analysis, the M1 marker region was used to identify cells undergoing NETosis. This was done to isolate the signal from cells undergoing NETosis. Despite the creation of the M1 marker, it is possible that a number of unhealthy (apoptotic or necrotic) dHL-60 cells were included in the gate, thus skewing not only the NETosis signals but the activation and degranulation markers (CD11b and CD63). Alternative gating methods may be required to more accurately isolate the NETosis signal.

Shear alone was found to increase both CD11b and CD63 expression in dHL-60 cells thus demonstrating that the biomaterial environment under those conditions triggered both activation and degranulation of the cells. In the case of CD63, additional activation with PMA under shear failed to significantly increase degranulation in dHL-60 cells, demonstrating that shear had a greater effect than PMA activation.

To begin investigating the mechanisms involved in triggering NETosis in dHL-60 cells on the biomaterial under shear conditions, 10 mM EDTA was added to the plasma-coated silicone in the chamber. The presence of 10 mM EDTA during the plasma coating resulted in a reduced number of cells undergoing NETosis, indicating that interactions between adsorbed complement proteins were contributing to NETosis.

Despite the ability of dHL-60 cells to respond to shear in the biomaterial environment, the lack of uniformity in their population makes the interpretation of the results more challenging. The presence of a damaged cell population, even prior to exposure to the shear and biomaterial, presents a confounding factor that will require additional analysis via different gating methods. Taken altogether, the results obtained using this experimental model indicate that dHL-60 cells were not an effective model of NETosis.

The aim of Chapter 4 was to apply the model used in Chapter 3 to investigate the effect of shear on PMN NETosis in the biomaterial environment, albeit at a lower PMA concentration and time. Experimental data revealed that the combination of shear and biomaterial increased the percentage of cells undergoing NETosis (via PMA stimulation) but this was not found to be significant. The expression of MPO was found to be greater in the plasma-containing shear condition but the citH3 signal showed no change. Difference in NETs structure and low PMA stimulation may

be explain the difference in NET marker expression in PMNs in this model. Further analysis revealed that this lack of signal increase in the bulk was likely due to the location of NETosis. Imaging revealed that many NET structures adhered to the plasma-coated silicone, stained positive for both NET markers, and were degraded by DNAse. If shear is capable of increasing the level of NETosis, particularly on the surface of the material, this would indicate that previous in-vitro models that studied NETs on material surfaces may have underestimated the true extent of NETosis that would occur under physiological conditions, thus limiting the application of their conclusions. Furthermore, previous work has examined NETs obtained from the blood of patients undergoing surgery and quantified them using flow cytometry [1]. Our results indicate that flow cytometry of a bulk solution does not accurately reflect NETosis occurring the biomaterial. As such, the presence of NETs in circulation is not painting an accurate picture of true NETosis levels (NETs likely accumulated on any materials associated with the surgical process).

As in Chapter 3, EDTA was added to investigate the role of complement. Inhibition of complement resulted in a decrease in NETosis in the circulating PMNs (and no change in MPO or citH3 expression), albeit it did not reach statistical level, suggesting the potential role of adsorbed complement activated products in material-induced NETosis under shear conditions. Visually, EDTA resulted in fewer aggregates on the plasma-coated silicone surface, however, NET structures were still evident. Further experiments will be needed to quantify NETs on the surface.

The results of chapter 3 and 4 can also be compared to each other to draw conclusions about modelling NETosis. While developing the protocol for this study, it became increasingly clear that different conditions were required for dHL-60 cells versus PMNs. Specifically, the concentration of PMA needed to generate a NETosis signal in dHL-60 cells was four times greater than what was used for PMNs and over twice as long. This confirms what has been previously reported on the differing activation thresholds for HL-60 cells and PMNs as mentioned in Chapter 2 [2],[3]. The cells can also be contrasted by their different response to EDTA. dHL-60 cells reduced NETosis (as evidenced by the significant decrease in the number of cells expressing NET markers and the reduction in citH3 expression) more readily in the presence of EDTA than PMNs. This demonstrates that these cells may interact with other immune components (including complement) via different mechanisms when it comes to NETs. Another notable difference was the morphology of NET structures on the silicone surface. NET structures released by the dHL-60 cells under shear did not aggregate to the same extent as PMNs and the DNA released did not extend as far from the cell. PMNs tended to aggregate in

large clusters with elongated strands of genetic material connecting these clusters across the silicone surface. Figures in Chapter 3 and 4 illustrate this difference to some extent but do not capture the full scale of the morphological difference observed.

The disparity in the threshold NETosis concentration suggests that the signaling pathways and regulatory mechanisms governing NETosis in dHL-60 cells may differ from those in PMNs, particularly in the presence of shear and/or a biomaterial. As such, caution should be exercised when extrapolating findings from HL-60 cell studies to infer the intricacies and physiological relevance of NETosis in human PMNs. To accurately understand the mechanisms and dynamics of NETosis on biomaterials under shear, it is crucial to utilize primary human neutrophils or more relevant ex vivo models that closely mimic the behaviour and responses of blood PMNs.

5.2 Future Work

This investigation concludes that dHL-60 cells are not a suitable model to investigate NETosis in the presence of shear and a biomaterial, however, it also acknowledges that a closer examination of the surface may be required. To characterize dHL-60 NETosis more accurately, the surface of the biomaterial could be further examined via staining. This will involve staining NET structures with DAPI, MPO, and citH3. This will confirm the spread and aggregation of NETs by dHL-60 cells at the chosen concentration of PMA and under constant shear conditions. Furthermore, additional gating strategies may be employed to isolate the population of cells undergoing NETosis more accurately.

With respect to PMNs, the results of this investigation suggest that the focus of studying NETosis in the presence of shear and biomaterial should shift to analyzing the surface. Given the accumulation of NETs on the material, it will be important to quantify the NETs that are present. Following this, the mechanisms involved can be further explored. For example, the non-specific inhibition by EDTA can be replaced with specific, targeted, complement inhibitors (such as those for complement receptor 3) added to the plasma coating. Furthermore, plasma can be replaced with serum at the biomaterial surface to eliminate the potential effect of fibrinogen. Lastly, additional physiological stimuli such as LPS, IL-8, and CI should replace PMA. Extensions of this work could also involve testing not only alternative stimuli, but also additional times points given that the progression of NETosis occurs over several hours. Furthermore, the shear stress could be modulated to determine if higher or lower shear stress changes the outcome of NETosis in the presence of the

biomaterial. Other biomaterials could also replace silicone within the parallel plate flow chamber, allowing for additional information to be obtained about NETosis at the biomaterial surface under shear.

Overall, the protocol developed over the course of this investigation can be easily adapted to explore a variety of stimuli concentrations, times, and surface interactions in order to increase the understanding of NETosis in the biomaterial environment under shear.

Letters of Copyright Permission

Figure 1.1

This Agreement between Andreea Palage ("You") and Elsevier ("Elsevier") consists of your license details and the terms and conditions provided by Elsevier and Copyright Clearance Center.

License Number	5558490874417
License date	May 29, 2023
Licensed Content Publisher	Elsevier
Licensed Content Publication	Biomaterials
Licensed Content Title	Biomaterial-associated thrombosis: roles of coagulation factors, complement, platelets and leukocytes
Licensed Content Author	Maud B. Gorbet,Michael V. Sefton
Licensed Content Date	Nov 1, 2004
Licensed Content Volume	25
Licensed Content Issue	26
Licensed Content Pages	23
Start Page	5681
End Page	5703
Type of Use	reuse in a thesis/dissertation
Portion	figures/tables/illustrations
Number of figures/tables/illustrations	1
Format	electronic
Are you the author of this Elsevier article?	No
Will you be translating?	No
Title	The Effect of the Shear-Biomaterial Environment on Neutrophil Extracellular Traps
Institution name	University of Waterloo
Expected presentation date	Jun 2023
Portions	FIgure 1

Figure 2.1

SPRINGER NATURE LICENSE
TERMS AND CONDITIONS

May 25, 2023

This Agreement between Andreea Palage ("You") and Springer Nature ("Springer Nature") consists of your license details and the terms and conditions provided by Springer Nature and Copyright Clearance Center.

License Number	5556170145619
License date	May 25, 2023
Licensed Content Publisher	Springer Nature
Licensed Content Publication	Springer eBook
Licensed Content Title	Human Neutrophil Isolation and Degranulation Responses to Yersinia pestis Infection
Licensed Content Author	Kara R. Eichelberger, William E. Goldman
Licensed Content Date	Jan 1, 2019
Type of Use	Thesis/Dissertation
Requestor type	academic/university or research institute
Format	electronic
Portion	figures/tables/illustrations
Number of figures/tables/illustrations	1
Will you be translating?	no
Circulation/distribution	1 - 29
Author of this Springer Nature content	no
Title	The Effect of the Shear-Biomaterial Environment on Neutrophil Extracellular Traps
Institution name	University of Waterloo
Expected presentation date	Jun 2023

Figure 2.2

JOHN WILEY AND SONS LICENSE
TERMS AND CONDITIONS

May 25, 2023

This Agreement between Andreea Palage ("You") and John Wiley and Sons ("John Wiley and Sons") consists of your license details and the terms and conditions provided by John Wiley and Sons and Copyright Clearance Center.

License Number	5556180734617
License date	May 25, 2023
Licensed Content Publisher	John Wiley and Sons
Licensed Content Publication	European Journal of Clinical Investigation
Licensed Content Title	Cytokine production by human neutrophils: Revisiting the “dark side of the moon”
Licensed Content Author	Marco A. Cassatella, Federica Calzetti, Sara Gasperini, et al
Licensed Content Date	May 30, 2018
Licensed Content Volume	48
Licensed Content Issue	S2
Licensed Content Pages	10
Type of use	Dissertation/Thesis
Requestor type	University/Academic
Format	Electronic
Portion	Figure/table
Number of figures/tables	1
Will you be translating?	No
Title	The Effect of the Shear-Biomaterial Environment on Neutrophil Extracellular Traps
Institution name	University of Waterloo
Expected presentation date	Jun 2023
Portions	Figure 1

Figure 2.7

AIP PUBLISHING LICENSE
TERMS AND CONDITIONS

May 23, 2023

This Agreement between Andreea Palage ("You") and AIP Publishing ("AIP Publishing") consists of your license details and the terms and conditions provided by AIP Publishing and Copyright Clearance Center.

License Number	5545380568569
License date	May 10, 2023
Licensed Content Publisher	AIP Publishing
Licensed Content Publication	Physics of Fluids
Licensed Content Title	The dynamics of parallel-plate and cone–plate flows
Licensed Content Author	Oza, Anand U.; Venerus, David C.
Licensed Content Date	Feb 18, 2021
Licensed Content Volume	33
Licensed Content Issue	2
Type of Use	Thesis/Dissertation
Requestor type	Student
Format	Electronic
Portion	Figure/Table
Number of figures/tables	1
Will you be translating?	No
Title	The Effect of the Shear-Biomaterial Environment on Neutrophil Extracellular Traps
Institution name	University of Waterloo
Expected presentation date	Jun 2023
Portions	Figure 2 to be used during the literature review chapter as the representative image of a cone and plate system.

References

Chapter 1 References

[1] V. Witko-Sarsat, P. Rieu, B. Descamps-Latscha, P. Lesavre, and L. Halbwachs-Mecarelli, "Neutrophils: Molecules, Functions and Pathophysiological Aspects," *Laboratory Investigation*, vol. 80, no. 5, pp. 617–653, May 2000, doi: 10.1038/labinvest.3780067.

[2] C. Rosales, "Neutrophil: A Cell with Many Roles in Inflammation or Several Cell Types?," *Front Physiol*, vol. 9, Feb. 2018, doi: 10.3389/fphys.2018.00113.

[3] A. Strohbach and R. Busch, "Predicting the in vivo performance of cardiovascular biomaterials: current approaches in vitro evaluation of blood-biomaterial interactions," *Int J Mol Sci*, vol. 22, no. 21, p. 11390, Oct. 2021, doi: 10.3390/ijms222111390.

[4] M. Gorbet, C. Sperling, M. F. Maitz, C. A. Siedlecki, C. Werner, and M. V Sefton, "The blood compatibility challenge. Part 3: Material associated activation of blood cascades and cells," *Acta Biomater*, vol. 94, pp. 25–32, 2019, doi: https://doi.org/10.1016/j.actbio.2019.06.020.

[5] N. E. Vrana, A. M. Ghaemmaghami, and P. Zorlutuna, "Editorial: Adverse Reactions to Biomaterials: State of the Art in Biomaterial Risk Assessment, Immunomodulation and in vitro Models for Biomaterial Testing," *Front Bioeng Biotechnol*, vol. 7, Feb. 2019, doi: 10.3389/fbioe.2019.00015.

[6] M. Weber *et al.*, "Blood-Contacting Biomaterials: In Vitro Evaluation of the Hemocompatibility," *Front Bioeng Biotechnol*, vol. 6, Jul. 2018, doi: 10.3389/fbioe.2018.00099.

[7] M. B. Gorbet and M. V. Sefton, "Leukocyte activation and leukocyte procoagulant activities after blood contact with polystyrene and polyethylene glycol–immobilized polystyrene beads," *Journal of Laboratory and Clinical Medicine*, vol. 137, no. 5, pp. 345–355, May 2001, doi: 10.1067/mlc.2001.114677.

[8] B. O. Ode Boni, L. Lamboni, T. Souho, M. Gauthier, and G. Yang, "Immunomodulation and cellular response to biomaterials: The overriding role of neutrophils in healing," *Materials Horizons*, vol. 6, no. 6. Royal Society of Chemistry, pp. 1122–1137, Jul. 01, 2019. doi: 10.1039/c9mh00291j.

[9] S. Jhunjhunwala, “Neutrophils at the biological-material interface,” *ACS Biomaterials Science and Engineering*, vol. 4, no. 4. American Chemical Society, pp. 1128–1136, Apr. 09, 2018. doi: 10.1021/acsbiomaterials.6b00743.

[10] M. B. Gorbet and M. V. Sefton, “Biomaterial-associated thrombosis: roles of coagulation factors, complement, platelets and leukocytes,” *Biomaterials*, vol. 25, no. 26, pp. 5681–5703, Nov. 2004, doi: 10.1016/j.biomaterials.2004.01.023.

[11] M. Zare, E. R. Ghomi, P. D. Venkatraman, and S. Ramakrishna, “Silicone-based biomaterials for biomedical applications: Antimicrobial strategies and 3D printing technologies,” *J Appl Polym Sci*, vol. 138, no. 38, p. 50969, Oct. 2021, doi: 10.1002/app.50969.

[12] I. Olsson and T. Olofsson, “Induction of differentiation in a human promyelocytic leukemic cell line (HL-60) *1Production of granule proteins,” *Exp Cell Res*, vol. 131, no. 1, pp. 225–230, Jan. 1981, doi: 10.1016/0014-4827(81)90422-5.

[13] G. R. Pullen and C. S. Hosking, “Differentiated HL60 promyelocytic leukaemia cells have a deficient myeloperoxidase/halide killing system.,” *Clin Exp Immunol*, vol. 62, no. 2, pp. 304–9, Nov. 1985.

[14] A. Clarke, E. LeBlanc, C. Angelatos, K. Russell, S. Karim, and L. A. Wells, “The effects of surface chemistry on the accumulation of extracellular traps on poly(methyl methacrylate) and the implications on other immune cells,” *J Mater Sci*, vol. 57, no. 22, pp. 10299–10312, Jun. 2022, doi: 10.1007/s10853-022-07264-y.

Chapter 2 References

[1] C. Rosales, “Neutrophil: A Cell with Many Roles in Inflammation or Several Cell Types?,” *Front Physiol*, vol. 9, Feb. 2018, doi: 10.3389/fphys.2018.00113.

[2] A. J. Stock, A. Kasus-Jacobi, and H. A. Pereira, “The role of neutrophil granule proteins in neuroinflammation and Alzheimer’s disease,” *J Neuroinflammation*, vol. 15, no. 1, p. 240, Dec. 2018, doi: 10.1186/s12974-018-1284-4.

[3] I. Naegelen, N. Beaume, S. Plançon, V. Schenten, E. J. Tschirhart, and S. Bréchard, "Regulation of Neutrophil Degranulation and Cytokine Secretion: A Novel Model Approach Based on Linear Fitting," *J Immunol Res*, vol. 2015, pp. 1–15, 2015, doi: 10.1155/2015/817038.

[4] B. K. A. Abdel-Salam and H. Ebaid, "Clinical immunology Expression of CD11b and CD18 on polymorphonuclear neutrophils stimulated with interleukin-2," *Central European Journal of Immunology*, vol. 2, pp. 209–215, 2014, doi: 10.5114/ceji.2014.43725.

[5] M. K. Rooney and K. A. Woodhouse, "Decreased tissue factor expression with increased CD11b upregulation on elastin-based biomaterial coatings," *Biomater Sci*, vol. 2, no. 10, p. 1377, Jun. 2014, doi: 10.1039/C4BM00099D.

[6] A. Strohbach and R. Busch, "Predicting the in vivo performance of cardiovascular biomaterials: current approaches in vitro evaluation of blood-biomaterial interactions," *Int J Mol Sci*, vol. 22, no. 21, p. 11390, Oct. 2021, doi: 10.3390/ijms222111390.

[7] K. R. Eichelberger and W. E. Goldman, "Human Neutrophil Isolation and Degranulation Responses to Yersinia pestis Infection," 2019, pp. 197–209. doi: 10.1007/978-1-4939-9541-7_14.

[8] W. Szlasa *et al.*, "Prognostic and Therapeutic Role of CD15 and CD15s in Cancer," *Cancers (Basel)*, vol. 14, no. 9, p. 2203, Apr. 2022, doi: 10.3390/cancers14092203.

[9] S. Watt *et al.*, "CD66 identifies a neutrophil-specific epitope within the hematopoietic system that is expressed by members of the carcinoembryonic antigen family of adhesion molecules," *Blood*, vol. 78, no. 1, pp. 63–74, Jul. 1991, doi: 10.1182/blood.V78.1.63.63.

[10] Y. Lu *et al.*, "CD16 expression on neutrophils predicts treatment efficacy of capecitabine in colorectal cancer patients," *BMC Immunol*, vol. 21, no. 1, p. 46, Dec. 2020, doi: 10.1186/s12865-020-00375-8.

[11] L. Lu, X. Jin, and Q. Zhang, "CD35 and CD64 of Neutrophils Can Differentiate Between Bacterial and Viral Infections in Children by Simultaneous Quantitative Analysis," *Medical Science Monitor*, vol. 25, pp. 7728–7734, Oct. 2019, doi: 10.12659/MSM.914527.

[12] J. M. Anderson, A. Rodriguez, and D. T. Chang, "Foreign body reaction to biomaterials," *Semin Immunol*, vol. 20, no. 2, pp. 86–100, Apr. 2008, doi: 10.1016/j.smim.2007.11.004.

[13] M. A. Wesdorp *et al.*, “A culture model to analyze the acute biomaterial-dependent reaction of human primary neutrophils in vitro,” *Bioact Mater*, vol. 20, pp. 627–637, Feb. 2023, doi: 10.1016/j.bioactmat.2022.05.036.

[14] S. Jhunjhunwala, “Neutrophils at the biological-material interface,” *ACS Biomaterials Science and Engineering*, vol. 4, no. 4. American Chemical Society, pp. 1128–1136, Apr. 09, 2018. doi: 10.1021/acsbiomaterials.6b00743.

[15] N. Tamassia *et al.*, “Cytokine production by human neutrophils: Revisiting the ‘dark side of the moon,’” *Eur J Clin Invest*, vol. 48, p. e12952, Nov. 2018, doi: 10.1111/eci.12952.

[16] V. Witko-Sarsat, P. Rieu, B. Descamps-Latscha, P. Lesavre, and L. Halbwachs-Mecarelli, “Neutrophils: Molecules, Functions and Pathophysiological Aspects,” *Laboratory Investigation*, vol. 80, no. 5, pp. 617–653, May 2000, doi: 10.1038/labinvest.3780067.

[17] B. O. Ode Boni, L. Lamboni, T. Souho, M. Gauthier, and G. Yang, “Immunomodulation and cellular response to biomaterials: The overriding role of neutrophils in healing,” *Materials Horizons*, vol. 6, no. 6. Royal Society of Chemistry, pp. 1122–1137, Jul. 01, 2019. doi: 10.1039/c9mh00291j.

[18] V. Brinkmann *et al.*, “Neutrophil extracellular traps kill bacteria,” *Science (1979)*, vol. 303, no. 5663, pp. 1532–1535, Mar. 2004, doi: 10.1126/science.1092385.

[19] M. J. Kaplan and M. Radic, “Neutrophil extracellular traps: double-edged swords of innate immunity,” *The Journal of Immunology*, vol. 189, no. 6, pp. 2689–2695, Sep. 2012, doi: 10.4049/jimmunol.1201719.

[20] Q. Remijsen, T. W. Kuijpers, E. Wirawan, S. Lippens, P. Vandenabeele, and T. vanden Berghe, “Dying for a cause: NETosis, mechanisms behind an antimicrobial cell death modality,” *Cell Death Differ*, vol. 18, no. 4, pp. 581–588, Apr. 2011, doi: 10.1038/cdd.2011.1.

[21] N. v. Vorobjeva and B. v. Chernyak, “NETosis: molecular mechanisms, role in physiology and pathology,” *Biochemistry (Moscow)*, vol. 85, no. 10, pp. 1178–1190, Oct. 2020, doi: 10.1134/S0006297920100065.

[22] Q. Remijsen, T. W. Kuijpers, E. Wirawan, S. Lippens, P. Vandenabeele, and T. vanden Berghe, “Dying for a cause: NETosis, mechanisms behind an antimicrobial cell death modality,” *Cell Death Differ*, vol. 18, no. 4, pp. 581–588, Apr. 2011, doi: 10.1038/cdd.2011.1.

[23] C. M. de Bont, W. C. Boelens, and G. J. M. Pruijn, “NETosis, complement, and coagulation: a triangular relationship,” *Cell Mol Immunol*, vol. 16, no. 1, pp. 19–27, Jan. 2019, doi: 10.1038/s41423-018-0024-0.

[24] B. G. Yipp and P. Kubes, “NETosis: how vital is it?,” *Blood*, vol. 122, no. 16, pp. 2784–2794, Oct. 2013, doi: 10.1182/blood-2013-04-457671.

[25] W. Stoiber, A. Obermayer, P. Steinbacher, and W.-D. Krautgartner, “The role of reactive oxygen species (ROS) in the formation of extracellular traps (ETs) in humans,” *Biomolecules*, vol. 5, no. 2, pp. 702–723, May 2015, doi: 10.3390/biom5020702.

[26] H. R. Thiam *et al.*, “NETosis proceeds by cytoskeleton and endomembrane disassembly and PAD4-mediated chromatin decondensation and nuclear envelope rupture”, doi: 10.1073/pnas.1909546117/-/DCSupplemental.

[27] H. Yang, M. H. Biermann, J. M. Brauner, Y. Liu, Y. Zhao, and M. Herrmann, “New insights into neutrophil extracellular traps: mechanisms of formation and role in inflammation,” *Front Immunol*, vol. 7, Aug. 2016, doi: 10.3389/fimmu.2016.00302.

[28] S. Collins, “The HL-60 promyelocytic leukemia cell line: proliferation, differentiation, and cellular oncogene expression,” *Blood*, vol. 70, no. 5, pp. 1233–1244, Nov. 1987, doi: 10.1182/blood.V70.5.1233.1233.

[29] J. M. Collins and K. A. Foster, “Differentiation of promyelocytic (HL-60) cells into mature granulocytes: mitochondrial-specific rhodamine 123 fluorescence.,” *Journal of Cell Biology*, vol. 96, no. 1, pp. 94–99, Jan. 1983, doi: 10.1083/jcb.96.1.94.

[30] G. Ciapetti *et al.*, “In vitro testing of the potential for orthopedic bone cements to cause apoptosis of osteoblast-like cells,” *Biomaterials*, vol. 23, no. 2, pp. 617–627, Jan. 2002, doi: 10.1016/S0142-9612(01)00149-1.

[31] A. Clarke, E. LeBlanc, C. Angelatos, K. Russell, S. Karim, and L. A. Wells, “The effects of surface chemistry on the accumulation of extracellular traps on poly(methyl methacrylate) and the implications on other immune cells,” *J Mater Sci*, vol. 57, no. 22, pp. 10299–10312, Jun. 2022, doi: 10.1007/s10853-022-07264-y.

[32] S. Abri, R. Attia, D. D. Pukale, and N. D. Leipzig, “Modulatory contribution of oxygenating hydrogels and polyhexamethylene biguanide on the antimicrobial potency of neutrophil-like

cells," *ACS Biomater Sci Eng*, vol. 8, no. 9, pp. 3842–3855, Sep. 2022, doi: 10.1021/acsbiomaterials.2c00292.

[33] R. Verdon *et al.*, "Neutrophil activation by nanomaterials in vitro: comparing strengths and limitations of primary human cells with those of an immortalized (HL-60) cell line," *Nanotoxicology*, vol. 15, no. 1, pp. 1–20, 2021, doi: 10.1080/17435390.2020.1834635.

[34] A. Manda-Handzlik *et al.*, "The influence of agents differentiating HL-60 cells toward granulocyte-like cells on their ability to release neutrophil extracellular traps," *Immunol Cell Biol*, vol. 96, no. 4, pp. 413–425, Apr. 2018, doi: 10.1111/imcb.12015.

[35] Z. Xu *et al.*, "Kindlin-3 negatively regulates the release of neutrophil extracellular traps," *J Leukoc Biol*, vol. 104, no. 3, pp. 597–602, Sep. 2018, doi: 10.1002/JLB.3AB0118-005R.

[36] Y. Takishita *et al.*, "Formation of neutrophil extracellular traps in mitochondrial DNA-deficient cells," *J Clin Biochem Nutr*, vol. 66, no. 1, pp. 15–23, 2020, doi: 10.3164/jcbn.19-77.

[37] Y. Guo *et al.*, "Differentiation of HL-60 cells in serum-free hematopoietic cell media enhances the production of neutrophil extracellular traps," *Exp Ther Med*, vol. 21, no. 4, p. 353, Feb. 2021, doi: 10.3892/etm.2021.9784.

[38] D. Nakazawa *et al.*, "Enhanced formation and disordered regulation of NETs in myeloperoxidase-ANCA–associated microscopic polyangiitis," *Journal of the American Society of Nephrology*, vol. 25, no. 5, pp. 990–997, May 2014, doi: 10.1681/ASN.2013060606.

[39] K. Kessenbrock *et al.*, "Netting neutrophils in autoimmune small-vessel vasculitis," *Nat Med*, vol. 15, no. 6, pp. 623–625, Jun. 2009, doi: 10.1038/nm.1959.

[40] D. Nakazawa *et al.*, "Abnormal conformation and impaired degradation of propylthiouracil-induced neutrophil extracellular traps: Implications of disordered neutrophil extracellular traps in a rat model of myeloperoxidase antineutrophil cytoplasmic antibody-associated vasculiti," *Arthritis Rheum*, vol. 64, no. 11, pp. 3779–3787, Nov. 2012, doi: 10.1002/art.34619.

[41] A. E. Fetz, W. E. King, B. A. Minden-Birkenmaier, and G. L. Bowlin, "Methods for Quantifying Neutrophil Extracellular Traps on Biomaterials," 2022, pp. 727–742. doi: 10.1007/978-1-0716-1811-0_38.

[42] S. Thakur, D. I. Cattoni, and M. Nöllmann, “The fluorescence properties and binding mechanism of SYTOX green, a bright, low photo-damage DNA intercalating agent,” *European Biophysics Journal*, vol. 44, no. 5, pp. 337–348, Jul. 2015, doi: 10.1007/s00249-015-1027-8.

[43] S. Jhunjhunwala *et al.*, “Neutrophil responses to sterile implant materials,” *PLoS One*, vol. 10, no. 9, p. e0137550, Sep. 2015, doi: 10.1371/journal.pone.0137550.

[44] T. Mohanty, O. E. Sørensen, and P. Nordenfelt, “NETQUANT: automated quantification of neutrophil extracellular traps,” *Front Immunol*, vol. 8, Jan. 2018, doi: 10.3389/fimmu.2017.01999.

[45] R. Rebernick *et al.*, “DNA area and NETosis analysis (DANA): a high-throughput method to quantify neutrophil extracellular traps in fluorescent microscope images,” *Biol Proced Online*, vol. 20, no. 1, p. 7, Dec. 2018, doi: 10.1186/s12575-018-0072-y.

[46] D. Nakazawa *et al.*, “Abnormal conformation and impaired degradation of propylthiouracil-induced neutrophil extracellular traps: Implications of disordered neutrophil extracellular traps in a rat model of myeloperoxidase antineutrophil cytoplasmic antibody-associated vasculiti,” *Arthritis Rheum*, vol. 64, no. 11, pp. 3779–3787, Nov. 2012, doi: 10.1002/art.34619.

[47] K. Kessenbrock *et al.*, “Netting neutrophils in autoimmune small-vessel vasculitis,” *Nat Med*, vol. 15, no. 6, pp. 623–625, Jun. 2009, doi: 10.1038/nm.1959.

[48] B. Matta, J. Battaglia, and B. J. Barnes, “Detection of neutrophil extracellular traps in patient plasma: method development and validation in systemic lupus erythematosus and healthy donors that carry IRF5 genetic risk,” *Front Immunol*, vol. 13, Jul. 2022, doi: 10.3389/fimmu.2022.951254.

[49] S. J. Donkel, F. J. Wolters, M. A. Ikram, and M. P. M. de Maat, “Circulating Myeloperoxidase (MPO)-DNA complexes as marker for Neutrophil Extracellular Traps (NETs) levels and the association with cardiovascular risk factors in the general population,” *PLoS One*, vol. 16, no. 8, p. e0253698, Aug. 2021, doi: 10.1371/journal.pone.0253698.

[50] B. Matta, J. Battaglia, and B. J. Barnes, “Detection of neutrophil extracellular traps in patient plasma: method development and validation in systemic lupus erythematosus and healthy donors that carry IRF5 genetic risk,” *Front Immunol*, vol. 13, Jul. 2022, doi: 10.3389/fimmu.2022.951254.

[51] H. Hayden *et al.*, “ELISA detection of MPO-DNA complexes in human plasma is error-prone and yields limited information on neutrophil extracellular traps formed in vivo,” *PLoS One*, vol. 16, no. 4, p. e0250265, Apr. 2021, doi: 10.1371/journal.pone.0250265.

[52] K. M. McKinnon, “Flow Cytometry: An Overview,” *Curr Protoc Immunol*, vol. 120, no. 1, Jan. 2018, doi: 10.1002/cpim.40.

[53] J. Perdomo *et al.*, “Neutrophil activation and NETosis are the major drivers of thrombosis in heparin-induced thrombocytopenia,” *Nat Commun*, vol. 10, no. 1, p. 1322, Mar. 2019, doi: 10.1038/s41467-019-09160-7.

[54] E. Schneck *et al.*, “Flow cytometry-based quantification of neutrophil extracellular traps shows an association with hypercoagulation in septic shock and hypocoagulation in postsurgical systemic inflammation—a proof-of-concept study,” *J Clin Med*, vol. 9, no. 1, p. 174, Jan. 2020, doi: 10.3390/jcm9010174.

[55] M. Gavillet *et al.*, “Flow cytometric assay for direct quantification of neutrophil extracellular traps in blood samples,” *Am J Hematol*, vol. 90, no. 12, pp. 1155–1158, Dec. 2015, doi: 10.1002/ajh.24185.

[56] C. P. Verschoor, A. Lelic, J. L. Bramson, and D. M. E. Bowdish, “An Introduction to Automated Flow Cytometry Gating Tools and Their Implementation,” *Front Immunol*, vol. 6, Jul. 2015, doi: 10.3389/fimmu.2015.00380.

[57] Y. K. Sung, D. R. Lee, and D. J. Chung, “Advances in the development of hemostatic biomaterials for medical application,” *Biomater Res*, vol. 25, no. 1, p. 37, Dec. 2021, doi: 10.1186/s40824-021-00239-1.

[58] M. M. Hale and S. H. Medina, “Biomaterials-enabled antithrombotics: recent advances and emerging strategies,” *Mol Pharm*, vol. 19, no. 12, pp. 4453–4465, Dec. 2022, doi: 10.1021/acs.molpharmaceut.2c00626.

[59] L. Vitkov *et al.*, “The initial inflammatory response to bioactive implants is characterized by NETosis,” *PLoS One*, vol. 10, no. 3, p. e0121359, Mar. 2015, doi: 10.1371/journal.pone.0121359.

[60] J. O. Abaricia, A. H. Shah, R. M. Musselman, and R. Olivares-Navarrete, “Hydrophilic titanium surfaces reduce neutrophil inflammatory response and NETosis,” *Biomater Sci*, vol. 8, no. 8, pp. 2289–2299, Apr. 2020, doi: 10.1039/c9bm01474h.

[61] J. O. Abaricia, A. H. Shah, and R. Olivares-Navarrete, “Substrate stiffness induces neutrophil extracellular trap (NET) formation through focal adhesion kinase activation,” *Biomaterials*, vol. 271, Apr. 2021, doi: 10.1016/j.biomaterials.2021.120715.

[62] T. Shay *et al.*, “Conservation and divergence in the transcriptional programs of the human and mouse immune systems,” *Proceedings of the National Academy of Sciences*, vol. 110, no. 8, pp. 2946–2951, Feb. 2013, doi: 10.1073/pnas.1222738110.

[63] A. M. Condliffe, “Sequential activation of class IB and class IA PI3K is important for the primed respiratory burst of human but not murine neutrophils,” *Blood*, vol. 106, no. 4, pp. 1432–1440, Aug. 2005, doi: 10.1182/blood-2005-03-0944.

[64] J. Bagaitkar, J. D. Matute, A. Austin, A. A. Arias, and M. C. Dinauer, “Activation of neutrophil respiratory burst by fungal particles requires phosphatidylinositol 3-phosphate binding to p40phox in humans but not in mice,” *Blood*, vol. 120, no. 16, pp. 3385–3387, Oct. 2012, doi: 10.1182/blood-2012-07-445619.

[65] L. Erpenbeck *et al.*, “Effect of adhesion and substrate elasticity on neutrophil extracellular trap formation,” *Front Immunol*, vol. 10, Oct. 2019, doi: 10.3389/fimmu.2019.02320.

[66] Q. Remijsen *et al.*, “Neutrophil extracellular trap cell death requires both autophagy and superoxide generation,” *Cell Res*, vol. 21, no. 2, pp. 290–304, Feb. 2011, doi: 10.1038/cr.2010.150.

[67] W. E. King and G. L. Bowlin, “Mechanical characterization and neutrophil NETs response of a novel hybrid geometry polydioxanone near-field electrospun scaffold,” *Biomedical Materials*, vol. 16, no. 6, p. 065002, Nov. 2021, doi: 10.1088/1748-605X/ac1e43.

[68] A. E. Fetz, I. Neeli, I. A. Rodriguez, M. Z. Radic, and G. L. Bowlin, “Electrospun Template Architecture and Composition Regulate Neutrophil NETosis in Vitro and in Vivo,” *Tissue Eng Part A*, vol. 23, no. 19–20, pp. 1054–1063, Oct. 2017, doi: 10.1089/ten.tea.2016.0452.

[69] A. E. Fetz *et al.*, “Localized delivery of Cl-amidine from electrospun polydioxanone templates to regulate acute neutrophil NETosis: A preliminary evaluation of the PAD4 inhibitor for tissue engineering,” *Front Pharmacol*, vol. 9, no. MAR, Mar. 2018, doi: 10.3389/fphar.2018.00289.

[70] A. E. Fetz, M. Z. Radic, and G. L. Bowlin, “Human neutrophil FcγRIIIb regulates neutrophil extracellular trap release in response to electrospun polydioxanone biomaterials,” *Acta Biomater*, vol. 130, pp. 281–290, Aug. 2021, doi: 10.1016/j.actbio.2021.06.007.

[71] C. Sperling, M. Fischer, M. F. Maitz, and C. Werner, “Neutrophil extracellular trap formation upon exposure of hydrophobic materials to human whole blood causes thrombogenic reactions,” *Biomater Sci*, vol. 5, no. 10, pp. 1998–2008, 2017, doi: 10.1039/C7BM00458C.

[72] Y. J. Lu *et al.*, “Mechanism of nanoformulated graphene oxide-mediated human neutrophil activation,” *ACS Appl Mater Interfaces*, vol. 12, no. 36, pp. 40141–40152, Sep. 2020, doi: 10.1021/acsami.0c12490.

[73] R. Bilyy *et al.*, “Inert coats of magnetic nanoparticles prevent formation of occlusive intravascular co-aggregates with neutrophil extracellular traps,” *Front Immunol*, vol. 9, no. OCT, Oct. 2018, doi: 10.3389/fimmu.2018.02266.

[74] L. E. Muñoz *et al.*, “Nanoparticles size-dependently initiate self-limiting NETosis-driven inflammation,” *Proc Natl Acad Sci U S A*, vol. 113, no. 40, pp. E5856–E5865, Oct. 2016, doi: 10.1073/pnas.1602230113.

[75] S. Keshavan, P. Calligari, L. Stella, L. Fusco, L. G. Delogu, and B. Fadeel, “Nano-bio interactions: a neutrophil-centric view,” *Cell Death and Disease*, vol. 10, no. 8. Nature Publishing Group, Aug. 01, 2019. doi: 10.1038/s41419-019-1806-8.

[76] P. W. Bisso, S. Gaglione, P. P. G. Guimarães, M. J. Mitchell, and R. Langer, “Nanomaterial interactions with human neutrophils,” *ACS Biomater Sci Eng*, vol. 4, no. 12, pp. 4255–4265, Dec. 2018, doi: 10.1021/acsbiomaterials.8b01062.

[77] H. Yang *et al.*, “Nanomaterial exposure induced neutrophil extracellular traps: a new target in inflammation and innate immunity,” *J Immunol Res*, vol. 2019, pp. 1–8, Feb. 2019, doi: 10.1155/2019/3560180.

[78] E. Huberman, G. R. Braslawsky, M. Callaham, and H. Fugiki, “Induction of differentiation of human promyelocytic leukemia (HL-60) cells by teleocidin and phorbol-12-myristate-13-acetate,” *Carcinogenesis*, vol. 3, no. 1, pp. 111–114, 1982, doi: 10.1093/carcin/3.1.111.

[79] S. Murao, M. A. Gemmell, M. F. Callaham, N. L. Anderson, and E. Huberman, “Control of macrophage cell differentiation in human promyelocytic HL-60 leukemia cells by 1,25-dihydroxyvitamin D3 and phorbol-12-myristate-13-acetate.,” *Cancer Res*, vol. 43, no. 10, pp. 4989–96, Oct. 1983.

[80] R. Winzen *et al.*, “Selective decrease in cell surface expression and mRNA level of the 55-kDa tumor necrosis factor receptor during differentiation of HL-60 cells into macrophage-like but not granulocyte-like cells.,” *J Immunol*, vol. 148, no. 11, pp. 3454–60, Jun. 1992.

[81] P. I. Padilla *et al.*, “Morphologic differentiation of HL-60 cells is associated with appearance of RPTPβ and induction of helicobacter pyloriVacA sensitivity,” *Journal of Biological Chemistry*, vol. 275, no. 20, pp. 15200–15206, May 2000, doi: 10.1074/jbc.275.20.15200.

[82] S. Launay *et al.*, “Lineage-specific modulation of calcium pump expression during myeloid differentiation.,” *Blood*, vol. 93, no. 12, pp. 4395–405, Jun. 1999.

[83] Y. Iwasaki, S.-I. Sawada, K. Ishihara, G. Khang, and H. B. Lee, “Reduction of surface-induced inflammatory reaction on PLGA/MPC polymer blend,” 2002.

[84] H. Y. Shin, D. M. Frechette, N. Rohner, X. Zhang, D. A. Puleo, and L. M. Bjursten, “Dependence of macrophage superoxide release on the pulse amplitude of an applied pressure regime: a potential factor at the soft tissue-implant interface,” *J Tissue Eng Regen Med*, vol. 10, no. 3, pp. E227–E238, Mar. 2016, doi: 10.1002/term.1789.

[85] D. Scieszka, Y.-H. Lin, W. Li, S. Choudhury, Y. Yu, and M. Freire, “Netome: the molecular characterization of neutrophil extracellular Traps (NETs)”, doi: 10.1101/2020.05.18.102772.

[86] R. Goggs, U. Jeffery, D. N. LeVine, and R. H. L. Li, “Neutrophil-extracellular traps, cell-free DNA, and immunothrombosis in companion animals: a review,” *Vet Pathol*, vol. 57, no. 1, pp. 6–23, Jan. 2020, doi: 10.1177/0300985819861721.

[87] G. Marsman, S. Zeerleder, and B. M. Luken, “Extracellular histones, cell-free DNA, or nucleosomes: differences in immunostimulation,” *Cell Death Dis*, vol. 7, no. 12, pp. e2518–e2518, Dec. 2016, doi: 10.1038/cddis.2016.410.

[88] J. Aucamp, A. J. Bronkhorst, C. P. S. Badenhorst, and P. J. Pretorius, “The diverse origins of circulating cell-free DNA in the human body: a critical re-evaluation of the literature,” *Biological Reviews*, vol. 93, no. 3, pp. 1649–1683, Aug. 2018, doi: 10.1111/brv.12413.

[89] A. M. Santos-Beneit and F. Mollinedo, “Expression of genes involved in initiation, regulation, and execution of apoptosis in human neutrophils and during neutrophil differentiation of HL-60 cells,” *J Leukoc Biol*, vol. 67, no. 5, pp. 712–724, May 2000, doi: 10.1002/jlb.67.5.712.

[90] R. W. G. Watson, O. D. Rotstein, J. Parodo, R. Bitar, D. Hackam, and J. C. Marshall, “Granulocytic differentiation of HL-60 cells results in spontaneous apoptosis mediated by increased caspase expression,” *FEBS Lett*, vol. 412, no. 3, pp. 603–609, Aug. 1997, doi: 10.1016/S0014-5793(97)00779-5.

[91] H. Sun and Y. Wang, “Apoptosis of human leukemic HL-60 cells induced to differentiate by treatment with RA or DMSO,” *Cell Res*, vol. 5, no. 2, pp. 181–186, Dec. 1995, doi: 10.1038/cr.1995.17.

[92] S. J. Martin, J. G. Bradley, and T. G. Cotter, “HL-60 cells induced to differentiate towards neutrophils subsequently die via apoptosis,” *Clin Exp Immunol*, vol. 79, no. 3, pp. 448–453, Jun. 2008, doi: 10.1111/j.1365-2249.1990.tb08110.x.

[93] E. Rincón, B. L. Rocha-Gregg, and S. R. Collins, “A map of gene expression in neutrophil-like cell lines,” *BMC Genomics*, vol. 19, no. 1, p. 573, Dec. 2018, doi: 10.1186/s12864-018-4957-6.

[94] K. E. Rennoll-Bankert, S. H. Sinclair, M. A. Lichay, and J. S. Dumler, “Comparison and characterization of granulocyte cell models for Anaplasma phagocytophilum infection,” *Pathog Dis*, vol. 71, no. 1, pp. 55–64, Jun. 2014, doi: 10.1111/2049-632X.12111.

[95] K. A. Babatunde, X. Wang, A. Hopke, N. Lannes, P.-Y. Mantel, and D. Irimia, “Chemotaxis and swarming in differentiated HL-60 neutrophil-like cells,” *Sci Rep*, vol. 11, no. 1, p. 778, Jan. 2021, doi: 10.1038/s41598-020-78854-6.

[96] E. F. Kenny *et al.*, “Diverse stimuli engage different neutrophil extracellular trap pathways,” *Elife*, vol. 6, Jun. 2017, doi: 10.7554/eLife.24437.

[97] S. L. Wong and D. D. Wagner, “Peptidylarginine deiminase 4: a nuclear button triggering neutrophil extracellular traps in inflammatory diseases and aging,” *The FASEB Journal*, vol. 32, no. 12, pp. 6258–6370, Sep. 2018, doi: 10.1096/fj.201800691R.

[98] A. S. Rohrbach, D. J. Slade, P. R. Thompson, and K. A. Mowen, “Activation of PAD4 in NET formation,” *Frontiers in Immunology*, vol. 3, no. NOV. 2012. doi: 10.3389/fimmu.2012.00360.

[99] I. Neeli, S. N. Khan, and M. Radic, “Histone deimination as a response to inflammatory stimuli in neutrophils,” *The Journal of Immunology*, vol. 180, no. 3, pp. 1895–1902, Feb. 2008, doi: 10.4049/jimmunol.180.3.1895.

[100] Y. Wang *et al.*, “Histone hypercitrullination mediates chromatin decondensation and neutrophil extracellular trap formation,” *Journal of Cell Biology*, vol. 184, no. 2, pp. 205–213, Jan. 2009, doi: 10.1083/jcb.200806072.

[101] R. Yaseen *et al.*, “Antimicrobial activity of HL-60 cells compared to primary blood-derived neutrophils against Staphylococcus aureus,” *J Negat Results Biomed*, vol. 16, no. 1, Feb. 2017, doi: 10.1186/s12952-017-0067-2.

[102] A. M. McInturff *et al.*, “Mammalian target of rapamycin regulates neutrophil extracellular trap formation via induction of hypoxia-inducible factor 1 α,” *Blood*, vol. 120, no. 15, pp. 3118–3125, Oct. 2012, doi: 10.1182/blood-2012-01-405993.

[103] T. Kawakami *et al.*, “Rab27a is essential for the formation of neutrophil extracellular traps (NETs) in neutrophil-like differentiated HL60 cells,” *PLoS One*, vol. 9, no. 1, p. e84704, Jan. 2014, doi: 10.1371/journal.pone.0084704.

[104] H. M. Alyami, L. S. Finoti, H. S. Teixeira, A. Aljefri, D. F. Kinane, and M. R. Benakanakere, “Role of NOD1/NOD2 receptors in Fusobacterium nucleatum mediated NETosis,” *Microb Pathog*, vol. 131, pp. 53–64, Jun. 2019, doi: 10.1016/j.micpath.2019.03.036.

[105] T. Tokuhiro *et al.*, “Oxidized phospholipids and neutrophil elastase coordinately play critical roles in NET formation,” *Front Cell Dev Biol*, vol. 9, Sep. 2021, doi: 10.3389/fcell.2021.718586.

[106] C. H. Lu *et al.*, “The fcγriii engagement augments pma-stimulated neutrophil extracellular traps (Nets) formation by granulocytes partially via cross-talk between syk-erk-nf-κb and pkc-ros signaling pathways,” *Biomedicines*, vol. 9, no. 9, Sep. 2021, doi: 10.3390/biomedicines9091127.

[107] L. P. Mendes *et al.*, “Monoclonal antibody 2C5 specifically targets neutrophil extracellular traps,” *MAbs*, vol. 12, no. 1, 2020, doi: 10.1080/19420862.2020.1850394.

[108] A. Manda-Handzlik *et al.*, “Nitric oxide and peroxynitrite trigger and enhance release of neutrophil extracellular traps,” *Cellular and Molecular Life Sciences*, vol. 77, no. 15, pp. 3059–3075, Aug. 2020, doi: 10.1007/s00018-019-03331-x.

[109] C. Spruell and A. B. Baker, “Analysis of a high-throughput cone-and-plate apparatus for the application of defined spatiotemporal flow to cultured cells,” *Biotechnol Bioeng*, vol. 110, no. 6, pp. 1782–1793, Jun. 2013, doi: 10.1002/bit.24823.

[110] A. U. Oza and D. C. Venerus, “The dynamics of parallel-plate and cone–plate flows,” *Physics of Fluids*, vol. 33, no. 2, p. 023102, Feb. 2021, doi: 10.1063/5.0036980.

[111] H. Y. Song, R. Salehiyan, X. Li, S. H. Lee, and K. Hyun, “A comparative study of the effects of cone-plate and parallel-plate geometries on rheological properties under oscillatory shear flow,” *Korea-Australia Rheology Journal*, vol. 29, no. 4, pp. 281–294, Nov. 2017, doi: 10.1007/s13367-017-0028-9.

[112] M. Franzoni, I. Cattaneo, B. Ene-Iordache, A. Oldani, P. Righettini, and A. Remuzzi, “Design of a cone-and-plate device for controlled realistic shear stress stimulation on endothelial cell monolayers,” *Cytotechnology*, vol. 68, no. 5, pp. 1885–1896, Oct. 2016, doi: 10.1007/s10616-015-9941-2.

[113] L. H. O. Hellström, M. A. Samaha, K. M. Wang, A. J. Smits, and M. Hultmark, “Errors in parallel-plate and cone-plate rheometer measurements due to sample underfill,” *Meas Sci Technol*, vol. 26, no. 1, p. 015301, Jan. 2015, doi: 10.1088/0957-0233/26/1/015301.

[114] A. Fuhrmann and A. J. Engler, “Acute shear stress direction dictates adherent cell remodeling and verifies shear profile of spinning disk assays,” *Phys Biol*, vol. 12, no. 1, p. 016011, Jan. 2015, doi: 10.1088/1478-3975/12/1/016011.

[115] H. Hino, S. Hashimoto, and Y. Takahasi, “Effect of Shear Stress in Flow on Cultured Cell: Using Rotating Disk at Microscope,” *SYSTEMICS, CYBERNETICS AND INFORMATICS*, vol. 14, no. 4, 2016.

[116] P. Sungkhaphaitoon, S. Wisutmethangoon, and T. Plookphol, “Influence of Process Parameters on Zinc Powder Produced by Centrifugal Atomisation,” *Materials Research*, vol. 20, no. 3, pp. 718–724, Apr. 2017, doi: 10.1590/1980-5373-mr-2015-0674.

[117] P. Pattanayak *et al.*, “Microfluidic chips: recent advances, critical strategies in design, applications and future perspectives,” *Microfluid Nanofluidics*, vol. 25, no. 12, p. 99, Dec. 2021, doi: 10.1007/s10404-021-02502-2.

[118] J. K. Nunes and H. A. Stone, “Introduction: Microfluidics,” *Chem Rev*, vol. 122, no. 7, pp. 6919–6920, Apr. 2022, doi: 10.1021/acs.chemrev.2c00052.

[119] A.-G. Niculescu, C. Chircov, A. C. Bîrcă, and A. M. Grumezescu, “Fabrication and Applications of Microfluidic Devices: A Review,” *Int J Mol Sci*, vol. 22, no. 4, p. 2011, Feb. 2021, doi: 10.3390/ijms22042011.

[120] C.-S. Lee, “Grand Challenges in Microfluidics: A Call for Biological and Engineering Action,” *Frontiers in Sensors*, vol. 1, Sep. 2020, doi: 10.3389/fsens.2020.583035.

[121] S. Wu, X. Wang, Z. Li, S. Zhang, and F. Xing, “Recent Advances in the Fabrication and Application of Graphene Microfluidic Sensors,” *Micromachines (Basel)*, vol. 11, no. 12, p. 1059, Nov. 2020, doi: 10.3390/mi11121059.

[122] P. H. Reinhardt, J. F. Elliott, and P. Kubes, “Neutrophils Can Adhere Via α4β1 -Integrin Under Flow Conditions,” *Blood*, vol. 89, no. 10, pp. 3837–3846, May 1997, doi: 10.1182/blood.V89.10.3837.

[123] Y. Zhang and S. Neelamegham, “Estimating the Efficiency of Cell Capture and Arrest in Flow Chambers: Study of Neutrophil Binding via E-selectin and ICAM-1,” *Biophys J*, vol. 83, no. 4, pp. 1934–1952, Oct. 2002, doi: 10.1016/S0006-3495(02)73956-8.

[124] D. P. Boso, Ferrari, Decuzzi, and Schrefler, “Optimizing particle size for targeting diseased microvasculature: from experiments to artificial neural networks,” *Int J Nanomedicine*, p. 1517, Jul. 2011, doi: 10.2147/IJN.S20283.

[125] J.-J. Chiu *et al.*, “Analysis of the effect of disturbed flow on monocytic adhesion to endothelial cells,” *J Biomech*, vol. 36, no. 12, pp. 1883–1895, Dec. 2003, doi: 10.1016/S0021-9290(03)00210-0.

[126] D. C. Brown and R. S. Larson, “Improvements to parallel plate flow chambers to reduce reagent and cellular requirements,” *BMC Immunol*, vol. 2, no. 1, p. 9, 2001, doi: 10.1186/1471-2172-2-9.

Chapter 3 References

[1] B. G. Yipp and P. Kubes, "NETosis: how vital is it?," *Blood*, vol. 122, no. 16, pp. 2784–2794, Oct. 2013, doi: 10.1182/blood-2013-04-457671.

[2] C. M. de Bont, W. C. Boelens, and G. J. M. Pruijn, "NETosis, complement, and coagulation: a triangular relationship," *Cell Mol Immunol*, vol. 16, no. 1, pp. 19–27, Jan. 2019, doi: 10.1038/s41423-018-0024-0.

[3] X. Yu and S. Diamond, "Fibrin Modulates Shear-Induced NETosis in Sterile Occlusive Thrombi Formed under Haemodynamic Flow," *Thromb Haemost*, vol. 119, no. 04, pp. 586–593, Apr. 2019, doi: 10.1055/s-0039-1678529.

[4] X. Yu, J. Tan, and S. L. Diamond, "Hemodynamic force triggers rapid NETosis within sterile thrombotic occlusions," *Journal of Thrombosis and Haemostasis*, vol. 16, no. 2, pp. 316–329, Feb. 2018, doi: 10.1111/jth.13907.

[5] C. Sperling, M. Fischer, M. F. Maitz, and C. Werner, "Neutrophil extracellular trap formation upon exposure of hydrophobic materials to human whole blood causes thrombogenic reactions," *Biomater Sci*, vol. 5, no. 10, pp. 1998–2008, 2017, doi: 10.1039/C7BM00458C.

[6] S. Jhunjhunwala *et al.*, "Neutrophil responses to sterile implant materials," *PLoS One*, vol. 10, no. 9, p. e0137550, Sep. 2015, doi: 10.1371/journal.pone.0137550.

[7] A. Strohbach and R. Busch, "Predicting the in vivo performance of cardiovascular biomaterials: current approaches in vitro evaluation of blood-biomaterial interactions," *Int J Mol Sci*, vol. 22, no. 21, p. 11390, Oct. 2021, doi: 10.3390/ijms222111390.

[8] W. Beaubien-Souligny, P.-E. Neagoe, D. Gagnon, A. Y. Denault, and M. G. Sirois, "Increased circulating levels of neutrophil extracellular traps during cardiopulmonary bypass," *CJC Open*, vol. 2, no. 2, pp. 39–48, Mar. 2020, doi: 10.1016/j.cjco.2019.12.001.

[9] A. E. Fetz, M. Z. Radic, and G. L. Bowlin, "Human neutrophil FcγRIIIb regulates neutrophil extracellular trap release in response to electrospun polydioxanone biomaterials," *Acta Biomater*, vol. 130, pp. 281–290, Aug. 2021, doi: 10.1016/j.actbio.2021.06.007.

[10] A. E. Fetz *et al.*, “Localized delivery of Cl-amidine from electrospun polydioxanone templates to regulate acute neutrophil NETosis: A preliminary evaluation of the PAD4 inhibitor for tissue engineering,” *Front Pharmacol*, vol. 9, no. MAR, Mar. 2018, doi: 10.3389/fphar.2018.00289.

[11] L. Vitkov *et al.*, “The initial inflammatory response to bioactive implants is characterized by NETosis,” *PLoS One*, vol. 10, no. 3, p. e0121359, Mar. 2015, doi: 10.1371/journal.pone.0121359.

[12] J. O. Abaricia, A. H. Shah, R. M. Musselman, and R. Olivares-Navarrete, “Hydrophilic titanium surfaces reduce neutrophil inflammatory response and NETosis,” *Biomater Sci*, vol. 8, no. 8, pp. 2289–2299, Apr. 2020, doi: 10.1039/c9bm01474h.

[13] R. S. Keshari, A. Verma, M. K. Barthwal, and M. Dikshit, “Reactive oxygen species-induced activation of ERK and p38 MAPK mediates PMA-induced NETs release from human neutrophils,” *J Cell Biochem*, vol. 114, no. 3, pp. 532–540, Mar. 2013, doi: 10.1002/jcb.24391.

[14] A. D. Verin *et al.*, “Role of Ras-dependent ERK activation in phorbol ester-induced endothelial cell barrier dysfunction,” *American Journal of Physiology-Lung Cellular and Molecular Physiology*, vol. 279, no. 2, pp. L360–L370, Aug. 2000, doi: 10.1152/ajplung.2000.279.2.L360.

[15] R. L. Degroote, M. Weigand, S. M. Hauck, and C. A. Deeg, “IL8 and PMA Trigger the Regulation of Different Biological Processes in Granulocyte Activation,” *Front Immunol*, vol. 10, Jan. 2020, doi: 10.3389/fimmu.2019.03064.

[16] M. P. Pruchniak and U. Demkow, “Potent NETosis inducers do not show synergistic effects in vitro,” *Central European Journal of Immunology*, vol. 44, no. 1, pp. 51–58, 2019, doi: 10.5114/ceji.2019.84017.

[17] A. Millius and O. D. Weiner, “Manipulation of Neutrophil-Like HL-60 Cells for the Study of Directed Cell Migration,” 2010, pp. 147–158. doi: 10.1007/978-1-60761-404-3_9.

[18] C. Tarella, D. Ferrero, E. Gallo, G. L. Pagliardi, and F. W. Ruscetti, “Induction of differentiation of HL-60 cells by dimethyl sulfoxide: evidence for a stochastic model not linked to the cell division cycle.,” *Cancer Res*, vol. 42, no. 2, pp. 445–9, Feb. 1982.

[19] S. J. Collins, F. W. Ruscetti, R. E. Gallagher, and R. C. Gallo, “Terminal differentiation of human promyelocytic leukemia cells induced by dimethyl sulfoxide and other polar

compounds.," *Proceedings of the National Academy of Sciences*, vol. 75, no. 5, pp. 2458–2462, May 1978, doi: 10.1073/pnas.75.5.2458.

[20] G. D. Birnie, "The HL60 cell line: a model system for studying human myeloid cell differentiation.," *Br J Cancer Suppl*, vol. 9, pp. 41–5, Dec. 1988.

[21] U. Siebenlist, P. Bressler, and K. Kelly, "Two Distinct Mechanisms of Transcriptional Control Operate on c- *myc* During Differentiation of HL60 Cells," *Mol Cell Biol*, vol. 8, no. 2, pp. 867–874, Feb. 1988, doi: 10.1128/mcb.8.2.867-874.1988.

[22] Y.-R. Lee *et al.*, "Dimethylsulfoxide induces upregulation of tumor suppressor protein PTEN through nuclear factor-κB activation in HL-60 cells," *Leuk Res*, vol. 29, no. 4, pp. 401–405, Apr. 2005, doi: 10.1016/j.leukres.2004.09.010.

[23] J. M. Collins and K. A. Foster, "Differentiation of promyelocytic (HL-60) cells into mature granulocytes: mitochondrial-specific rhodamine 123 fluorescence.," *Journal of Cell Biology*, vol. 96, no. 1, pp. 94–99, Jan. 1983, doi: 10.1083/jcb.96.1.94.

[24] N. Yokoyama *et al.*, "Kras promotes myeloid differentiation through Wnt/β-catenin signaling," *FASEB Bioadv*, vol. 1, no. 7, pp. 435–449, Jul. 2019, doi: 10.1096/fba.2019-00004.

[25] I. D. Trayner, T. Bustorff, A. E. Etches, G. J. Mufti, Y. Foss, and F. Farzaneh, "Changes in antigen expression on differentiating HL60 cells treated with dimethylsulphoxide, all-trans retinoic acid, alpha1,25-dihydroxyvitamin D3 or 12-O-tetradecanoyl phorbol-13-acetate.," *Leuk Res*, vol. 22, no. 6, pp. 537–47, Jun. 1998, doi: 10.1016/s0145-2126(98)00041-1.

[26] D. J. Gee, L. K. Wright, J. Zimmermann, K. Cole, K. Soule, and M. Ubowski, "Dimethylsulfoxide exposure modulates HL-60 cell rolling interactions," *Biosci Rep*, vol. 32, no. 4, pp. 375–382, Aug. 2012, doi: 10.1042/BSR20110109.

[27] Y. Yoshii, H. Wake, Y. Nishimura, K. Teshigawara, D. Wang, and M. Nishibori, "An Evaluation of the Activity of Histidine-Rich Glycoprotein on Differentiated Neutrophil-Like Cells from Human Cell Lines," *Journal of Pharmacology and Experimental Therapeutics*, vol. 375, no. 3, pp. 406–413, Dec. 2020, doi: 10.1124/jpet.120.000182.

[28] L. C. Meagher and T. G. Cotter, "The degranulation response in differentiated HL-60 cells.," *Clin Exp Immunol*, vol. 74, no. 3, pp. 483–8, Dec. 1988.

[29] Y. Guo *et al.*, “Differentiation of HL-60 cells in serum-free hematopoietic cell media enhances the production of neutrophil extracellular traps,” *Exp Ther Med*, vol. 21, no. 4, p. 353, Feb. 2021, doi: 10.3892/etm.2021.9784.

[30] T. Kawakami *et al.*, “Rab27a is essential for the formation of neutrophil extracellular traps (NETs) in neutrophil-like differentiated HL60 cells,” *PLoS One*, vol. 9, no. 1, p. e84704, Jan. 2014, doi: 10.1371/journal.pone.0084704.

[31] A. Clarke, E. LeBlanc, C. Angelatos, K. Russell, S. Karim, and L. A. Wells, “The effects of surface chemistry on the accumulation of extracellular traps on poly(methyl methacrylate) and the implications on other immune cells,” *J Mater Sci*, vol. 57, no. 22, pp. 10299–10312, Jun. 2022, doi: 10.1007/s10853-022-07264-y.

[32] S. L. Wong and D. D. Wagner, “Peptidylarginine deiminase 4: a nuclear button triggering neutrophil extracellular traps in inflammatory diseases and aging,” *The FASEB Journal*, vol. 32, no. 12, pp. 6258–6370, Sep. 2018, doi: 10.1096/fj.201800691R.

[33] I. Neeli, S. N. Khan, and M. Radic, “Histone deimination as a response to inflammatory stimuli in neutrophils,” *The Journal of Immunology*, vol. 180, no. 3, pp. 1895–1902, Feb. 2008, doi: 10.4049/jimmunol.180.3.1895.

[34] K.-H. Kim, J. Y. Seoh, and S. J. Cho, “Phenotypic and Functional Analysis of HL-60 Cells Used in Opsonophagocytic-Killing Assay for *Streptococcus pneumoniae*,” *J Korean Med Sci*, vol. 30, no. 2, p. 145, 2015, doi: 10.3346/jkms.2015.30.2.145.

[35] K. A. Babatunde, X. Wang, A. Hopke, N. Lannes, P.-Y. Mantel, and D. Irimia, “Chemotaxis and swarming in differentiated HL-60 neutrophil-like cells,” *Sci Rep*, vol. 11, no. 1, p. 778, Jan. 2021, doi: 10.1038/s41598-020-78854-6.

[36] J. Tomczok, W. Sliwa-tomczok, C. L. Klein, T. G. Van Kooten, and C. J. Kirkpatrick, “Biomaterial-induced alterations of human neutrophils under fluid shear stress: scanning electron microscopical study in vitro,” *Biomaterials*, vol. 17, no. 14, pp. 1359–1367, Jul. 1996, doi: 10.1016/0142-9612(96)87275-9.

[37] M. S. Shive, W. G. Brodbeck, and J. M. Anderson, “Activation of caspase 3 during shear stress-induced neutrophil apoptosis on biomaterials,” *J Biomed Mater Res*, vol. 62, no. 2, pp. 163–168, Nov. 2002, doi: 10.1002/jbm.10225.

[38] W. Sun, S. Wang, J. Zhang, K. Arias, B. P. Griffith, and Z. J. Wu, “Neutrophil injury and function alterations induced by high mechanical shear stress with short exposure time,” *Artif Organs*, vol. 45, no. 6, pp. 577–586, Jun. 2021, doi: 10.1111/aor.13874.

[39] J. O. Abaricia, A. H. Shah, and R. Olivares-Navarrete, “Substrate stiffness induces neutrophil extracellular trap (NET) formation through focal adhesion kinase activation,” *Biomaterials*, vol. 271, Apr. 2021, doi: 10.1016/j.biomaterials.2021.120715.

[40] J. O. Abaricia, A. H. Shah, and R. Olivares-Navarrete, “Substrate stiffness induces neutrophil extracellular trap (NET) formation through focal adhesion kinase activation,” *Biomaterials*, vol. 271, no. February, p. 120715, 2021, doi: 10.1016/j.biomaterials.2021.120715.

[41] M. Zare, E. R. Ghomi, P. D. Venkatraman, and S. Ramakrishna, “Silicone-based biomaterials for biomedical applications: Antimicrobial strategies and 3D printing technologies,” *J Appl Polym Sci*, vol. 138, no. 38, p. 50969, Oct. 2021, doi: 10.1002/app.50969.

[42] E. I. B. Peerschke, S. Panicker, and J. Bussel, “Classical complement pathway activation in immune thrombocytopenia purpura: inhibition by a novel C1s inhibitor,” *Br J Haematol*, vol. 173, no. 6, pp. 942–945, Jun. 2016, doi: 10.1111/bjh.13648.

[43] H. Gaikwad *et al.*, “Complement Inhibitors Block Complement C3 Opsonization and Improve Targeting Selectivity of Nanoparticles in Blood,” *Bioconjug Chem*, vol. 31, no. 7, pp. 1844–1856, Jul. 2020, doi: 10.1021/acs.bioconjchem.0c00342.

[44] C. M. de Bont, W. C. Boelens, and G. J. M. Pruijn, “NETosis, complement, and coagulation: a triangular relationship,” *Cell Mol Immunol*, vol. 16, no. 1, pp. 19–27, 2019, doi: 10.1038/s41423-018-0024-0.

[45] L. Waters, “Promyelocyte HL-60 Cell-line Demonstrates the Involvement of NETosis-Related Proteins in Neutrophil Nuclear Morphology Dynamics,” Thesis , University of California San Diego , 2018.

[46] P.-Y. Chen, J.-H. Yen, R.-H. Kao, and J.-H. Chen, “Down-Regulation of the Oncogene PTTG1 via the KLF6 Tumor Suppressor during Induction of Myeloid Differentiation,” *PLoS One*, vol. 8, no. 8, p. e71282, Aug. 2013, doi: 10.1371/journal.pone.0071282.

[47] D. Hickenson, A. Back, and S. Collins, “Regulation of expression of the CD11b and CD18 subunits of the neutrophil adherence receptor during human myeloid differentiation,” *The Journal of Biological Chemistry* , 1989.

[48] A. Manda-Handzlik *et al.*, “Flow cytometric quantification of neutrophil extracellular traps: Limitations of the methodological approach,” *Am J Hematol*, vol. 91, no. 3, pp. E9–E10, Mar. 2016, doi: 10.1002/ajh.24257.

[49] D. Scieszka, Y.-H. Lin, W. Li, S. Choudhury, Y. Yu, and M. Freire, “Netome: the molecular characterization of neutrophil extracellular Traps (NETs)”, doi: 10.1101/2020.05.18.102772.

[50] J. Kumbrink and K. H. Kirsch, “p130Cas acts as survival factor during PMA-induced apoptosis in HL-60 promyelocytic leukemia cells,” *Int J Biochem Cell Biol*, vol. 45, no. 3, pp. 531–535, Mar. 2013, doi: 10.1016/j.biocel.2012.12.017.

[51] A. Arroyo *et al.*, “NADPH Oxidase-dependent Oxidation and Externalization of Phosphatidylserine during Apoptosis in Me2SO-differentiated HL-60 Cells,” *Journal of Biological Chemistry*, vol. 277, no. 51, pp. 49965–49975, Dec. 2002, doi: 10.1074/jbc.M204513200.

[52] S. An *et al.*, “Neutrophil extracellular traps (NETs) contribute to pathological changes of ocular graft-vs.-host disease (oGVHD) dry eye: Implications for novel biomarkers and therapeutic strategies,” *Ocul Surf*, vol. 17, no. 3, pp. 589–614, Jul. 2019, doi: 10.1016/j.jtos.2019.03.010.

[53] T. A. Fuchs *et al.*, “Extracellular DNA traps promote thrombosis,” *Proc Natl Acad Sci U S A*, vol. 107, no. 36, pp. 15880–15885, 2010, doi: 10.1073/pnas.1005743107.

[54] M. L. Akenhead, X. Zhang, and H. Y. Shin, “Characterization of the shear stress regulation of CD18 surface expression by HL60-derived neutrophil-like cells,” *Biomech Model Mechanobiol*, vol. 13, no. 4, pp. 861–870, Aug. 2014, doi: 10.1007/s10237-013-0541-9.

[55] M. J. Mitchell and M. R. King, “Shear-Induced Resistance to Neutrophil Activation via the Formyl Peptide Receptor,” *Biophys J*, vol. 102, no. 8, pp. 1804–1814, Apr. 2012, doi: 10.1016/j.bpj.2012.03.053.

[56] A. Sheshachalam, N. Srivastava, T. Mitchell, P. Lacy, and G. Eitzen, “Granule Protein Processing and Regulated Secretion in Neutrophils,” *Front Immunol*, vol. 5, Sep. 2014, doi: 10.3389/fimmu.2014.00448.

[57] M. B. Gorbet and M. V. Sefton, “Biomaterial-associated thrombosis: roles of coagulation factors, complement, platelets and leukocytes,” *Biomaterials*, vol. 25, no. 26, pp. 5681–5703, Nov. 2004, doi: 10.1016/j.biomaterials.2004.01.023.

[58] B. G. Yipp *et al.*, “Infection-induced NETosis is a dynamic process involving neutrophil multitasking in vivo,” *Nat Med*, vol. 18, no. 9, pp. 1386–1393, Sep. 2012, doi: 10.1038/nm.2847.

[59] L. J. Palmer, C. Damgaard, P. Holmstrup, and C. H. Nielsen, “Influence of complement on neutrophil extracellular trap release induced by bacteria,” *J Periodontal Res*, vol. 51, no. 1, pp. 70–76, Feb. 2016, doi: 10.1111/jre.12284.

[60] M. Saffarzadeh *et al.*, “Characterization of rapid neutrophil extracellular trap formation and its cooperation with phagocytosis in human neutrophils,” *Discoveries*, vol. 2, no. 2, p. e19, Jun. 2014, doi: 10.15190/d.2014.11.

[61] Z. Chen *et al.*, “Review: The Emerging Role of Neutrophil Extracellular Traps in Sepsis and Sepsis-Associated Thrombosis,” *Front Cell Infect Microbiol*, vol. 11, Mar. 2021, doi: 10.3389/fcimb.2021.653228.

[62] J. Yuen *et al.*, “NETosing Neutrophils Activate Complement Both on Their Own NETs and Bacteria via Alternative and Non-alternative Pathways,” *Front Immunol*, vol. 7, Apr. 2016, doi: 10.3389/fimmu.2016.00137.

[63] K. H. Krause, W. Schlegel, C. B. Wollheim, T. Andersson, F. A. Waldvogel, and P. D. Lew, “Chemotactic peptide activation of human neutrophils and HL-60 cells. Pertussis toxin reveals correlation between inositol trisphosphate generation, calcium ion transients, and cellular activation.,” *Journal of Clinical Investigation*, vol. 76, no. 4, pp. 1348–1354, Oct. 1985, doi: 10.1172/JCI112109.

[64] Z. Ahmed, G. Shaw, V. P. Sharma, C. Yang, E. McGowan, and D. W. Dickson, “Actin-binding Proteins Coronin-1a and IBA-1 are Effective Microglial Markers for Immunohistochemistry,” *Journal of Histochemistry & Cytochemistry*, vol. 55, no. 7, pp. 687–700, Jul. 2007, doi: 10.1369/jhc.6A7156.2007.

[65] A. B. Hauert, S. Martinelli, C. Marone, and V. Niggli, “Differentiated HL-60 cells are a valid model system for the analysis of human neutrophil migration and chemotaxis,” *Int J Biochem Cell Biol*, vol. 34, no. 7, pp. 838–854, Jul. 2002, doi: 10.1016/S1357-2725(02)00010-9.

[66] O. Teufelhofer, “Promyelocytic HL60 Cells Express NADPH Oxidase and Are Excellent Targets in a Rapid Spectrophotometric Microplate Assay for Extracellular Superoxide,” *Toxicological Sciences*, vol. 76, no. 2, pp. 376–383, Nov. 2003, doi: 10.1093/toxsci/kfg234.

Chapter 4 References

[1] C. Rosales, “Neutrophil: A Cell with Many Roles in Inflammation or Several Cell Types?,” *Front Physiol*, vol. 9, Feb. 2018, doi: 10.3389/fphys.2018.00113.

[2] B. G. Yipp and P. Kubes, “NETosis: how vital is it?,” *Blood*, vol. 122, no. 16, pp. 2784–2794, Oct. 2013, doi: 10.1182/blood-2013-04-457671.

[3] R. S. Keshari, A. Verma, M. K. Barthwal, and M. Dikshit, “Reactive oxygen species-induced activation of ERK and p38 MAPK mediates PMA-induced NETs release from human neutrophils,” *J Cell Biochem*, vol. 114, no. 3, pp. 532–540, Mar. 2013, doi: 10.1002/jcb.24391.

[4] A. D. Verin *et al.*, “Role of Ras-dependent ERK activation in phorbol ester-induced endothelial cell barrier dysfunction,” *American Journal of Physiology-Lung Cellular and Molecular Physiology*, vol. 279, no. 2, pp. L360–L370, Aug. 2000, doi: 10.1152/ajplung.2000.279.2.L360.

[5] R. L. Degroote, M. Weigand, S. M. Hauck, and C. A. Deeg, “IL8 and PMA Trigger the Regulation of Different Biological Processes in Granulocyte Activation,” *Front Immunol*, vol. 10, Jan. 2020, doi: 10.3389/fimmu.2019.03064.

[6] M. P. Pruchniak and U. Demkow, “Potent NETosis inducers do not show synergistic effects in vitro,” *Central European Journal of Immunology*, vol. 44, no. 1, pp. 51–58, 2019, doi: 10.5114/ceji.2019.84017.

[7] M. Siddiqi, Z. C. Garcia, D. S. Stein, T. N. Denny, and Z. Spolarics, “Relationship between oxidative burst activity and CD11b expression in neutrophils and monocytes from healthy

individuals: Effects of race and gender," *Cytometry*, vol. 46, no. 4, pp. 243–246, Aug. 2001, doi: 10.1002/cyto.1134.

[8] A. J. Murphy *et al.*, "Neutrophil Activation Is Attenuated by High-Density Lipoprotein and Apolipoprotein A-I in In Vitro and In Vivo Models of Inflammation," *Arterioscler Thromb Vasc Biol*, vol. 31, no. 6, pp. 1333–1341, Jun. 2011, doi: 10.1161/ATVBAHA.111.226258.

[9] B. K. A. Abdel-Salam and H. Ebaid, "Clinical immunology Expression of CD11b and CD18 on polymorphonuclear neutrophils stimulated with interleukin-2," *Central European Journal of Immunology*, vol. 2, pp. 209–215, 2014, doi: 10.5114/ceji.2014.43725.

[10] D. Dömer, T. Walther, S. Möller, M. Behnen, and T. Laskay, "Neutrophil Extracellular Traps Activate Proinflammatory Functions of Human Neutrophils," *Front Immunol*, vol. 12, Jun. 2021, doi: 10.3389/fimmu.2021.636954.

[11] S. Mol *et al.*, "Efficient Neutrophil Activation Requires Two Simultaneous Activating Stimuli," *Int J Mol Sci*, vol. 22, no. 18, p. 10106, Sep. 2021, doi: 10.3390/ijms221810106.

[12] J. O. Abaricia, A. H. Shah, R. M. Musselman, and R. Olivares-Navarrete, "Hydrophilic titanium surfaces reduce neutrophil inflammatory response and NETosis," *Biomater Sci*, vol. 8, no. 8, pp. 2289–2299, Apr. 2020, doi: 10.1039/c9bm01474h.

[13] J. O. Abaricia, A. H. Shah, R. M. Musselman, and R. Olivares-Navarrete, "Hydrophilic titanium surfaces reduce neutrophil inflammatory response and NETosis," *Biomater Sci*, vol. 8, no. 8, pp. 2289–2299, 2020, doi: 10.1039/c9bm01474h.

[14] S. Jhunjhunwala, "Neutrophils at the biological-material interface," *ACS Biomaterials Science and Engineering*, vol. 4, no. 4. American Chemical Society, pp. 1128–1136, Apr. 09, 2018. doi: 10.1021/acsbiomaterials.6b00743.

[15] B. O. Ode Boni, L. Lamboni, T. Souho, M. Gauthier, and G. Yang, "Immunomodulation and cellular response to biomaterials: The overriding role of neutrophils in healing," *Materials Horizons*, vol. 6, no. 6. Royal Society of Chemistry, pp. 1122–1137, Jul. 01, 2019. doi: 10.1039/c9mh00291j.

[16] J. O. Abaricia, A. H. Shah, and R. Olivares-Navarrete, "Substrate stiffness induces neutrophil extracellular trap (NET) formation through focal adhesion kinase activation," *Biomaterials*, vol. 271, Apr. 2021, doi: 10.1016/j.biomaterials.2021.120715.

[17] C. Sperling, M. Fischer, M. F. Maitz, and C. Werner, “Neutrophil extracellular trap formation upon exposure of hydrophobic materials to human whole blood causes thrombogenic reactions,” *Biomater Sci*, vol. 5, no. 10, pp. 1998–2008, 2017, doi: 10.1039/C7BM00458C.

[18] Y. J. Lu *et al.*, “Mechanism of nanoformulated graphene oxide-mediated human neutrophil activation,” *ACS Appl Mater Interfaces*, vol. 12, no. 36, pp. 40141–40152, Sep. 2020, doi: 10.1021/acsami.0c12490.

[19] P. W. Bisso, S. Gaglione, P. P. G. Guimarães, M. J. Mitchell, and R. Langer, “Nanomaterial interactions with human neutrophils,” *ACS Biomater Sci Eng*, vol. 4, no. 12, pp. 4255–4265, Dec. 2018, doi: 10.1021/acsbiomaterials.8b01062.

[20] A. E. Fetz, M. Z. Radic, and G. L. Bowlin, “Human neutrophil FcγRIIIb regulates neutrophil extracellular trap release in response to electrospun polydioxanone biomaterials,” *Acta Biomater*, vol. 130, pp. 281–290, Aug. 2021, doi: 10.1016/j.actbio.2021.06.007.

[21] L. Erpenbeck *et al.*, “Effect of adhesion and substrate elasticity on neutrophil extracellular trap formation,” *Front Immunol*, vol. 10, Oct. 2019, doi: 10.3389/fimmu.2019.02320.

[22] R. Yaseen *et al.*, “Antimicrobial activity of HL-60 cells compared to primary blood-derived neutrophils against Staphylococcus aureus,” *J Negat Results Biomed*, vol. 16, no. 1, Feb. 2017, doi: 10.1186/s12952-017-0067-2.

[23] H. Gaikwad *et al.*, “Complement Inhibitors Block Complement C3 Opsonization and Improve Targeting Selectivity of Nanoparticles in Blood,” *Bioconjug Chem*, vol. 31, no. 7, pp. 1844–1856, Jul. 2020, doi: 10.1021/acs.bioconjchem.0c00342.

[24] E. I. B. Peerschke, S. Panicker, and J. Bussel, “Classical complement pathway activation in immune thrombocytopenia purpura: inhibition by a novel C1s inhibitor,” *Br J Haematol*, vol. 173, no. 6, pp. 942–945, Jun. 2016, doi: 10.1111/bjh.13648.

[25] C.-J. Jung, C.-Y. Yeh, R.-B. Hsu, C.-M. Lee, C. Shun, and J.-S. Chia, “Endocarditis Pathogen Promotes Vegetation Formation by Inducing Intravascular Neutrophil Extracellular Traps Through Activated Platelets,” *Circulation*, vol. 131, Dec. 2014, doi: 10.1161/CIRCULATIONAHA.114.011432.

[26] T. W. R. Halverson, M. Wilton, K. K. H. Poon, B. Petri, and S. Lewenza, “DNA Is an Antimicrobial Component of Neutrophil Extracellular Traps,” *PLoS Pathog*, vol. 11, no. 1, p. e1004593, Jan. 2015, doi: 10.1371/journal.ppat.1004593.

[27] A. Hosseinnejad *et al.*, “DNase I functional microgels for neutrophil extracellular trap disruption,” *Biomater Sci*, vol. 10, no. 1, pp. 85–99, 2022, doi: 10.1039/D1BM01591E.

[28] A. Clarke, E. LeBlanc, C. Angelatos, K. Russell, S. Karim, and L. A. Wells, “The effects of surface chemistry on the accumulation of extracellular traps on poly(methyl methacrylate) and the implications on other immune cells,” *J Mater Sci*, vol. 57, no. 22, pp. 10299–10312, Jun. 2022, doi: 10.1007/s10853-022-07264-y.

[29] K. H. Lee *et al.*, “Quantification of NETs-associated markers by flow cytometry and serum assays in patients with thrombosis and sepsis,” *Int J Lab Hematol*, vol. 40, no. 4, pp. 392–399, Aug. 2018, doi: 10.1111/ijlh.12800.

[30] T. Hoppenbrouwers *et al.*, “In vitro induction of NETosis: Comprehensive live imaging comparison and systematic review,” *PLoS One*, vol. 12, no. 5, p. e0176472, May 2017, doi: 10.1371/journal.pone.0176472.

[31] D. Pai, M. Gruber, S.-M. Pfaehler, A. Bredthauer, K. Lehle, and B. Trabold, “Polymorphonuclear Cell Chemotaxis and Suicidal NETosis: Simultaneous Observation Using fMLP, PMA, H7, and Live Cell Imaging,” *J Immunol Res*, vol. 2020, pp. 1–10, Aug. 2020, doi: 10.1155/2020/1415947.

[32] J. S. Holsapple *et al.*, “Expansion microscopy of neutrophil nuclear structure and extracellular traps,” *Biophysical Reports*, vol. 3, no. 1, p. 100091, Mar. 2023, doi: 10.1016/j.bpr.2022.100091.

[33] A. Obermayer *et al.*, “New Aspects on the Structure of Neutrophil Extracellular Traps from Chronic Obstructive Pulmonary Disease and In Vitro Generation,” *PLoS One*, vol. 9, no. 5, p. e97784, May 2014, doi: 10.1371/journal.pone.0097784.

[34] Y. Wang *et al.*, “Histone hypercitrullination mediates chromatin decondensation and neutrophil extracellular trap formation,” *Journal of Cell Biology*, vol. 184, no. 2, pp. 205–213, Jan. 2009, doi: 10.1083/jcb.200806072.

[35] M. Saffarzadeh *et al.*, “Neutrophil Extracellular Traps Directly Induce Epithelial and Endothelial Cell Death: A Predominant Role of Histones,” *PLoS One*, vol. 7, no. 2, p. e32366, Feb. 2012, doi: 10.1371/journal.pone.0032366.

[36] D. Zhang *et al.*, “Neutrophil ageing is regulated by the microbiome,” *Nature*, vol. 525, no. 7570, pp. 528–532, Sep. 2015, doi: 10.1038/nature15367.

[37] A. Manda-Handzlik *et al.*, “Flow cytometric quantification of neutrophil extracellular traps: Limitations of the methodological approach,” *Am J Hematol*, vol. 91, no. 3, pp. E9–E10, Mar. 2016, doi: 10.1002/ajh.24257.

[38] D. Gunawardena, I. Priyankara, H. Jayamanne, and S. Suresh, “Modified Giemsa Stain: A solution to improve the quality of hypercellular bone marrow smears,” *Int J Lab Hematol*, vol. 44, no. 3, pp. 504–509, Jun. 2022, doi: 10.1111/ijlh.13824.

[39] M. Bins, W. Huiges, T. Timmers, E. S. Gelsema, and M. R. Halie, “Neutrophil granulation stained with May Gruenwald Giemsa or pure Azure B-eosin Y quantified by image analysis,” *Blut*, vol. 58, no. 2, pp. 79–82, Feb. 1989, doi: 10.1007/BF00320653.

[40] T. Tanaka, “Leukocyte Adhesion Molecules,” in *Encyclopedia of Immunobiology*, Elsevier, 2016, pp. 505–511. doi: 10.1016/B978-0-12-374279-7.07015-6.

[41] S. Y. Park *et al.*, “Autophagy Primes Neutrophils for Neutrophil Extracellular Trap Formation during Sepsis,” *Am J Respir Crit Care Med*, vol. 196, no. 5, pp. 577–589, Sep. 2017, doi: 10.1164/rccm.201603-0596OC.

[42] C. Sanchez, M. C. Alessi, N. Saut, M. F. Aillaud, And P. E. Morange, “Relation between the antithrombin Cambridge II mutation, the risk of venous thrombosis, and the endogenous thrombin generation,” *Journal of Thrombosis and Haemostasis*, vol. 6, no. 11, pp. 1975–1977, Nov. 2008, doi: 10.1111/j.1538-7836.2008.03144.x.

[43] X. Chang, “Shear Effect on Material Induced Blood Cell Activation,” 2011.

[44] C. Lewis, “Effects of Short Exposure to High Shear on Neutrophil State and Function,” 2018.

[45] M. L. Akenhead, X. Zhang, and H. Y. Shin, “Characterization of the shear stress regulation of CD18 surface expression by HL60-derived neutrophil-like cells,” *Biomech Model Mechanobiol*, vol. 13, no. 4, pp. 861–870, Aug. 2014, doi: 10.1007/s10237-013-0541-9.

[46] A. Sheshachalam, N. Srivastava, T. Mitchell, P. Lacy, and G. Eitzen, “Granule Protein Processing and Regulated Secretion in Neutrophils,” *Front Immunol*, vol. 5, Sep. 2014, doi: 10.3389/fimmu.2014.00448.

[47] S. Mol *et al.*, “Efficient Neutrophil Activation Requires Two Simultaneous Activating Stimuli,” *Int J Mol Sci*, vol. 22, no. 18, p. 10106, Sep. 2021, doi: 10.3390/ijms221810106.

[48] G. Rai, “Factors regulating NETosis,” in *Netosis*, Elsevier, 2019, pp. 57–88. doi: 10.1016/B978-0-12-816147-0.00003-4.

[49] C. M. de Bont, W. C. Boelens, and G. J. M. Pruijn, “NETosis, complement, and coagulation: a triangular relationship,” *Cell Mol Immunol*, vol. 16, no. 1, pp. 19–27, Jan. 2019, doi: 10.1038/s41423-018-0024-0.

[50] J. Yuen *et al.*, “NETosing Neutrophils Activate Complement Both on Their Own NETs and Bacteria via Alternative and Non-alternative Pathways,” *Front Immunol*, vol. 7, Apr. 2016, doi: 10.3389/fimmu.2016.00137.

[51] L. J. Palmer, C. Damgaard, P. Holmstrup, and C. H. Nielsen, “Influence of complement on neutrophil extracellular trap release induced by bacteria,” *J Periodontal Res*, vol. 51, no. 1, pp. 70–76, Feb. 2016, doi: 10.1111/jre.12284.

[52] B. G. Yipp *et al.*, “Infection-induced NETosis is a dynamic process involving neutrophil multitasking in vivo,” *Nat Med*, vol. 18, no. 9, pp. 1386–1393, Sep. 2012, doi: 10.1038/nm.2847.

[53] M. Saffarzadeh *et al.*, “Characterization of rapid neutrophil extracellular trap formation and its cooperation with phagocytosis in human neutrophils,” *Discoveries*, vol. 2, no. 2, p. e19, Jun. 2014, doi: 10.15190/d.2014.11.

[54] A. E. Fetz, M. Z. Radic, and G. L. Bowlin, “Human neutrophil FcγRIIIb regulates neutrophil extracellular trap release in response to electrospun polydioxanone biomaterials,” *Acta Biomater*, vol. 130, pp. 281–290, 2021, doi: 10.1016/j.actbio.2021.06.007.

[55] A. Hakkim *et al.*, “Activation of the Raf-MEK-ERK pathway is required for neutrophil extracellular trap formation,” *Nat Chem Biol*, vol. 7, no. 2, pp. 75–77, Feb. 2011, doi: 10.1038/nchembio.496.

[56] S. Shalekoff, L. Page-Shipp, and C. T. Tiemessen, “Effects of Anticoagulants and Temperature on Expression of Activation Markers CD11b and HLA-DR on Human Leukocytes,” *Clinical Diagnostic Laboratory Immunology*, vol. 5, no. 5, pp. 695–702, Sep. 1998, doi: 10.1128/CDLI.5.5.695-702.1998.

[57] L. Koenderman, J. van der Linden, H. Honing, and L. Ulfman, “Integrins on neutrophils are dispensable for migration into three-dimensional fibrin gels,” *Thromb Haemost*, vol. 104, no. 09, pp. 599–608, Nov. 2010, doi: 10.1160/TH09-10-0740.

[58] L. J. Miller, D. F. Bainton, N. Borregaard, and T. A. Springer, “Stimulated mobilization of monocyte Mac-1 and p150,95 adhesion proteins from an intracellular vesicular compartment to the cell surface.,” *Journal of Clinical Investigation*, vol. 80, no. 2, pp. 535–544, Aug. 1987, doi: 10.1172/JCI113102.

[59] h. De la Corte Rodriguez, e. C. Rodriguez-Merchan, and v. Jimenez-Vuste, “Radiosynovectomy in hemophilia: quantification of its effectiveness through the assessment of 10 articular parameters,” *Journal of Thrombosis and Haemostasis*, vol. 9, no. 5, pp. 928–935, May 2011, doi: 10.1111/j.1538-7836.2011.04246.x.

[60] T. A. Fuchs *et al.*, “Extracellular DNA traps promote thrombosis,” *Proc Natl Acad Sci U S A*, vol. 107, no. 36, pp. 15880–15885, 2010, doi: 10.1073/pnas.1005743107.

[61] R. Bilyy *et al.*, “Neutrophil Extracellular Traps Form a Barrier between Necrotic and Viable Areas in Acute Abdominal Inflammation,” *Front Immunol*, vol. 7, Oct. 2016, doi: 10.3389/fimmu.2016.00424.

[62] A. Mangold *et al.*, “Coronary Neutrophil Extracellular Trap Burden and Deoxyribonuclease Activity in ST-Elevation Acute Coronary Syndrome Are Predictors of ST-Segment Resolution and Infarct Size,” *Circ Res*, vol. 116, no. 7, pp. 1182–1192, Mar. 2015, doi: 10.1161/CIRCRESAHA.116.304944.

[63] V. Brinkmann *et al.*, “Neutrophil Extracellular Traps Kill Bacteria,” *Science (1979)*, vol. 303, no. 5663, pp. 1532–1535, Mar. 2004, doi: 10.1126/science.1092385.

Chapter 5 References

[1] W. Beaubien-Souligny, P.-E. Neagoe, D. Gagnon, A. Y. Denault, and M. G. Sirois, “Increased circulating levels of neutrophil extracellular traps during cardiopulmonary bypass,” *CJC Open*, vol. 2, no. 2, pp. 39–48, 2020. doi:10.1016/j.cjco.2019.12.001

[2] I. Neeli, S. N. Khan, and M. Radic, “Histone deimination as a response to inflammatory stimuli in neutrophils,” *The Journal of Immunology*, vol. 180, no. 3, pp. 1895–1902, Feb. 2008, doi: 10.4049/jimmunol.180.3.1895.

[3] Y. Wang *et al.*, “Histone hypercitrullination mediates chromatin decondensation and neutrophil extracellular trap formation,” *Journal of Cell Biology*, vol. 184, no. 2, pp. 205–213, Jan. 2009, doi: 10.1083/jcb.200806072.

Appendix A: Lactoferrin

During NETosis, lactoferrin (LF) is released and adheres to expelled genetic material alongside MPO and NE. Additionally, work in our lab has revealed that stimulation with fMLP results in LF release from neutrophils within 15 minutes. To date, no group has used LF alongside MPO and H3 to assess NETosis using flow cytometry. We attempted to develop a protocol that could be used to quantify LF expression from parallel plate samples. This was done solely in PMNs as we have also seen that HL-60 cells do not release LF upon stimulation. Cells were incubated with 1uM fMLP for 1 hour at 37 degrees. Initial attempts were made to pair PE-LF with FITC-MPO to more specifically target NETs, however, there was a substantial signal leak into the neutrophil marker CD15 channel with the PE-LF secondary antibody. The settings were adjusted to account for this however the LF signal decreased upon fMLP stimulation, indicating that an issue remained. To obtain a greater positive control peak for MPO, the channel voltage was increased however the reduction in the LF signal with fMLP remained obvious. At this stage, several adjustments were made. To prevent overlap and interference, MPO was removed and a new set of settings using FITC-LF and Cy5.5-CD45 were tested. These new settings and its protocol had previously been validated for LF release from tear film neutrophils. fMLP was also replaced with the more reliable NETosis stimuli PMA at a concentration of 6nM. Under these conditions, the LF signal continued to decrease in the static conditions despite PMA stimulation. At this stage, it was determined that LF could not be used reliably to identify NETs via flow cytometry.

Appendix B: HL-60

Table A.1: Fluorescence of cells identified by the M1 histogram marker for samples activated with 1uM fMLP for 2 hours.

Sample	MPO	H3
Static	191.30	13.96
	166.12	13.34
	161.00	15.24
fMLP Static	210.12	13.38
	167.49	13.50
	148.92	15.53
Plate	163.16	13.53
	93.63	12.06
	117.73	14.55
fMLP Plate	111.58	13.33
	89.25	12.81
	130.23	13.73

fMLP: 1uM fMLP. Fluorescence for both NETosis markers did not change meaningfully with fMLP stimulation in either static or sheared samples. Samples were incubated without platelet-poor plasma.

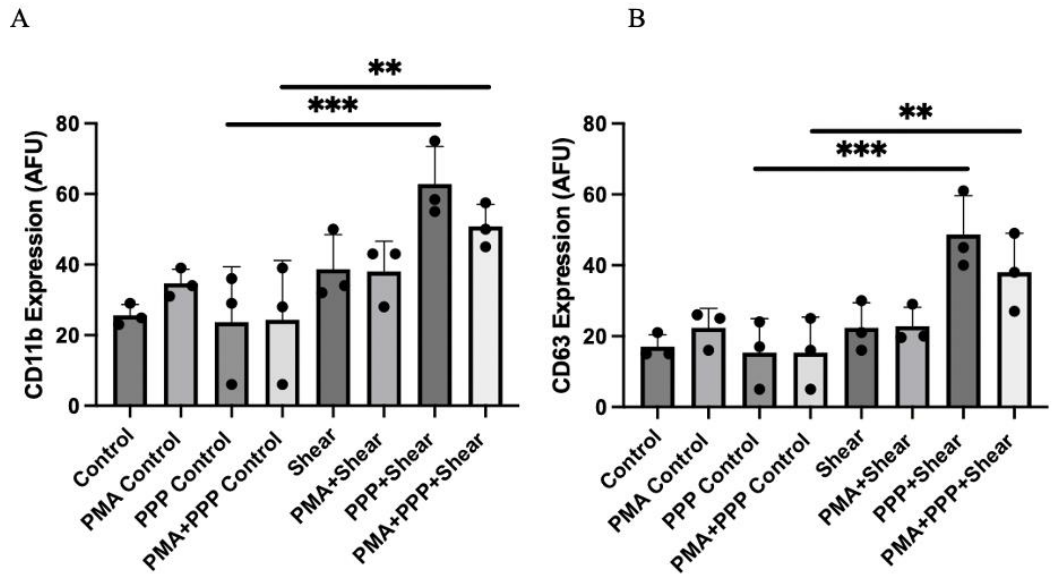

Figure A.1: CD11b (A) and CD63 (B) expression (AFU) of cells in the triple population gate (R1, R2, and R3) for all samples. n =3. ** indicates $p < 0.01$ and *** indicates $p < 0.01$.

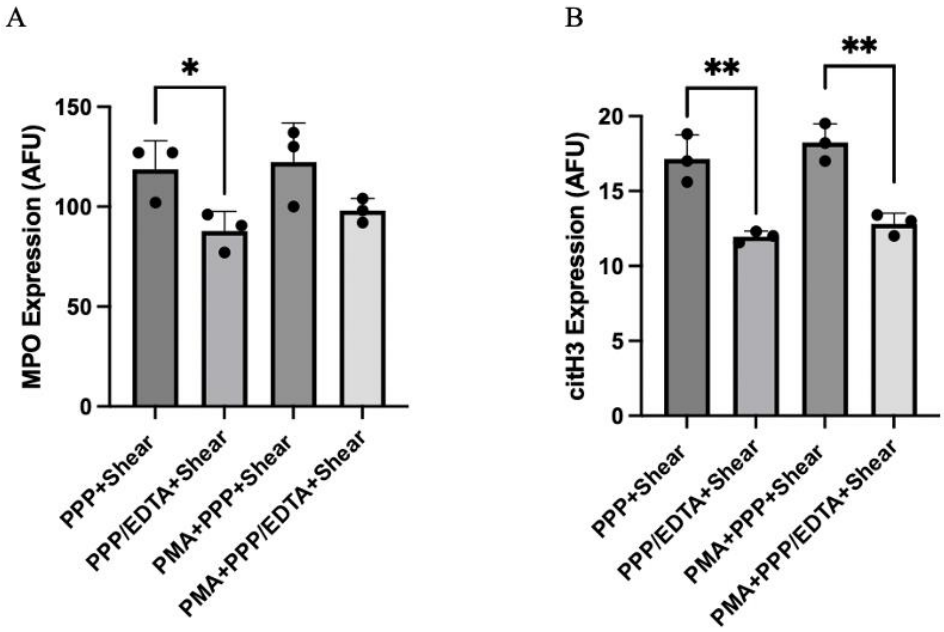

Figure A.2: MPO (FITC)(A) and citH3 (PE) (B) expression on dHL-60 cells in gate 1 (including R1, R2, and R3) following 2-hour exposure to silicone with plasma with or without 10mM EDTA. n = 3. Significance * $p < 0.05$ and ** is $p < 0.01$.

Appendix C: PMN Values

Table A.2: MPO and citH3 expression values (AFU) of PMN samples exposed to shear with or without plasma and with or without 1uM fMLP.

Sample	Fluorescence MPO (AFU)	Fluorescence citH3 (AFU)	Mean ± SD for MPO	Mean ± SD for citH3
+ PPP Static	2.68	4.08	2.40 ± 0.22	3.74 ± 0.33
	2.13	3.32		
	2.36	4.06		
	2.28	3.52		
	2.54	3.72		
fMLP+PPP Static	2.95	3.56	3.07 ± 0.13	3.66 ± 0.63
	3.11	3.33		
	3.0	3.58		
	3.28	4.74		
	3.02	3.10		
PPP+Shear	2.83	4.17	2.55 ± 0.24	3.45 ± 0.57
	2.50	2.87		
	2.23	3.83		
	2.45	3.47		
	2.74	2.91		
fMLP+PPP+Shear	4.44	4.88	4.28 ± 0.54	3.99 ± 0.53
	5.13	4.06		
	3.69	3.63		
	4.09	3.77		
	4.05	3.62		

PMA: 6nM PMA, fMLP: 1uM fMLP, PPP: platelet poor plasma

Table A.3: CD11b and CD63 expression values (AFU) of PMN samples exposed to shear with or without plasma and with or without 1uM fMLP.

Sample	Fluorescence CD11b (AFU)	Fluorescence CD63 (AFU)	Mean ± SD for CD11b	Mean ± SD for CD63
PPP Static	146	7.82	121.54 ± 24.96	6.90 ± 0.99
	114	5.62		
	104.11	6.7		
	94.1	6.4		
	149.48	7.98		
fMLP+PPP Static	299	25	285.87 ± 17.27	21.26 ± 6.64
	297	15.31		
	257.97	30.99		
	280.25	16.97		
	295.15	17.53		
PPP+Shear	159	8.57	132.48 ± 25.21	7.57 ± 0.89
	132.7	6.83		
	94.72	6.55		
	124.72	7.56		
	151.28	8.33		
fMLP+PPP+Shear	282	25.19	256.97 ± 28.45	21.51 ± 4.62
	231.66	15.24		
	271.95	26.27		
	278.24	22.38		
	221	18.49		

PMA: 6nM PMA, fMLP: 1uM fMLP, PPP: platelet poor plasma

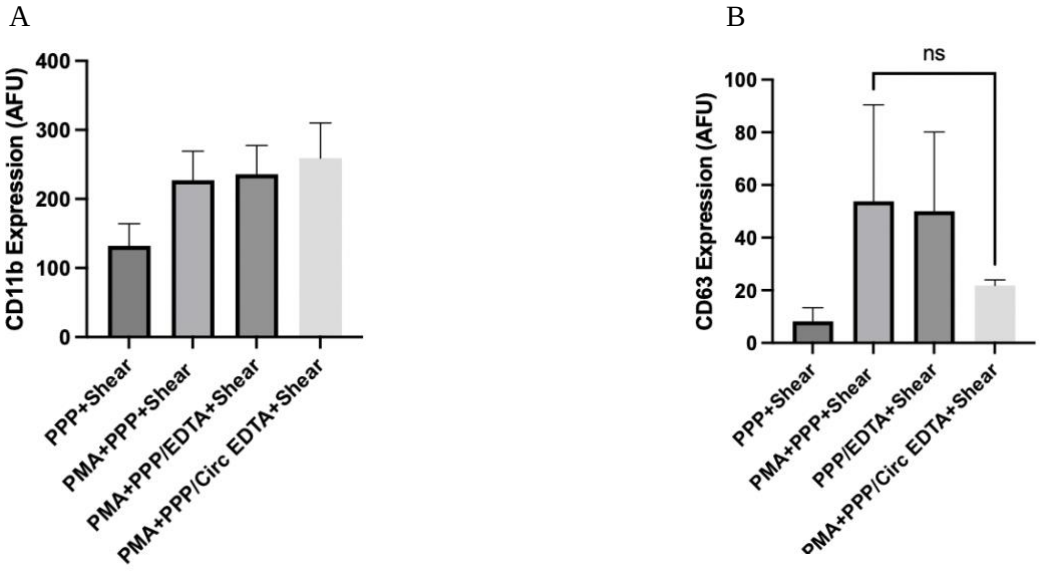

Figure A.3: CD11b (A) and CD63 (B) expression in PMNs following 1-hour exposure to plasma-coated silicone under shear conditions with or without 6 nM PMA and 10mM EDTA. PPP: platelet poor plasma. PPP/EDTA: platelet poor plasma with 10mM EDTA. PPP/Circ EDTA: platelet poor plasma with 10mM EDTA and an additional 10mM EDTA circulating in the bulk solution. n = 7 for PPP+Shear and PMA+PPP+Shear. n=5 for PMA+PPP/EDTA+Shear. n = 3 for PMA+PPP/Circ EDTA+Shear A) percentage of cells staining for both MPO (FITC) and citH3 (PE). B) MPO and citH3 expression on PMNs cells. mean ± standard deviation. All experiments were run for 1 hour at 37ºC.

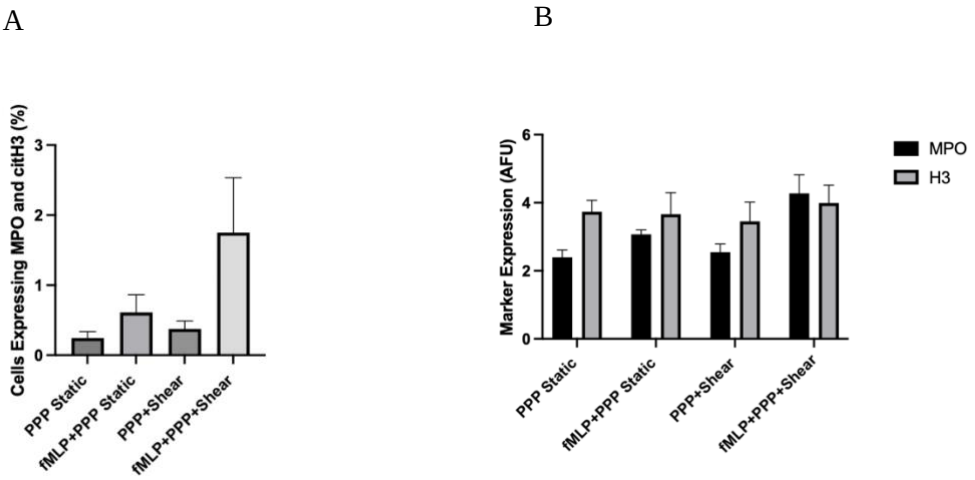

Figure A.4: NETosis in PMNs following 1-hour exposure to plasma-coated silicone under shear conditions with or without 1μM fMLP PPP: platelet poor plasma. n=5 A) percentage of cells staining for both MPO (FITC) and citH3 (PE). B) MPO and citH3 expression on PMNs cells. mean ± standard deviation. All experiments were run for 1 hour at 37ºC.

Table A.4: Percentage of cells lost in the shear-biomaterial environment following either no stimulation, or activation with 6nM PMA or 1uM fMLP for 1 hour.

Sample	Mean ± SD of the Percentage of Cells Lost
PPP+Shear	67.45 ± 10.91
PMA + PPP+Shear	82.26 ± 9.11
fMLP +PPP+Shear	89.46 ± 5.71
+ PPP/EDTA+Shear	73.55 ± 11.75
PMA + PPP/EDTA+Shear	83.12 ± 7.87
PMA + PPP/Circ EDTA Shear	76.80 ± 1.28

PMA: 6nM PMA, fMLP: 1uM fMLP, PPP: platelet poor plasma, EDTA: 10mM EDTA incubated with the PPP, Circ EDTA: 10mM Circulating EDTA through the bulk solution.